PCCP

Accepted Manuscript

ROYAL SOCIETY OF CHEMISTRY

www.rsc.org/pccp

Reactions of Allylic Radicals that Impact Molecular Weight Growth Kinetics

Kun Wang, Stephanie M. Villano, and Anthony M. Dean*

Chemical and Biological Engineering Dept., Colorado School of Mines, Golden, CO 80401

*corresponding author: amdean@mines.edu

Abstract: The reactions of allylic radicals have the potential to play a critical role in molecular weight growth (MWG) kinetics during hydrocarbon oxidation and/or pyrolysis. Due to their stability (when compared to alkyl radicals), they can accumulate to relatively high concentrations. Thus, even though the rate coefficients for their various reactions are small, the rates of these reactions may be significant. In this work, we use electronic structure calculations to examine the recombination, addition, and abstraction reactions of allylic radicals. For the recombination reaction of allyl radicals, we assign a high pressure rate rule that is based on experimental data. Once formed, the recombination product can potentially undergo an H-atom abstraction reaction followed by unimolecular cyclization and β-scission reactions. Depending upon the conditions (e.g., higher pressures) these pathways can lead to the formation of stable MWG species. The addition of allylic radicals to olefins can also lead to MWG species formation. Once again, cyclization of the adduct followed by β-scission is an important energy accessible route. Since the recombination and addition reactions produce chemically-activated adducts, we have explored the pressure- and temperature-dependence of the overall rate constants as well as that for the multiple product channels. We describe a strategy for estimating these pressure-dependencies for systems where detailed electronic structure information is not available. We also derive generic rate rules for hydrogen abstraction reactions from olefins and diolefins by methyl and allyl radicals.

Keywords: Allylic radicals, molecular weight growth, kinetic model, recombination reactions, addition reactions, hydrogen abstraction reactions

1. INTRODUCTION

Olefins are a component of gasoline. They are also key intermediates in the combustion and pyrolysis of paraffins. For example, ethylene, propene, and isobutene play important roles in the pyrolysis and oxidation of ethane[1, 2], propane[3, 4], and isooctane[5, 6], respectively. Therefore understanding the pyrolysis kinetics of olefins is essential for the proper characterization of the detailed kinetic mechanisms of larger alkanes. One significant kinetic feature of olefin pyrolysis (especially at temperatures near 1000K) is that high concentrations of resonantly-stabilized allylic radicals are formed. These radicals are formed from dissociation and/or hydrogen abstraction reactions of the parent olefin, due to its relatively weak C-C and C-H bonds. Once formed, the higher stability of these radicals means that their subsequent reactions are slow compared to the analogous reactions of "normal" (i.e., non-resonantly stabilized) alkyl radicals. For instance, hydrogen abstraction reactions by these radicals are generally slow due to the unfavorable energetics. Radical addition reactions are also often slower since the adduct that is formed is generally not resonantly stabilized. As a result, the entrance channel well is less deep than in the corresponding alkyl radical addition reaction. Similarly, the recombination reactions also result in a relatively shallow entrance channel well and dissociation back to the reactants is often favored. These features may impact the pyrolysis kinetics by: (1) The conversion of alkyl radicals to allylic radicals via H-atom abstraction from olefins will likely inhibit the pyrolysis kinetics by lowering the reactivity of the radical pool, and (2) The higher concentrations of allylic radicals may favor addition and recombination reactions, even though the rate constants are relatively small, leading to formation of higher molecular weight growth (MWG) species. These factors are especially important in the analysis of olefin and biomass systems, where the presence of weaker C-C and/or C–H bonds increases the potential to form allylic radicals.

The recombination reactions of resonantly-stabilized radicals have been considered to be important for the formation of MWG species. A number of experimental and theoretical studies[7-10] have been performed for the self-recombination reaction of propargyl (C_3H_3) radicals and the reaction pathways leading to the formation of benzene have been well documented. The kinetics for the self-reaction of allyl (C_3H_5) radicals[11, 12] and the cross-reaction between C_3H_3 and C_3H_5 radicals[11-14] have also been characterized. The self-recombination of cyclopentadienyl radicals to

ultimately form naphthalene (after isomerization and loss of hydrogen) has been proposed by several groups[15-20]. Other recombination reactions have also been proposed, including: allyl + cyclopentadienyl leading to formation of styrene[18], propargyl + cyclopentadienyl to form phenylacetylene[18], and propargyl + benzyl to form naphthalene[18, 21].

Another pathway leading to the formation of MWG species involves addition of these stabilized radicals to a double bond in olefins or conjugated dienes, or a triple bond in alkynes. The resulting adduct may then cyclize and β-scission to form a stable MWG species. However, the fact that the initially-formed adduct is generally less stable due to loss of resonance means that it is often more likely to re-dissociate back to reactants. This situation is exacerbated by the fact that the cyclization of the linear adduct causes an entropy loss. The loss in entropy will become increasingly important at higher temperatures, shifting the equilibrium back toward reactants. As a general rule, the formation of MWG species will be favored if the initially-formed linear adduct is unusually stable and if the cyclic adduct is significantly more stable than the linear one.

Although H-abstraction reactions by resonantly stabilized radicals are often energetically disfavored, abstraction from the parent or product olefins to form other resonantly stabilized radicals is approximately thermoneutral. There are several studies[17, 22, 23] that have taken this type of reaction into consideration by either assigning the rate constants by estimation, or by analogy to a "normal" H-abstraction reactions. The various rate constant estimates in the literature differ significantly from one another. Recently, Sabbe et al.[24] employed electronic structure calculations to investigate the influence of resonance stabilization on the kinetics of hydrogen abstractions. Their analysis considered several "thermoneutral" reactions, but did not provide generic rate rules. Since the concentration of allylic radicals in olefin pyrolysis could be higher than that of "normal" alkyl radicals (by ~1-2 orders of magnitude), the overall abstraction rate may compete with abstractions by "normal" radicals, thereby impacting the radical pool.

The objective of this work is to use electronic structure calculations to identify primary reaction pathways for the recombination, addition, and H-abstraction reactions involving allylic radicals. Since the addition and recombination reactions produce chemically-activated adducts,

we have systematically explored the pressure- and temperature-dependence of the overall rate constants as well as that for the multiple product channels. We describe a strategy for estimating the pressure-dependencies for systems where detailed electronic structure information is not available. We derive generic rate rules for hydrogen abstraction reactions from olefins and diolefins by methyl and allyl radicals. The intent is that this information will allow for self-consistent descriptions of the reactions of allylic radicals in pyrolysis and oxidation mechanisms. We anticipate that the inclusion of the rate constant estimates, although approximate, will provide sufficient accuracy to allow for a meaningful sensitivity analysis. If this sensitivity analysis indicates that some of the reactions are important for a particular modeling application, then specific rate constants can be examined in more detail to assess their accuracy.

2. THEORETICAL METHODS

Electronic structure calculations were carried out using the Gaussian 03 and 09 suite of programs[25, 26]. The CBS-QB3 composite method[27] was used to calculate optimized geometries, frequencies, and electronic energies for the lowest energy conformer of the reactants, products, and transition states for a variety of reactions. This method has been shown to predict heats of formation for a large test set of molecules with an accuracy of just over 1 kcal/mol[27]. Low frequency vibrational modes that resemble torsions around single bonds were treated as hindered internal rotors rather than as harmonic oscillators. Hindrance potentials were calculated at the B3LYP/6-31G(d) level of theory via relaxed surface scans with a step size of 10 degrees. Thermodynamic properties (e.g., $\Delta_f H_{298}$, S_{298}, and C_p values) were calculated using standard statistical mechanics methods. The electronic energy of each species was converted to its heat of formation using the atomization method. High-pressure rate constants were computed using canonical transition state theory (TST) with tunneling corrections based on asymmetric Eckart potentials.[28] Rate constants were fit to a modified Arrhenius form over a temperature range of 300-2500 K. The error in the activation energy is estimated to be ~1 kcal/mol, while the uncertainty in the pre-exponential factor is estimated to be a factor of ~2. This leads to an uncertainty of ~3 at 1000 K in the calculated rate coefficients. This uncertainty arises from errors such as variations in optimized reactant(s) and transition state geometries as

well as errors in the harmonic frequencies and hindered rotor calculations. More detailed descriptions can be found in earlier publications[29, 30].

Pressure- and temperature-dependent rate constants for the multiwell and multichannel potential energy surface (PES) were calculated based on a steady state analysis in which the energy-dependent unimolecular rate coefficients, k(E), were computed using Quantum-Rice-Ramsperger-Kassel (QRRK) theory. The density of states was calculated from three representative frequencies, which were extracted from an analysis of the CBS-QB3 heat capacity. Collisional stabilization rate constants were calculated using the modified strong collision (MSC)[31] assumption. More details of the methodology can be found in the work of Chang et al[32]. The Lennard-Jones collision diameters (σ_{LJ}) and well depths (ε_{LJ}) were estimated for adducts/isomers. For almost all of the QRRK/MSC calculations, the average energy transferred per collision for the collider N_2, $\langle\Delta E_{all}\rangle$, is assigned to be -440 cal/mol. The one exception is the calculation for allyl recombination for which the collider is Kr and $\langle\Delta E_{all}\rangle$ = -334 cal/mol. Although this approach is clearly more approximate than a Rice-Ramsperger-Kassel-Marcus (RRKM)/Master Equation approach, several previous studies have shown that it produce results with similar reliability[33-39]. Furthermore, because of the approximate nature of this approach, it can be used to efficiently generate results for large reaction mechanisms that often contain hundreds or even thousands of pressure dependent reactions.

In several places throughout the text, tables, and figures, we employ a chemical notation that omits the hydrogen atoms. For C_3 and larger species, the radical site is indicated by a bullet and a double bond by an equal sign. The units employed are kcal, sec, and mol.

3. RESULTS AND DISCUSSION

3.1 Recombination Reactions

The self-recombination of propargyl (C_3H_3) radicals is unusual in that the initially-formed linear adduct can isomerize via a series of relatively-low energy pathways to form benzene[10, 11]. In contrast, both experimental and theoretical studies of the self-recombination of allyl (C_3H_5) radicals concluded that the initial recombination product, 1,5-hexadiene, was the predominant

species formed[11, 12, 14] and there did not appear to be any evidence for a direct molecular cyclization pathway. The enthalpy changes (derived from group additivity) for the self and cross recombination reactions of allyl and methyl-allyl are shown below; the enthalpies of the various reactions are similar.

C=CC• + C=CC• ⇄ C=CCCC=C	ΔH_{298} = -61.4 kcal/mol	(1)
C=CC•C + C=CC•C ⇄ C=CC(C)C(C)C=C	ΔH_{298} = -60.2 kcal/mol	(2)
CC=CC• + CC=CC• ⇄ CC=CCCC=CC	ΔH_{298} = -61.3 kcal/mol	(3)
C=CC• + CC=CC• ⇄ C=CCCC=CC	ΔH_{298} = -61.7 kcal/mol	(4)
C=CC• + C=CC•C ⇄ C=CCC(C)C=C	ΔH_{298} = -60.8 kcal/mol	(5)

Several experimental studies have measured the rate constant for the recombination of two allyl radicals at the high pressure limit[11, 12, 14, 40, 41]. As shown in Figure 1, the measured values are quite consistent, and are higher than the Tsang recommendation[42]. The theoretical calculation by Georgievskii et al.[11] captures the magnitude of the rate constants, but has a more negative temperature dependence. For modeling efforts we propose a high-pressure value based on the experimental measurements:

$$k(T) = 1.12E13 * exp\left(\frac{306cal/mol}{RT}\right) cm^3/mol/s$$

Recently, Lynch et al.[43] investigated the recombination of allyl radicals, using krypton as the collider, at higher temperature where the falloff kinetics could be observed. Figure 2 compares the pressure- and temperature-dependent rate constants for the allyl recombination calculated using the above high-pressure value as input for a QRRK/MSC analysis with the measurements of Lynch et al.[43] Given the uncertainty associated with assignment of the energy transfer parameter ($\langle\Delta E_{all}\rangle$ = -334 cal/mol), the agreement with experiment is reasonable. Although the calculated fall-off is shifted to slightly higher temperatures, the impact of changing temperature and pressure is captured. Fall-off effects begin to become important above ~1000 K, even when the pressure is at 10 atm. The same approach was used to estimate the pressure- and temperature-

dependence for the self- or cross-recombination reactions of allyl and 1-methyl-allyl radicals. Figure 3 shows the predicted impact of temperature on the fall-off behavior. The necessity for accounting for fall-off effects at higher temperatures is apparent. The high pressure limit rate constants for forward and reverse reactions for the several similar recombination reactions (i.e., reactions (2)-(5) above), as well as the apparent rate constants over the temperature range of 300-2500 K and at pressures from 0.001-50 atm are listed the Supporting Information (Table S1).

To provide an effective route to MWG species formation, the recombination product needs to have a reaction pathway that can compete with the reverse reaction back to the reactants. One possibility is a direct molecular cyclization pathway, but there does not appear to be any literature evidence for such a reaction. Instead, radicals might abstract from the weaker allylic bond(s) in the recombination adduct to form another stabilized radical, which could then cyclize (in competition with β-scission of this radical). The cyclized radical could then form a stable cyclic product via β-scission of an H atom or an alkyl group. Ultimately, the cyclic products could then form aromatic species. This sequence of reactions is shown for the recombination of two allyl radicals in Figure 4. The sequential reactions and product distributions are different for the recombination between two methyl-allyl radicals or methyl-allyl and allyl, although they still lead to the formation of aromatic species. For example, the recombination between methyl-allyl and allyl forms cyclopentadiene, benzene, and toluene after H-atom abstraction. The reaction schematic for this reaction is shown in the Supporting Information (Figure S1).

The C_6H_9 PES is shown in Figure 5. Note that species (1) may be formed from H-atom abstraction of 1,5-hexadiene, which is the recombination product of two allyl radicals. This surface has previously been investigated by Sharma et al.[44] using the CBS-QB3 method; in subsequent work, Xu et al.[1] updated this surface by including the addition reaction of vinyl to 1,3-butadiene. The current calculations include the vinyl addition to 1,3-butadiene reaction (VII) and also a pathway leading to methylenecyclopentene + H (VI). In general, the results are consistent with those of Sharma et al.[44] and Xu et al.[1] As shown in Figure 5, the barriers for formation of the cyclic isomers (cyclohexen-4-yl (3) and cyclopentene-4-carbinyl (4)) are significantly lower than the other channels and these channels are expected to dominate at lower temperatures. As the

temperature increases, the 1,4 H-shift reaction forming (2) and the β-scission pathways from (3) forming the stable cyclic species, 1,3-cyclohexadiene +H (III) and 1,4-cyclohexadiene +H (IV), should become important, thus "locking in" the higher molecular weight species. These species, after subsequent H-abstraction and β-scission, can form benzene, as indicated in Figure 4.

The high-pressure rate constants calculated for this sequence of reactions were used in QRRK/MSC calculations to predict the pressure- and temperature-dependence for the various product channels. The results at 1 atm, shown in Figure 6, are consistent with the qualitative expectations based on the system energetics. The formation of the (collisionally-stabilized) cyclic radicals ((3) and (4)) dominates at the lower temperature range (i.e., T < 1000 K), while direct formation the β-scission products, vinyl + 1,3-butadiene (VII) and the cyclohexadiene isomers + H ((III) and (IV)) become more important at higher temperatures. Subsequent reactions of the cyclic radicals also need to be considered (e.g., H-atom abstraction by cyclohexene-4-yl (3) and cyclopentene-4-carbinyl (4) to form cyclohexene and methyl-cyclopentene, respectively). The rate constants for the various products of the C_6H_9 reaction sequence over the temperature range of 300-2500 K and pressures at 1 atm are listed in the Supporting Information (Table S3). Also provided are the high-pressure rate constants obtained from CBS-QB3 calculation that were used as input for the pressure-dependent analysis (Table S2).

3.2 Addition Reactions

An earlier analysis of ethane pyrolysis[1] demonstrated the importance of the addition reactions involving methyl and vinyl in the formation of MWG species. The increased concentration of allylic radicals in pyrolysis of C_3 and higher olefins is the motivation for considering addition reactions of these species in this work. In many reactions involving the addition of resonantly-stabilized radicals, the stability of the initially formed adduct is reduced due to the loss of resonance; this increases the likelihood that the adduct will simply re-dissociate, thereby not leading to the generation of MWG species. As a result, only certain such reactions are likely to be important in terms of MWG kinetics. In this section we consider several addition reactions involving allyl radicals that may be important.

Allyl Addition to Ethylene

The simplest resonantly stabilized radical addition reaction is the addition of allyl to ethylene, which is part of the C_5H_9 PES. A simplified version of this PES is shown in Figure 7; CBS-QB3 derived enthalpies are provided along with estimated values in parenthesis that will be discussed in Section 5. (A more complete version of this PES is provided in the Supporting Information in Figure S3.) It can be accessed either by allyl addition to ethylene (I), methyl addition to 1,3-butadiene (III), or H addition to either cyclopentene (II), 1,3-pentadiene (IV), 1,4-pentadiene (V), and methylene-cyclobutane (VI). Considering allyl addition to ethylene (I), once the initial adduct is formed the barriers to form cyclobutyl-carbinyl (4) and cyclopentyl (5) radicals are lower than that returning to reactants, although the pre-exponential factors will be smaller. The barrier for β-scission of cyclopentyl ((5) to (II)) is comparable to the reverse ring-opening reaction ((5) to (1)), and this leads to formation of cyclopentene and an H atom (II). Subsequent reactions of cyclopentene can lead to cyclo-1,3-pentadiene [45, 46], which is known to be an important intermediate in formation of even larger MWG species. However, the barrier for β-scission of cyclobutyl-carbinyl radical ((4) to (VI)) is much too high for this pathway to be significant. The H-atom shift reactions of the initially formed linear adduct to form other linear radicals ((1) to (2) and (1) to (3)) have higher barriers. In contrast to the allyl addition to ethylene (I), entering the surface from methyl addition to 1,3-butadiene (III) does not readily provide access to any of the lower energy exit channels. Although this channel is favored by a lower barrier and a deeper initial well (3), the subsequent reaction to form cyclopentene is inhibited by the higher isomerization barrier ((3) to (1)).

Our calculated high pressure limit rate constant for addition of allyl to ethylene at 1000 K is about 60% higher than that calculated by Sabbe et al.[47] The calculated high pressure limit rate constant for methyl addition to 1,3-butadiene is similar (within 10%) to that calculated by Sabbe et al.[47] The calculated rate constant at 1 atm for the formation of cyclopentene + H from the addition of allyl to ethylene is in reasonable agreement with the experimental observations of Sakai and Nohara[48], as shown in the Supporting Information (Figure S4). The high-pressure rate constants for the reactions on the C_5H_9 surface are included in the Supporting Information (Table

S4), with the values at 1 atm listed in Table S5. The predictions also qualitatively agree with an earlier experimental observation by Bryce and Ruzicka[49], in which cyclopentene is the dominant product.

Figure 8 shows the predicted rate constants for the major product channels at 1 atm when entering the PES via addition of allyl to ethylene (reaction (I) to (1) in Figure 7). The high pressure rate constant (k_∞) is also plotted. At low temperatures, formation of the initial adduct, C=CCCC• (1), is dominant. As the temperature increases, fall-off is evident since more of the adduct goes back to reactants, as indicated by the increasing difference between k_{total} and k_∞. The formation of cyclopentene + H (II) also become increasingly important. Channel (II) is significantly important because it not only leads to the formation of a stable MWG species, but it effectively converts allyl radical to a reactive H-atom. The rate constant for formation of cyclobutyl-carbinyl radical (4) is relatively low since it can easily dissociate back to (1).

Figure 9 shows the predictions for methyl addition to the terminal carbon in 1,3-butadiene ((III) to (3) in Figure 7). Here the addition rate is much faster than that of allyl + ethylene, and the deeper well means that dissociation back to the reactants is not so important at the lower temperatures. In spite of the higher addition rate constant, the formation of cyclic species is predicted to be much lower than that for allyl addition over the entire temperature range. This results from the high barrier associated with isomerization to a linear species (1) that can then cyclize. Formation of the initial, resonantly stabilized adduct (3) dominates at lower temperatures. At higher temperatures, the formation of 1,3-pentadiene and H (IV) is important, followed by the formation of allyl and ethylene (I).

The differences between the addition of allylic and alkyl radicals can be seen by comparing the C_5H_{11} PES for n-propyl addition to ethylene (Figure 10) to that for allyl addition to ethylene (Figure 7). Similar to the methyl addition to 1,3-butadiene ((III) to (3)), the entrance channel of the C_5H_9 PES, n-propyl addition to ethylene ((I) to (1)), has a lower barrier and a deeper initial well (1), which means that the addition rate will be faster with slower dissociation back to the reactants for propyl addition than for allyl addition. The high-pressure rate constants and the rate constants for the various channels at 1 atm are listed in the Supporting Information (Tables

S6 and S7, respectively). Figure 11 shows the predicted rate constants at 1 atm for the reactions on this PES. The rate of product formation is much higher for this system than for the analogous allyl addition. However, note that no cyclic compounds are formed by propyl addition since there is no double bond in the adduct to allow for ring closure. The channels that lead to MWG species (channels (III) and (IV)) are unimportant since the initial adduct must undergo a high energy H-atom shift ((1) to (3)) prior to β-scission. The major bimolecular product is ethyl + propene (II). A subsequent H-atom abstraction from propene to form allyl is needed to initiate MWG kinetics. Thus in olefin pyrolysis there are two factors that lead to enhanced MWG species formation: (1) Higher concentrations of allylic radicals, thus offsetting the slower addition rates, and (2) Presence of a double bond in the stabilized radical to allow for cyclization. These cyclic species ultimately may then be converted to aromatic species.

These addition reactions are also important for the formation of larger polycyclic aromatic hydrocarbons (PAH). Wornat and co-workers[50] investigated the growth mechanisms of PAHs that lead to the formation of solids by performing supercritical pyrolysis experiments with n-decane, a model alkane fuel. 2-methylnaphthalene and 1-methylnaphthalene were each added as a dopant to provide a resonantly-stabilized radical source. The PAH product analysis indicated that stabilized radical addition to ethylene was the starting point for subsequent addition to various olefins, leading to formation of MWG species.

Allyl Addition to 1,3-Butadiene

Allyl addition to the terminal carbon in 1,3-butadiene introduces another factor that can promote the formation of MWG species. In this instance the initially-formed linear adduct is itself resonantly-stabilized, leading to a deeper well than in the case of allyl addition to ethylene. Figure 12 shows the simplified C_7H_{11} PES of allyl addition to 1,3-butadiene ((I) to (1)). The barrier for the addition is lower than that for addition to ethylene (7.5 kcal/mol versus 12.1 kcal/mol). Once the initial adduct is formed, it can isomerize to form a linear stabilized radical (2) or cyclize to form (10), (11), and (12). The resonantly stabilized (2) can readily isomerize into the cyclic radical (3) that can form 1,4-cyclohexadiene and methyl (II) via β-scission. There are multiple exit channels that are lower in energy than the entrance barrier on this PES (indicated by the dotted line).

Therefore, once the initial adduct is formed, isomerization, cyclization, and formation of a stable ring compounds via β-scissions are energetically favored. Allyl addition to 1,3-butadiene can lead to the formation of five-, six- and seven-member ring species: cyclopentadiene (III), methyl-cyclopentadiene (IV), and 1,4-cyclohexadiene (II), 4-methylene-cyclohexene (VII), vinyl-cyclopentene isomers (VIII and IX), and 1,4-cycloheptadiene (X). An interesting feature for the isomerization reactions involving an allylic radical is that the predicted barriers are higher than that of an alkyl or alkenyl radical by ~8-12 kcal/mol. One such comparison is the formation of a cyclic 5-member ring radical in Figure 12 (e.g., (1) to (11)) with a barrier of ~23 kcal/mol to the similar reaction forming a cyclic radical in Figure 7 (e.g., (1) to (5)) with an ~15 kcal/mol barrier.

Figure 13 shows the predicted apparent rate constants for the product channels resulting from the addition of allyl to 1,3-butadiene at 1 atm. Formation of the initially-stabilized linear adduct (1) is dominant over the entire temperature range, with much lower production of other stabilized adducts ((2) and (4)). At higher temperatures, chemically-activated product channels, first 1,4-cyclohexadiene and methyl (II), followed by 4-methylene-cyclohexene and H atom (VII) and vinyl-cyclopentene isomers and H atoms ((VIII) and (IX)), begin to contribute. The rate constants for the various products of this reaction sequence over the temperature range of 300-2500 K and pressure at 1 atm are listed in the Supporting Information (Table S9) along with the high pressure values that were used as input for this analysis (Table S8). A comparison of the product predictions for allyl addition to butadiene versus ethylene reveals similar rate constants for the production of cyclic species, although for different reasons. The total rate constant is larger for addition to butadiene, reflecting the lower entrance channel barrier. But the branching ratio for cyclic formation is higher for addition to ethylene, such that the rate constant for cyclic formation is comparable for both systems.

These predictions can be compared to the experiments of Nohara and Sakai[51], who studied the pyrolysis of diallyl oxalate in the presence of butadiene at 430-510 ^{o}C under atmospheric pressure. Diallyl oxalate dissociates rapidly to form allyl and its reaction with butadiene produces cyclopentadiene, cyclohexadiene, benzene, and several unidentified C_7 hydrocarbons, consistent with the above analysis.

3.3 Hydrogen Abstraction Reactions

In general, hydrogen abstractions by allylic radicals from alkanes are slow since these reactions are endothermic by 8-15 kcal/mol. Rate rules have previously been generated by analysis of a series of electronic structure calculations for such reactions[52-54]. In contrast, H-atom abstractions from olefins will often be close to thermoneutral if another resonantly-stabilized radical is formed. Recently, Sabbe et al.[24] employed electronic structure calculations to investigate the influence of resonance stabilization on the kinetics of hydrogen abstraction reactions. Their analysis considered several such approximately thermoneutral reactions, but did not generate generic rate rules. In this study, CBS-QB3 calculations have been performed to investigate a series of H-atom abstraction reactions at the allylic position of a variety of alkenes and dienes by allyl and methyl radicals. In addition to being a basis for comparison, analysis of the abstractions by methyl serves two purposes: (1) Much more information is available on such abstractions, thus providing an important validation check, (2) H-atom abstraction from olefins by methyl may generate allylic radicals, so additional information about such systems provides greater confidence in the rate constant assignments for these reactions. Our results are used to derive rate rules that can be readily incorporated into kinetic mechanisms.

The abstraction of an H-atom from an allylic site of an alkene or diene by a methyl radical is more exothermic than abstraction of an H-atom from an alkane, so it is not clear whether the extrapolation of the rate estimation rules developed for normal C-H groups to allylic C-H abstractions is appropriate. In this study, we address this issue by developing a complete set of rate rules that account for the effects of ring structure, nature of the allylic C-H site (primary, secondary, or tertiary), and extent of resonance stabilization (allylic versus more extended resonance). Table 1 presents the results for a series of H-atom abstraction reactions by methyl. Note that the pre-exponential factors are normalized to reflect the number of degenerate hydrogen atoms at the abstraction site. In the modified Arrhenius fits, the value of $n \sim 3$ means that all of these abstraction reactions have very significant upward curvature on an Arrhenius plot. Thus, the use of the modified Arrhenius form is essential to properly describe the temperature dependence. Nevertheless, simple Arrhenius parameters were evaluated (using E_a

= $E + nRT$ and $A_H' = k/Exp(-E_a/RT)$) at T = 1000 K to allow for a more straightforward comparison of the rate expressions. Inspection of these results reveals the following: (1) Within each subgroup, both the modified and simple forms of the Arrhenius expressions for each reaction are quite similar, as reflected in the standard deviations, with no apparent correlation to the structure of the olefin within the subset. Rate rules have been developed for each subset by averaging the individual rate constants within the subset at a given temperature and then fitting the data from 300 to 2500 K to a modified Arrhenius form. These rules can predict the individual rate constants to within a factor of 2 at 1000 K for almost all of the reactions calculated. (2) In general, the more exothermic reactions have lower activation energies. (3) The pre-exponential factors (per H) for all of the subgroups are quite similar, within a factor of 3, with the higher values for the cyclic species. (4) The higher rate constants for formation of cyclic radicals, when compared to their linear counterparts with similar exothermicities, is due to the combination of a higher pre-exponential factor and a lower barrier. (5) Although reactions involving species with a conjugated double bond are more exothermic than those of simple alkenes, the rate constants at 1000 K are only slightly larger, with the lower barriers offset by lower pre-exponential factors.

One complication that arises in application of the rate rules is due to small differences between the reaction enthalpies (~1.5 kcal/mol) and entropies (~1.5 cal/mol-K) obtained from the CBS-QB3 results and those derived from group additivity (e.g., using THERM[55]). This issue has been recognized previously[1]. Thus, the use of the rate rules developed in conjunction with equilibrium constants that are derived from group additivity would yield incorrect values for the reverse rate constants. To address this issue, we include in Table 1 the average equilibrium constant for each subset that is obtained from the ratio of forward and reverse CBS-QB3 rate constants. These fits should be used to obtain the rate rule for the reverse rate constants for each subset. A table listing the reverse rate constants for the reactions in Table 1 is included in the Supporting Information (Table S10).

Several groups have investigated the H-atom abstraction reaction of propene by methyl. Baldwin et al.[56] measured the rate constant at 480 ^{o}C. Miyoshi and Brinton[57] and Cvetanović and Irwin[58] measured rate constants over the range 100-170 ^{o}C and 80-180 ^{o}C, respectively. Kinsman

and Roscoe[59] measured rate constants during the photolysis of mixtures of acetone and propene from 300 to 580 K. Reviews by Warnatz[60] and Tsang[42] recommended rate parameters over the temperature range of 300-2500 K. Hidaka et al.[61] estimated a rate constants for modeling propene pyrolysis in shock tube experiments over the range 1200-1800 K. Sabbe et al.[24] performed ab initio calculations for this reaction. Figure 14 compares these values with the results of this study. The agreement of the present calculations with the earlier work is encouraging.

H-atom abstraction reactions of olefins by allylic radicals are predicted to be significantly slower than those by alkyl radicals. Table 2 compares the results for H-atom abstractions by allyl to those by methyl. The rate constants are shown in both modified and normal Arrhenius forms. The large values of *n* again signifies substantial upward curvature on an Arrhenius plot; thus the modified Arrhenius fits should be used in modeling studies. The normalized pre-exponential factors for H-atom abstraction by allyl are comparable to those by methyl; however, the activation energies are ~8 kcal/mol higher, leading to significantly smaller rate constants. It is interesting to note that this increase in activation energy is similar to that observed above for isomerization of allylic versus alkyl radicals. An analysis of a large series of H-atom abstraction by allyl reactions from the allylic sites of a variety of olefins (shown in Table 3) suggests that it is possible to develop a series of rate rules for these subsets as well. Again the average CBS-QB3 derived equilibrium constant for each subset is provided. The corresponding reverse rate constants are provided in the Supporting Information (Table S11).

There are several studies that have considered abstraction by resonantly-stabilized radicals. Glaude et al.[62] and Dente et al.[63] estimated rate rules. The Livermore mechanism[64] describing iso-octane oxidation and ignition estimate the rate constants by analogy to normal H-abstractions, with E_a ~12 kcal/mol for a thermoneutral reaction and a decreased pre-exponential factor. Recently, Sabbe et al.[24] employed electronic structure calculations to examine these reactions. Figure 15 compares the rate constant for hydrogen abstraction from 1-butene by allyl that is calculated in this study to these earlier results. A few points deserve comment: (1) The rate rule developed in this work is very consistent with our specific calculated result for this

reaction. (2) The calculated rate constant agrees very well with that by Sabbe et al.[24] (3) The earlier estimates differ significantly from those predicted by electronic structure calculations, most notably in terms of not accounting for upward curvature in the Arrhenius plots. The rate constants obtained in this study and that of Sabbe et al.[24] suggest that abstraction reactions by resonantly-stabilized radicals may be substantially more important in high temperature systems than previously thought. One consequence is that the distribution of such radicals in these systems could be shifted more readily, thereby changing the relative distribution. Given the importance of these species in terms of the formation of MWG species, this redistribution has the potential to affect the various MWG pathways (e.g., the recombination and addition reactions that are discussed above).

The activation energies shown in Tables 1 and 3 vary over a very broad range and correlate with the enthalpy change of the reaction (e.g., the more exothermic reactions have lower activation energies). Figure 16 illustrates that the results are consistent with an Evans-Polanyi correlation[65]. Though there is significant scatter, the same Evans-Polanyi relationship can be observed for abstraction by both methyl and allyl. An important caveat is that this particular correlation was developed using activation energies computed at 1000 K. The substantial non-Arrhenius behavior of these abstraction reactions implies that the Evans-Polanyi parameters will change significantly at different temperatures.

4. COMPETITION BETWEEN ADDITION AND H-ABSTRACTION REACTIONS

When a radical encounters an olefin, it can either add to the double bond or abstract a hydrogen atom from the olefin (the allylic site is lowest energy abstraction pathway). Given the high concentration of both allylic radicals and olefins in alkene pyrolysis, we examined several reactions of allyl radicals with selected olefins to determine the branching ratio for these two competing channels. Table 4 compares the CBS-QB3 predictions for these reactions. With the notable exception of ethylene, where abstraction is much slower due to the very strong vinylic C-H bond, it is seen that addition and abstraction are generally comparable at temperatures ranging from 500 K to 1500 K. At lower temperatures, the addition reactions dominate due to

their lower activation energies. Thus there is substantial potential for allylic radicals to participate in addition reactions, which can lead to MWG species formation, in this temperature range.

5. APPROXIMATE METHOD TO ANALYZE THE PRESSURE-DEPENDENT REACTIONS

Among the three types of reactions discussed above, the recombination and addition reactions are pressure-dependent. While generic rate rules could be derived for the H-abstraction reactions and estimated high pressure rate rules are also available for the recombination reactions, the addition reactions are much more complicated, with the possibility of subsequent isomerization, cyclization, and β-scission reactions. As discussed above, the individual reactions can be analyzed in terms of initially constructing a PES based on relatively high-level theoretical methods. However this detailed analysis is time consuming and indeed impractical for reactions of larger species. An alternative approach is to estimate the high pressure limit rate constants for the various unimolecular reactions that are expected to occur and use these as input for a QRRK/MSC analysis to estimate the pressure- and temperature-dependent rate constants.

Several previous studies have provided a detailed discussion of rate constant estimation methods[35, 66, 67]. There has also been several studies devoted to determining theoretically based rate estimation rules for a variety of reaction types that are relevant to combustion and/or pyrolysis[29, 30, 36, 68]. Specifically related to the reactions of interest in this study are high-pressure rate rules for β-scission/radical addition[42, 69], H-atom abstraction[47, 70], H-atom shift [71, 72], and cycloaddition reactions[72, 73]. Recently, we systematically investigated the intramolecular H-atom shift reactions of alkyl radicals and cycloaddition reactions of alkenyl radicals at the CBS-QB3 level of theory and used these results to develop reactivity-structure based rate estimation rules for these two types of reactions[72]. The barriers for these two intramolecular reactions are estimated according to the Benson model[74] via the expression: $E_a = E_{bimolecular} + E_{strain}$. The first term, $E_{bimolecular}$, is based on what the barrier would be if the reaction were a bimolecular abstraction or addition reaction; this estimate explicitly accounts for the reaction enthalpy. The second term, E_{strain}, accounts for the ring strain in the transition state. The pre-exponential factors are

estimated by accounting for the change in entropy (i.e., due to the loss of hindered rotors in the transition state). Quantitative relationships between the pre-exponential factors and rotor loss were derived for the H-shift isomerization and cycloaddition reactions. The enthalpies of the reactants, products, and adducts were calculated by group additivity (using THERM[55]).

This approach is applied to the C_5H_9 PES (allyl addition to ethylene) to generate an approximate version. The estimated enthalpies at 298 K are shown in parenthesis in Figure 7. The activation energy for the 1,2-H shift reaction ((1) to (2)) was estimated from the sum of the analogous bimolecular reaction of ethyl radical abstracting a secondary H-atom from propane, in which $E_{bimolecular}$ = 11.8 kcal/mol, and E_{strain} = 25.9 kcal/mol to account for the three-membered ring transition state. Similarly, the barrier for the 1,3-H shift ((1) to (3)) was estimated from the reaction of ethyl abstracting an allylic H from 1-butene, with $E_{bimolecular}$ = 7.9 kcal/mol, and E_{strain} = 24.1 kcal/mol to account for the four-member ring transition state. The barrier for the endo-cyclization reaction ((1) to (5)) was estimated from the analogous addition reaction of ethyl plus propene to form 2-pentyl radical ($E_{bimolecular}$ = ~7.0 kcal/mol) [42] plus E_{strain} = 8.2 kcal/mol to account for the five-membered ring transition state. For the exo-cyclization reaction ((1) to (4)), the analogous addition reaction was ethyl plus propene to form 2-methyl-1-butyl radical ($E_{bimolecular}$ = ~7.9 kcal/mol) [42] with E_{strain} = 6.7 kcal/mol to account for the four-membered ring transition state. The barriers for the entrance and exit channel addition reactions are estimated from similar reactions in the literature[36, 42, 69]. In each case, the rate parameters for the reverse reactions were obtained from the estimated rate parameters for the forward reaction and the group additivity based equilibrium constant. These estimated rate parameters are provided in the Supporting Information (Table S4).

A comparison of the estimated and CBS-QB3 enthalpies for the stable species in Figure 7 indicates that generally the group additivity enthalpies are lower than the CBS-QB3 values. Similarly, the estimated transition state enthalpies are lower, meaning that barriers are quite similar. However, note that reverse reaction ((5) to (1)) is ~1.9 kcal/mol higher on the CBS-QB3 surface than on the estimated one. Additionally, the calculated barrier for β-scission of the 1-hexen-5-yl radical back to the reactants ((1) to (I)) is lower than the estimated one by ~2.6

kcal/mol. Thus, one might expect to see more of (I) converted to (5) on the estimated surface. The predicted rate constants that are based on the estimated values at 1 atm are compared to those obtained from CBS-QB3 calculations in Figure 17. At lower temperatures, the formation of adduct (1) is predicted to be dominant by both approaches. At lower temperatures, the difference in the two predictions is due to the different values for k_∞ for the C=CC• + C_2H_4 entrance channel (I). At higher temperatures the differences are primarily due to the deeper estimated well (1) which results in less re-dissociation out of the entrance channel and a more rapid decrease in the rate constant for formation of (5) on the estimated surface, consistent with the difference in barriers discussed above. Fortunately, the difference in (5) occurs where this channel is only a minor contributor to the overall rate. Overall, the approximate surface yields results that are reasonably consistent with the more rigorous treatment.

Another comparison considers entering the same PES surface via the addition of methyl to butadiene. The predictions at 1 atm using the two surfaces are shown in Figure 18. Both surfaces predict that adduct (3) is dominant over the entire temperature range. As discussed above, the deep well combined with much higher energy exit channels preclude formation of other products. Although the CBS-QB3 barriers for methyl addition to 1,3-butadiene ((III) to (3)) and H addition to 1,3-pentadiene ((IV) to (3)) are lower than the estimated ones, the initial well depth is similar for both surfaces. Thus, one can expect that the formation of (IV) from the calculated surface would be faster than that from the estimated surface. The rate constants in Figure 18 confirm this expectation. The rate estimate method was also applied to the other cases discussed above (i.e., the C_6H_9 and C_5H_{11} PESs). Good agreement was observed for these cases; these results are provided in the Supporting Information (Figures S2 and S5/S6, respectively).

The above comparisons suggest that the approach of estimating the high-pressure rate constants as input parameters for a chemical activation analysis can provide a reasonable starting point for rate constant assignments. It allows the modeler to estimate rate constants for various reactions when it is not feasible to perform high-level calculations. One expects that these estimates will at least be sufficiently accurate such that a subsequent sensitivity analysis of the mechanism will properly identify the importance of the reactions. If a particular reaction turns

out to be significant, it might then warrant additional attention. In any event, these estimated values allow for reactions to be incorporated into the mechanism that might otherwise not be included.

We now provide a final example using the estimation technique for a reaction that is an important pathway to form MWG species. Figure 19 shows the C_6H_{11} PES for the addition of 1-methyl-allyl, including two resonance structures C=CC•C and CC=CC•, to ethylene. The estimated high pressure rate parameters were obtained as described above and are provided in the Supporting Information (Table S12) with the values at 1 atm listed in Table S13. Similar to allyl addition to ethylene (Figure 7), isomerization of (1) to (6), which can then lead to the formation of CH_3 + cyclopentene (III), can compete with dissociation back to the entrance channel (I). Thus, we expect the formation of the cyclic species to be significant. The predicted pressure-dependent rate constants at 1 atm (shown in Figure 20) confirm this expectation. While stabilization to form (1) dominates over the investigated temperature range, at higher temperatures a significant fraction of the reactants are converted to cyclopentene + CH_3 (III) and to 1,3-butadiene + C_2H_5 (VIII). As discussed above, the subsequent addition of allylic radicals to 1,3-butadiene provides an additional pathway for the formation of MWG species.

6. SUMMARY AND CONCLUSIONS

The objective of this study is to characterize the kinetics of allylic radicals and understand their role in promoting the formation of molecular weight growth (MWG) species during alkane and alkene pyrolysis. Three important reaction types, recombination, addition, and hydrogen abstraction, were studied. A high pressure limit rate constant for the recombination of two allyl radicals was assigned on the basis of experimental data. We then applied this high-pressure value to the recombination of other allylic radicals. Following recombination, a subsequent H-atom abstraction reaction is needed before cyclization can occur. Thus, this pathway to MWG species formation is only expected to become important at high pressures and lower temperatures (where there is a shift in the equilibrium toward the recombination product). Under conditions that favor the subsequent abstraction (i.e., higher pressures), multiple reaction pathways that

can lead to the formation of MWG species were identified. The high-pressure rate constants were used as the basis for estimating temperature- and pressure-dependent rate constants.

The addition of allylic radicals to olefins can also lead to the formation of MWG species. The PES for allyl addition to ethylene indicates that once the initial adduct is formed, it is energetically more favorable to form cyclopentyl radical than it is to dissociate back to reactants. The barrier for β-scission of cyclopentyl to form cyclopentene + H is comparable to the reverse ring-opening reaction. The double bond within the allyl radical is essential to allow formation of cyclic species that can then react to ultimately form aromatic species. Similarly, the addition of allyl to 1,3-butadiene will lead to the formation of C_5-C_7 cyclic species; the pathways forming MWG species are favored by a lower entrance barrier, a deeper initial well, and low energy exit channels. The high-pressure CBS-QB3 rate constants were used to estimate the temperature- and pressure-dependent rate constants.

Rate rules for H-atom abstraction reactions were developed by calculating a series of rate constants for abstraction by methyl and allyl from a variety of olefins and dienes at the allylic site and grouping the results into appropriate subsets. The reactions exhibit highly non-Arrhenius temperature dependences. However, by evaluating the modified Arrhenius activation energy at a particular temperature, the activation energies were shown to follow an Evans-Polanyi correlation over a wide range of reaction enthalpies. These rate rules, combined with previously developed rate rules for radical addition, isomerization, and cyclization reactions allow for rate constants for to be readily incorporated into kinetic mechanisms. The latter three provide the means to estimate an approximate PES for those systems where high-level electronic structure calculations are not feasible. This approach provides a straightforward way to assign reasonable estimates for the temperature- and pressure-dependence for chemically-activated addition and recombination reactions that can be included in pyrolysis and combustion kinetic models.

Acknowledgements

We thank Dr. Hans-Heinrich Carstensen at Ghent University for helpful discussions. This work was supported by the Petroleum Institute and the National Advanced Biofuels Consortium.

Supporting Information Available: Additional tables and figures are available in the Supporting Information. This material is available free of charge via the Internet at http://pubs.RSC.uk.

Author Information

Corresponding Author: *E-mail: amdean@mines.edu.

References

1 C. Xu, A. S. Al Shoaibi, C. G. Wang, H.-H. Carstensen, and A. M. Dean, *J. Phys. Chem. A,* 2011, **115**, 10470-10490.

2 O. Park, P. S. Veloo and F. N. Egolfopoulos, *Proc. Combust. Inst.,* 2013, **34**, 711-718.

3 C. K. Westbrook and W. J. Pitz, *Comb. Sci. Tech.,* 1984, **37**, 117-152.

4 P. Dagaut, M. Cathonnet, and J.-C. Boettner, *Int. J. Chem. Kinet.,* 1992, **24**, 813-837.

5 P. Dagaut, M. Reuillon, and M. Cathonnet, *Comb. Sci. Tech.,* 1993, **95**, 233-260.

6 H. J. Curran, P. Gaffuri, W. J. Pitz and C. K. Westbrook, *Combust. Flame,* 2002, **129**, 253-280.

7 R. X. Fernandes, H. Hippler, and M. Olzmann, *Proc. Combust. Inst.,* 2005, **30**, 1033-1038.

8 R. S. Tranter, X. L. Yang, and J. H. Kiefer, *Proc. Combust. Inst.*, 2011, **33**, 259-265.

9 J. A. Miller and C. F. Melius, *Combust. Flame,* 1992, **91**, 21-39.

10 J. A. Miller and S. J. Klippenstein, *J. Phys. Chem. A*, 2003, **107**, 7783-7799.

11 Y. Georgievskii, J. A. Miller, and S. J. Klippenstein, *Phys. Chem. Chem. Phys.,* 2007, **9**, 4259-4268.

12 T. M. Selby, G. Meloni, F. Goulay, S. R. Leone, A. Fahr, C. A. Taatjes and D. L. Osborn, *J. Phys. Chem. A*, 2008, **112**, 9366-9373.

13 J. A. Miller, S. J. Klippenstein, Y. Georgievskii, L. B. Harding, W. D. Allen and A. C. Simmonett, *J. Phys. Chem. A*, 2010, **114**, 4881-4890.

14 A. Matsugi, K. Suma and A. Miyoshi, *J. Phys. Chem. A*, 2011, **115**, 7610-7624.

15 A. M. Dean, *J. Phys. Chem.* 1990, **94**, 1432-1439.

16 C. F. Melius, M. E. Colvin, N. M. Marinov, W. J. Pitz and S. M. Senkan, *Proc. Combust. Inst.,* 1996, **26**, 685-692.

17 N. M. Marinov, W. J. Pitz, C. K. Westbrook, A. M. Vincitore, M. J. Castaldi and S. M. Senkan, *Combust. Flame,* 1998, **114**, 192-213.

18 P. Lindstedt, L. Maurice and M. Meyer, *Faraday Discuss.,* 2002, **119**, 409-432.

19 A. M. Mebel and V. V. Kislov, *J. Phys. Chem. A*, 2009, **113**, 9825-9833.

20 C. Cavallotti and D. Polino, *Proc. Combust. Inst.,* 2013, **34**, 557-564.

21 A. Matsugi and A. Miyoshi, *Int. J. Chem. Kinet.,* 2012, **44**, 206-218.

22 I. Ziegler, R. Fournet and P. M. Marquaire, *J. Anal. Appl. Pyrolysis,* 2005, **73**, 212-230.

23 X. Zhong and J. W. Bozzelli, *J. Phys. Chem. A,* 1998, **102**, 3537-3555.

24 M. K. Sabbe, A. G. Vandeputte, M.-F. Reyniers, M. Waroquier and G. B. Marin, *Phys. Chem. Chem. Phys.*, 2010, **12**, 1278-1298.

25 M. J. Frisch, G. W. Trucks, H. B. Schlegel, G. E. Scuseria, M. A. Robb, J. R. Cheeseman, J. A., Jr. Montgomery, T. Vreven, K. N. Kudin and J. C. Burant, et al., Gaussian 03, Revision A. 1, Gaussian, Inc: Pittsburgh, PA, 2003

26 M. J. Frisch, G. W. Trucks, H. B. Schlegel, G. E. Scuseria, M. A. Robb, J. R. Cheeseman, G. Scalmani, V. Barone, B. Mennucci and G. A. Petersson, et al., Gaussian 09, Revision A. 1, Gaussian, Inc: Wallingford, CT, 2009

27 J. J. A. Montgomery, M. J. Frisch, J. W. Ochterski and G. A. Petersson, *J. Chem. Phys.*, 2000, **112**, 6532-6542.

28 C. Eckart, *Phys. Rev.*, 1930, **35**, 1303-1309.

29 S. M. Villano, L. K. Huynh, H.-H. Carstensen and A. M. Dean, *J. Phys. Chem. A*, 2011, **115**, 13425-13442.

30 S. M. Villano, L. K. Huynh, H.-H. Carstensen and A. M. Dean, *J. Phys. Chem. A*, 2012, **116**, 5068-5089.

31 J. Troe, *Ber. Bunsen-Ges. Phys. Chem.*, 1983, **87**, 161-169.

32 A. Y. Chang, J. W. Bozzelli and A. M. Dean, *Z. Phys. Chem.*, 2000, **214**, 1533-1568.

33 C. Sheng, Ph.D. Dissertation, New Jersey Institute of Technology, 2002.

34 H. Richter and J. B. Howard, *Phys. Chem. Chem. Phys.*, 2002, **4**, 2038-2055

35 D. M. Matheu, W. H., Jr. Green and J. M. Grenda, *Int. J. Chem. Kinet.*, 2003, **35**, 95-119.

36 H.-H. Carstensen and A. M. Dean, In *Comprehensive Chemical Kinetics*; ed. R. Carr, Elsevier: New York, 2007, **42**, 105-187.

37 H.-H. Carstensen and A. M. Dean, *Int. J. Chem. Kinet.*, 2011, **44**, 75-89.

38 S. M. Villano, H.-H. Carstensen and A. M. Dean, *J. Phys. Chem. A*, 2013, **117**, 6458-6473.

39 K. P. Somers, Ph.D. Dissertation, National University of Ireland, Galway, 2014.

40 M. E. Jenkin, T. P. Murrells, S. J. Shalliker and G. D. J. Hayman, *Chem. Soc. Faraday Trans.*, 1993, **89**, 433-446.

41 A. A. Boyd, B. Noziere and R. Lesclaux, *J. Phys. Chem.*, 1995, **99**, 10815-10823.

42 W. Tsang, *J. Phys. Chem. Ref. Data*, 1991, **20**, 221-273.

43 P. T. Lynch, C. J. Annesley, C. J. Aul, X. L. Yang and R. S. Tranter, *J. Phys. Chem. A*, 2013, **117**, 4750-4761.

44 S. Sharma, M. R. Harper and W. H. Green, *Combust. Flame*, 2010, **157**, 1331-1345.

45 D. K. Lewis, J. Bergmann, R. Manjoney, R. Paddock, B. L. Kaira, *J. Phys. Chem.*, 1984, **88**, 4112-4116.

46 S. F. Rickborn, D. S. Rogers, M. A. Ring, H. E. O'Neal, *J. Phys. Chem.*, 1986, **90**, 408-414.

47 M. K. Sabbe, M.-F. Reyniers, V. V. Speybroeck, M. Waroquier and G. B. Marin, *Chem. Phys. Chem.*, 2008, **9**, 124-140.

48 T. Sakai, D. Nohara and T. Kunugi, In *Ind. Lab. Pyrolysis* 1986**,** ch. **10**, pp. 152-177.

49 W. A. Bryce and D. J. Ruzicka, *Can. J. Phys.*, 1960, **38**, 835-844.

50 S. V. Kalpathy, N. B. Poddar, S. P. Bagley and Wornat M. J., *Proc. Combust. Inst.*, 2014, http://dx.doi.org/10.1016/j.proci.2014.06.129

51 D. Nohara and T. Sakai, *Ind. Eng. Chem. Res.*, 1988, **27**, 1925-1929.

52 R. Sumathi, H.-H. Carstensen and W. H. Jr Green, *J. Phys. Chem. A*, 2001, **105**, 6910-6925.

53 N. Kungwan and T. N. Truong, *J. Phys. Chem. A*, 2005, **109,** 7742-7750.

54 H.-H. Carstensen and A. M. Dean, *J. Phys. Chem. A*, 2009, **113**, 367-380.

55 C. J. Chen and J. W. Bozzelli, *J. Phys. Chem. A*, 2000, **104**, 4997-5012.

56 R. R. Baldwin, A. Keen and R. W. Walker, *J. Chem. Soc. Faraday Trans. 2.*, 1987, **83**, 759-766.

57 M. Miyoshi and R. K. Brinton, *J. Chem. Phy.*, 1962, **32**, 3019-3030.

58 R. J. Cvetanović and R. S. Irwin, *J. Chem. Phy.*, 1967, **46**, 1694-1702.

59 A. C. Kinsman and J. M. Roscoe, *Int. J. Chem. Kinet.*, 1994, **26**, 191-200.

60 J. Warnatz, in *Combustion Chemistry*, ed. W. C. Jr Gardiner, Springer Verlag, New York, 1984, ch. **5**, 197-360.

61 Y. Hidaka, T. Nakamura, H. Tanaka, A. Jinno and H. Kawano, *Int. J. Chem. Kinet.,* 1992, **24**, 761-780.

62 P. A. Glaude, R. Fournet and V. Warth, *Ind. Eng. Chem. Res.*, 2005, **44**, 4212-4220.

63 M. Dente, G. Bozzano, T. Faravelli, A. Marongiu, S. Pierucci and E. Ranzi, In *Advances in Chemical Engineering.* 2007, **32**, 51-166.

64 H. J. Curran, P. Gaffuri, W. J. Pitz and C. K. Westbrook, *Combust. Flame,* 1998*,* **114**, 149-177.

65 M. G. Evans and M. Polanyi, *Trans. Faraday Soc.*, 1938, **34**, 11-24.

66 H. J. Curran, P. Gaffuri, W. J. Pitz and C. K. Westbrook, *Combust. Flame*, 2002, **129**, 253-280.

67 P. A. Glaude, V. Conraud, R. Fournet, F. Battin-Leclerc, G. M. Come, G. Scacchi, P. Dagaut and M. Cathonnet, *Energy Fuels*, 2002**, 16**, 1186-1195.

68 A. Miyoshi, *J. Phys. Chem. A*, 2011, **115**, 3301-3325.

69 M. Saeys, M.-F. Reyniers, G. B. Marin, V. V. Speybroeck and M. Waroquier, *AIChE J.*, 2004, **50**, 426-444.

70 M. Saeys, M.-F. Reyniers, V. V. Speybroeck, M. Waroquier and G. B. Marin, *ChemPhysChem*, 2006, **7**, 188-199.

71 B. Sirjean, E. Dames, H. Wang and W. Tsang, *J. Phys. Chem. A*, 2012, **116**, 319-332.

72 K. Wang, S. M. Villano and A. M. Dean, *J. Phys. Chem. A*, 2014, submitted.

73 B. Sirjean, P. A. Glaude, M. F. Ruiz-Lopèz and R. Fournet, *J. Phys. Chem. A*, 2008, **112**, 11598-11610.

74 S. W. Benson, *Thermochemical Kinetics*, 2nd ed.; Wiley: New York, 1976.

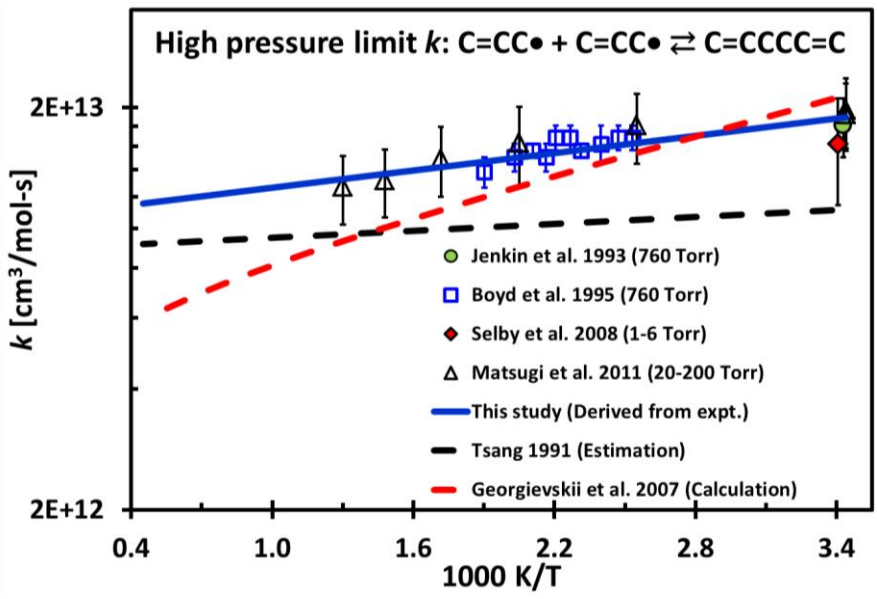

Figure 1: Comparison of the high pressure rate constants for allyl recombination used in this study to those derived in other work.

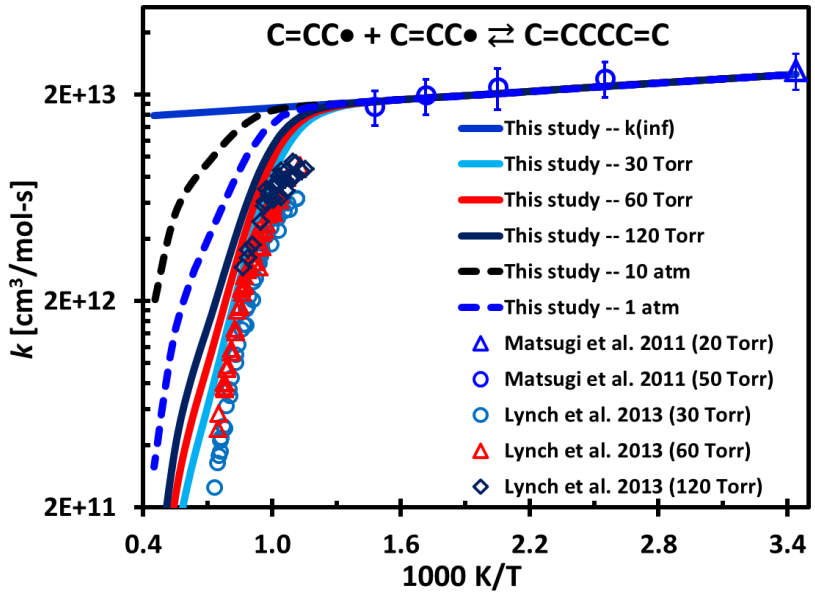

Figure 2: Comparison of the calculated pressure- and temperature-dependent rate constant for allyl recombination to experimental measurements.

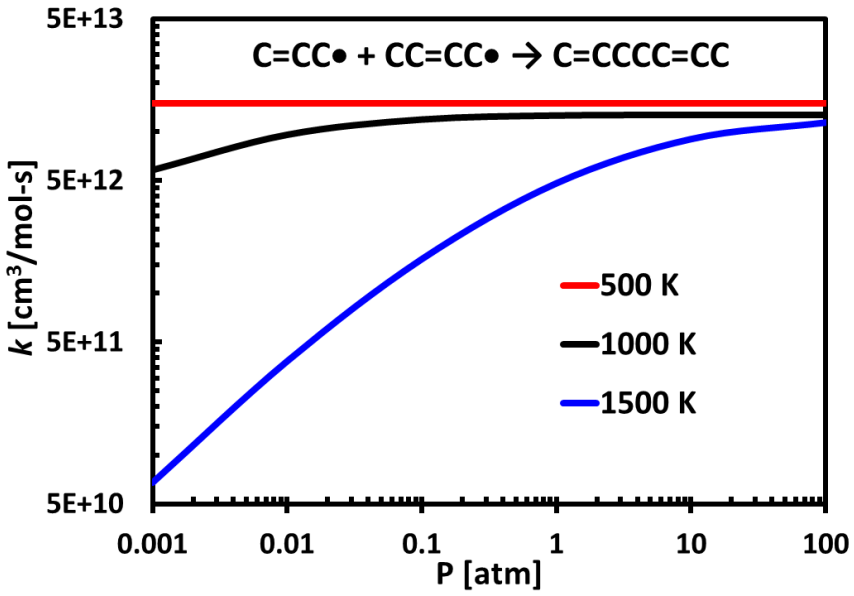

Figure 3: Predicted pressure- and temperature-dependent rate constants for the recombination of allyl and 1-methyl-allyl.

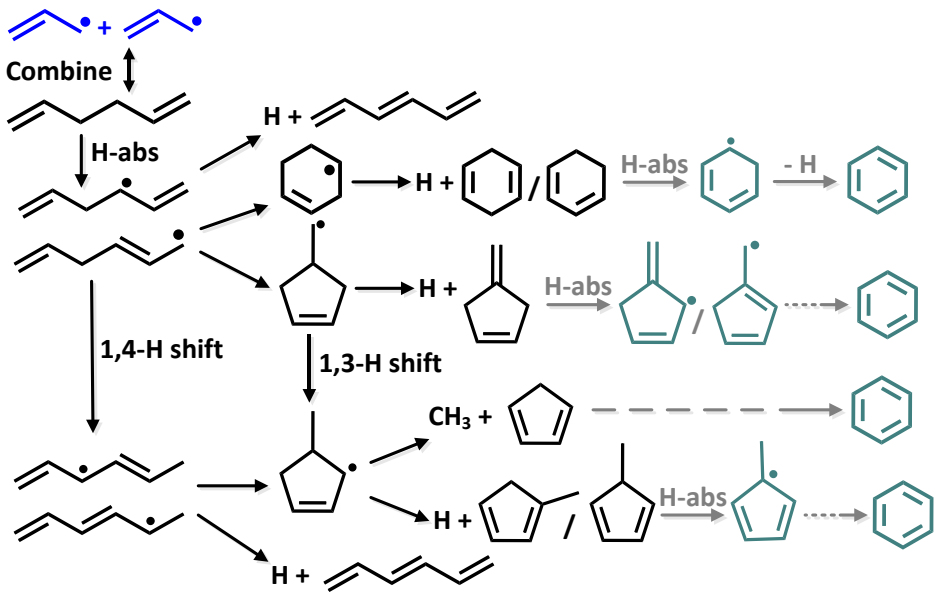

Figure 4: Pathways leading to formation of aromatic species after the recombination of allyl radicals.

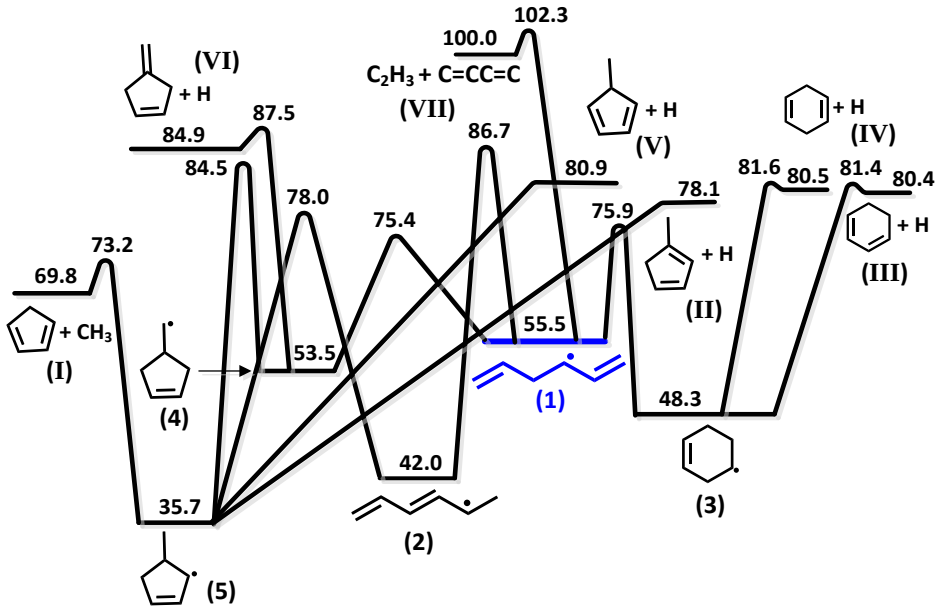

Figure 5: Simplified C_6H_9 PES depicting the energetics of the reaction sequence at 298 K (based on CBS-QB3 calculations, numbers showing enthalpies in kcal/mol). For simplicity only one resonant form is shown for (1), (2), and (5).

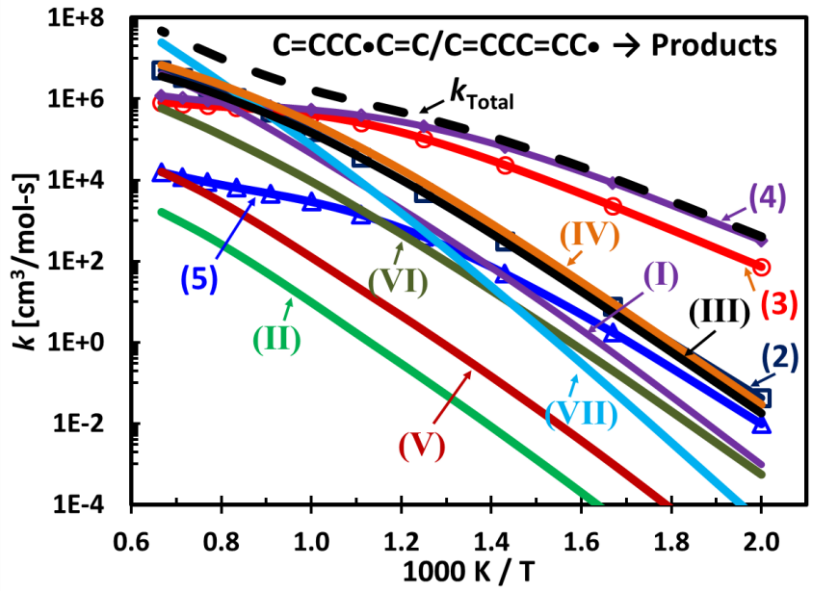

Figure 6: Predicted apparent rate constants for the products resulting from reaction of C=CCC•C=C/C=CCC=CC• at 1 atm in N_2. (Lines with symbols are intermediate isomers and those without symbols are bimolecular products. Product structures are shown in Figure 5: (2) C=CC=CC•C, (3) cyclohexene-4-yl, (4) cyclopentene-4-carbinyl, (5) 4-methyl-cyclopentene-3-yl, (I) 1,3-cyclopentadiene + CH_3, (II) 1-methylcyclopentadiene + H, (III) 1,3-cyclohexadiene + H, (IV) 1,4-cyclohexadiene + H, (V) 3-methyl-cyclopentadiene + H, (VI) methylene-cyclopentene + H, and (VII) C_2H_3 + C=CC=C.)

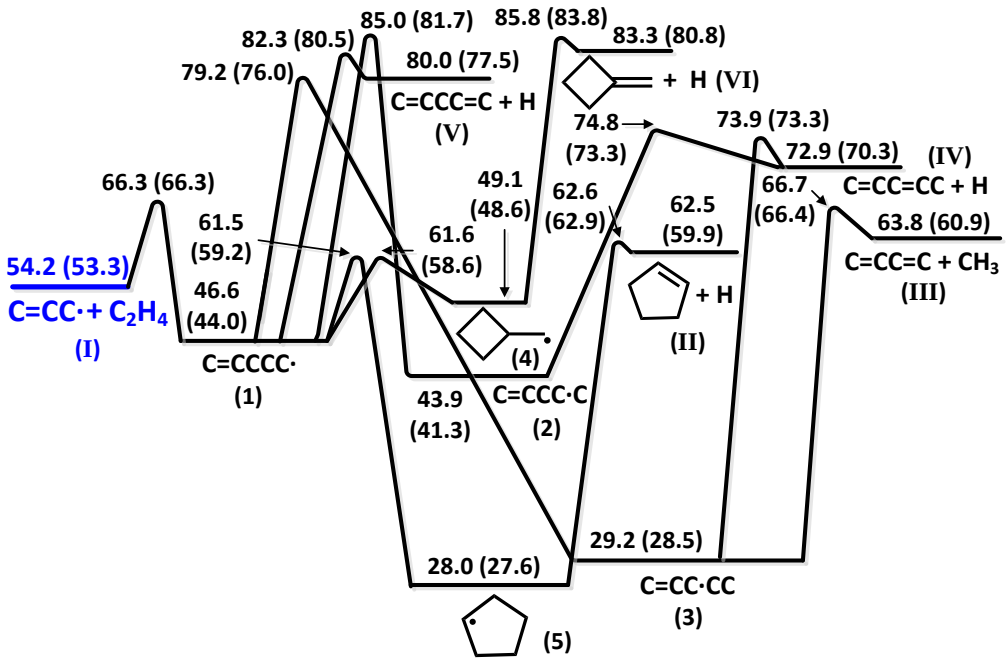

Figure 7: Simplified PES for C_5H_9 calculated at the CBS-QB3 level of theory, showing enthalpies in kcal/mol at 298 K. The numbers in parenthesis are based on estimates using rate rules. For simplicity only one resonance structure is shown for (3).

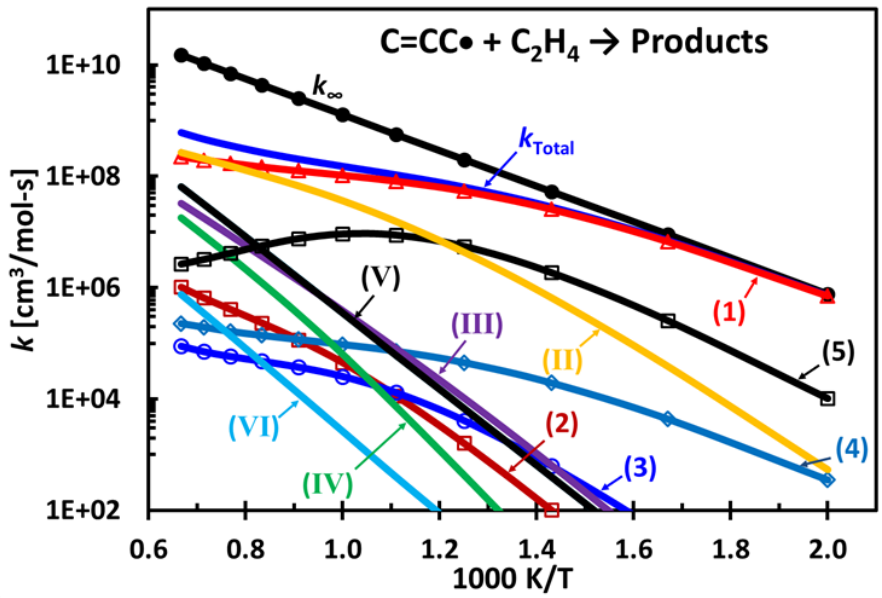

Figure 8: Predicted apparent rate constants for the product channels resulting from the addition of allyl to ethylene (C=CC• + C_2H_4) at 1 atm in N_2. (Lines with symbols are intermediate isomers and without symbols are bimolecular products. Product structures are shown in Figure 7: (1) C=CCCC•, (2) C=CCC•C, (3) C=CC•CC, (4) cyclobutyl-carbinyl, (5) cyclopentyl, (II) cyclopentene + H, (III) CH_3 + C=CC=C, (IV) C=CC=CC + H, (V) C=CCC=C + H, and (VI) methylene-cyclobutane + H.)

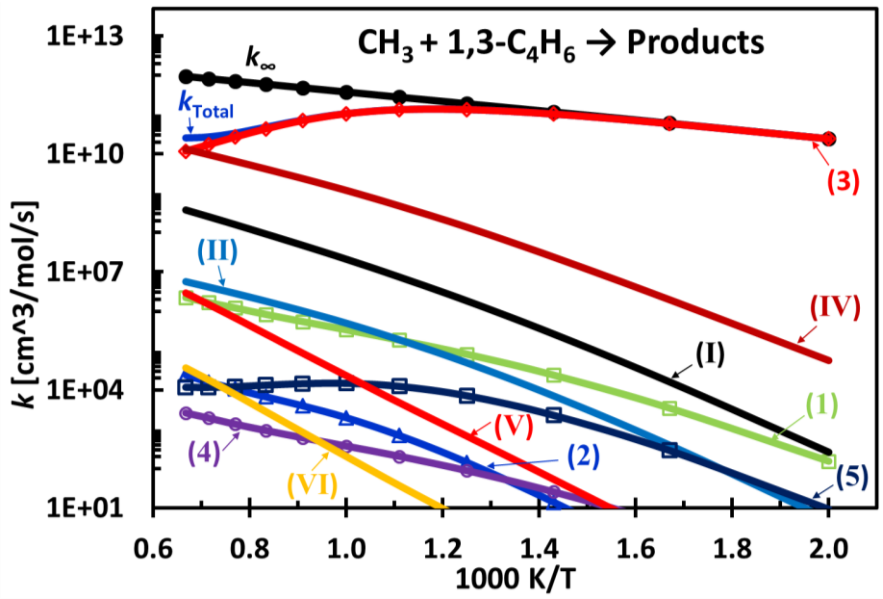

Figure 9: Predicted apparent rate constants for the product channels resulting from the addition of methyl to 1,3-butadiene (CH_3 + 1,3-C_4H_6) at 1 atm in N_2. (Lines with symbols are intermediate isomers and without symbols are bimolecular products. Product structures are shown in Figure 7: (1) C=CCCC•, (2) C=CCC•C, (3) C=CC•CC, (4) cyclobutyl-carbinyl, (5) cyclopentyl, (I) C=CC• + C_2H_4, (II) cyclopentene + H, (IV) C=CC=CC + H, (V) C=CCC=C + H, and (VI) methylene-cyclobutane + H.)

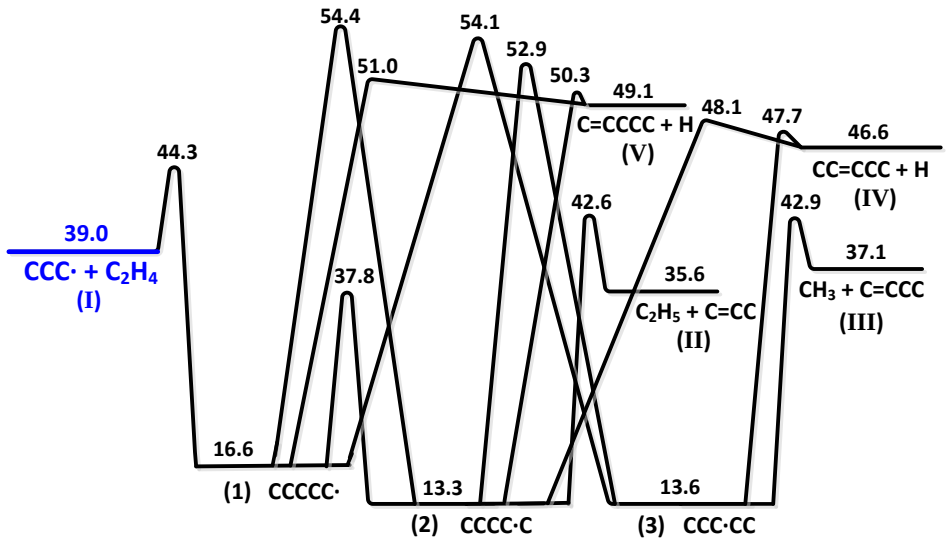

Figure 10: PES for C_5H_{11} calculated at the CBS-QB3 level of theory, showing enthalpies in kcal/mol at 298 K.

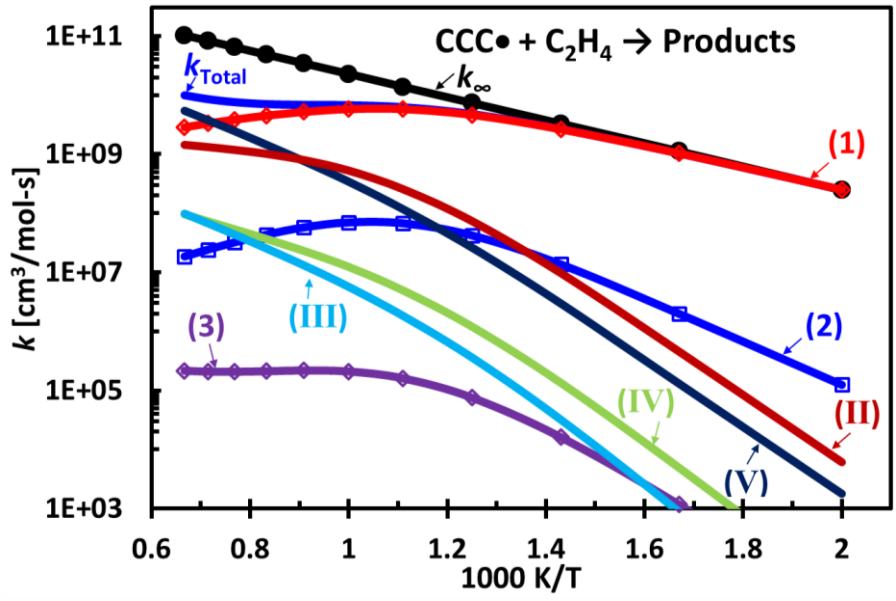

Figure 11: Predicted apparent rate constants for the product channels resulting from the addition of n-propyl to ethylene (CCC• + C_2H_4) at 1 atm in N_2. (Lines with symbols are intermediate isomers and without symbols are bimolecular products. (1) CCCCC•, (2) CCCC•C, (3) CCC•CC, (II) C_2H_5 + C=CC, (III) CH_3 + C=CCC, (IV) CC=CCC + H, and (V) C=CCCC + H.)

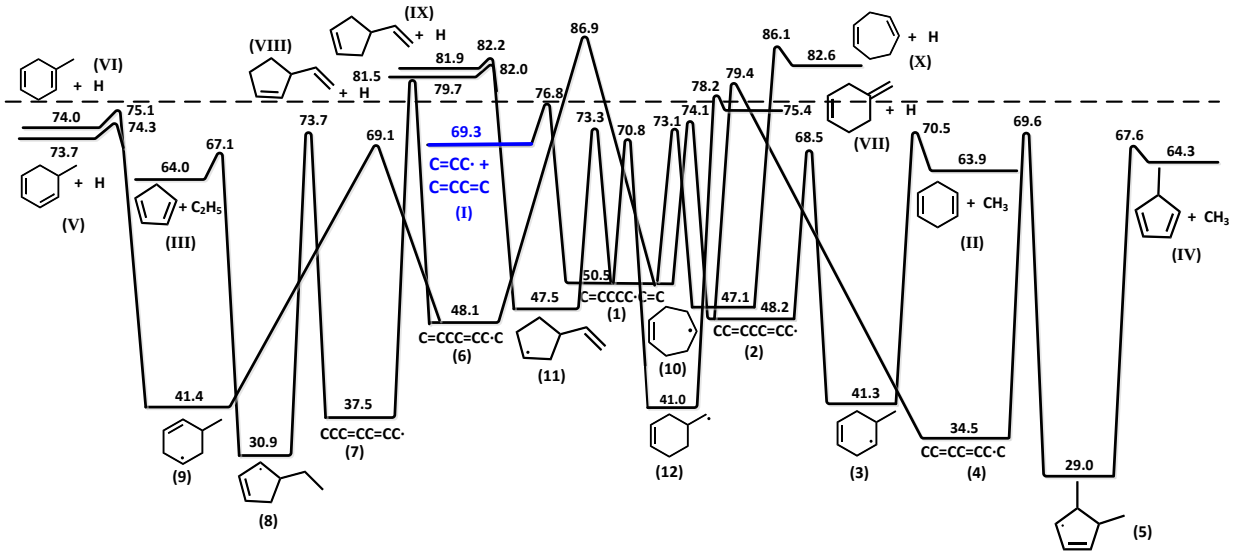

Figure 12: Simplified PES for the addition of allyl to 1,3-butadiene (C=CC• + C=CC=C) calculated at the CBS-QB3 level of theory, showing enthalpies in kcal/mol at 298 K. For simplicity only one resonant form is shown for (1), (2), (4), (5), (6), (7), and (8).

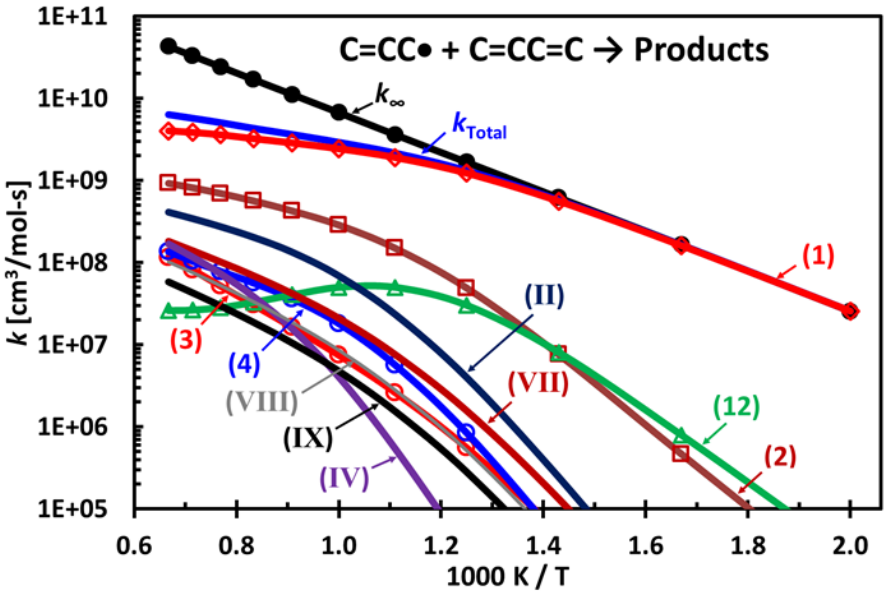

Figure 13: Predicted apparent rate constants for the product channels resulting from the addition of allyl to 1,3-butadiene (C=CC• + C=CC=C) at 1 atm in N_2. (Lines with symbols are intermediate isomers and without symbols are bimolecular products. Product structures are shown in Figure 12: (1) C=CCCC•C=C, (2) CC=CCC=CC•, (3) 4-methyl-cyclohexene-5-yl, (4) CC=CC=CC•C, (12) 4-CH_2•-cyclohexene, (II) 1,4-cyclohexadiene + CH_3, (IV) 3-methyl-cyclopentadiene + CH_3, (VII) 4-methylene-cyclohexene + H, (VIII) 3-vinyl-cyclopentene + H, and (IX) 4-vinyl-cyclopentene + H.)

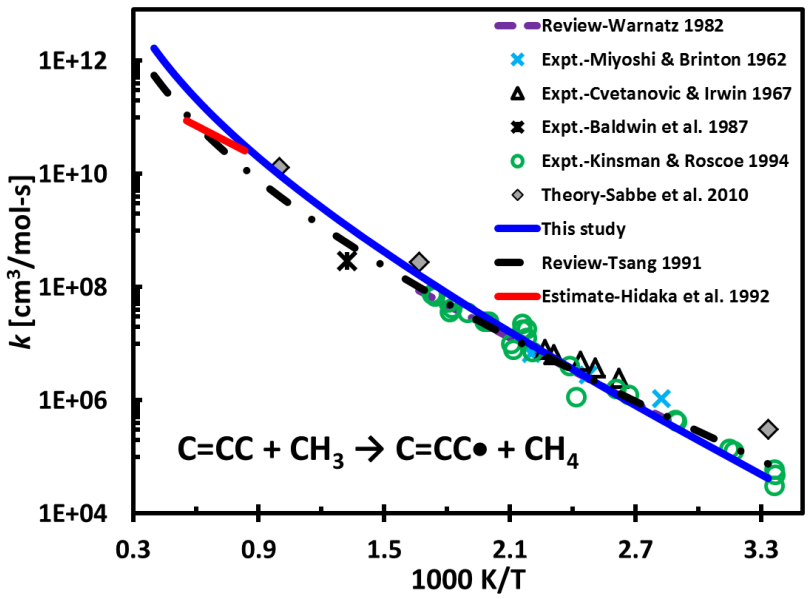

Figure 14: Comparison of literature rate constants for the H-abstraction of propene by methyl to that calculated in this study.

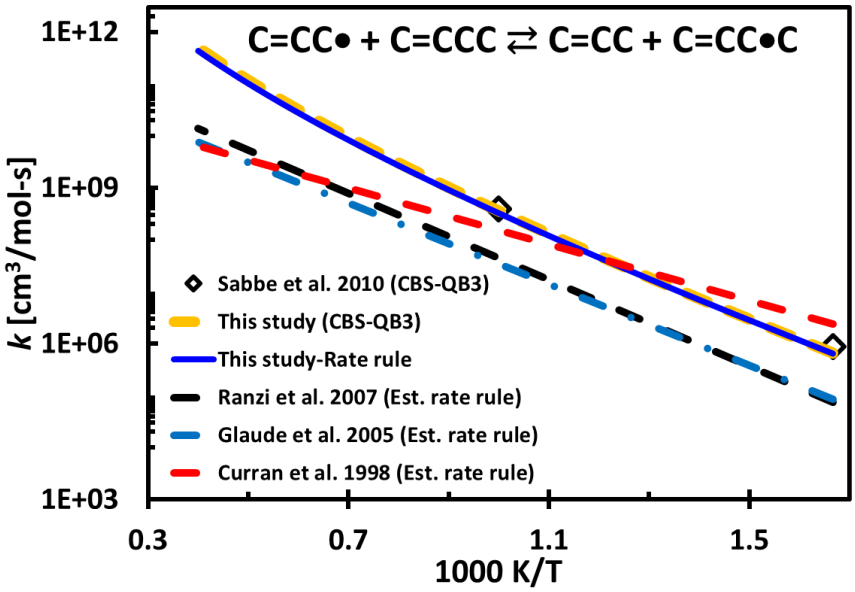

Figure 15: Comparison of literature rate constants for the H-abstraction of 1-butene by allyl to that calculated in this study.

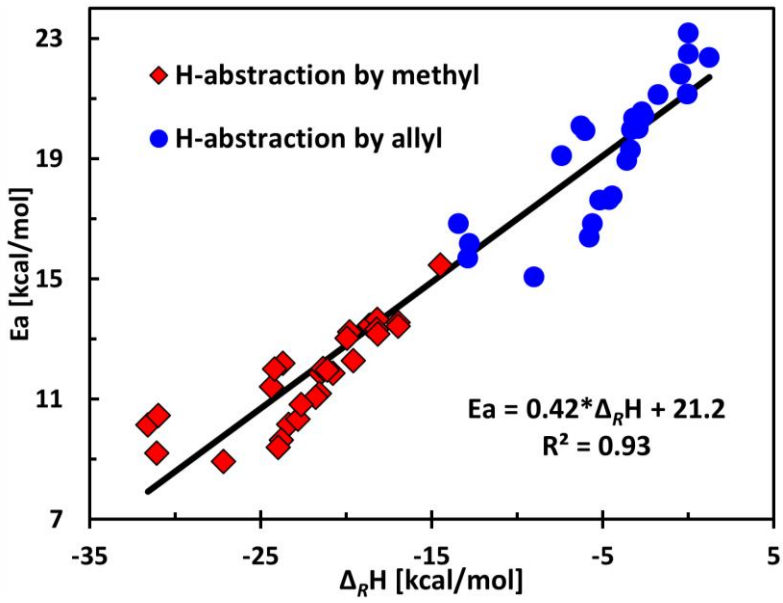

Figure 16: Evans-Polanyi plot for the reactions in Tables 1 and 3 (E_a calculated at 1000 K).

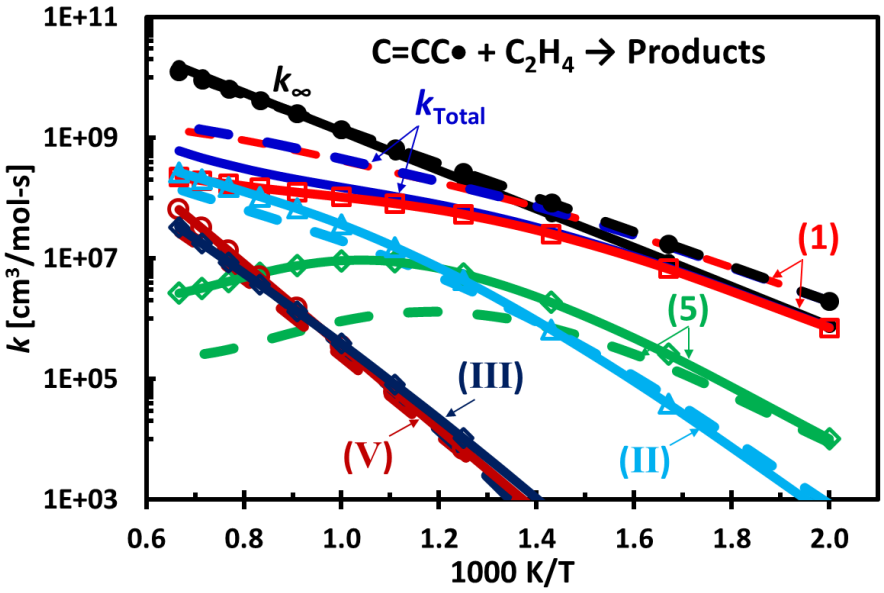

Figure 17: Comparison of the predicted apparent rate constants based on CBS-QB3 calculations (solid lines with symbols) to those estimated using rate rules (dashed lines) for the product channels resulting from the addition of allyl to ethylene (C=CC• + C_2H_4) at 1 atm in N_2. (1) C=CCCC•, (5) cyclopentyl, (II) cyclopentene + H, (III) CH_3 + C=CC=C, and (V) C=CCC=C + H.)

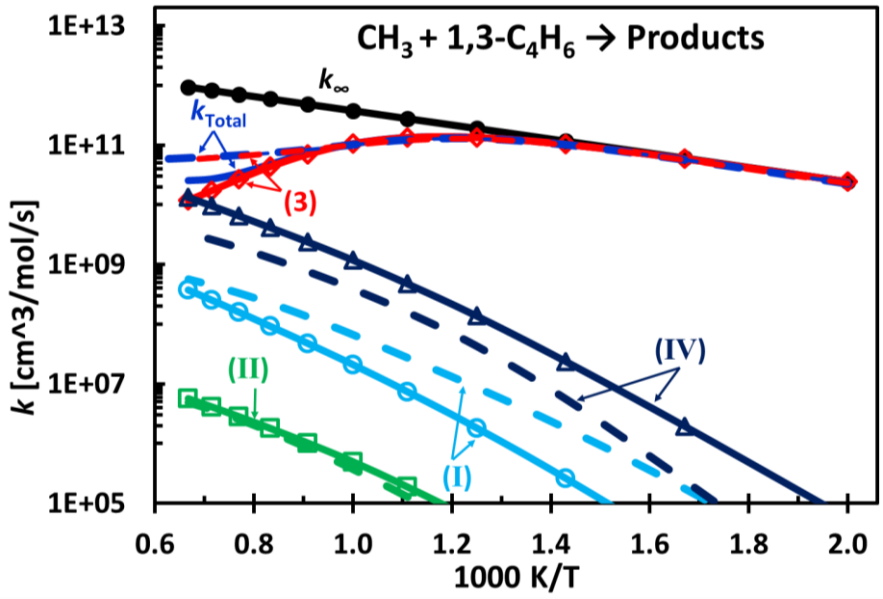

Figure 18: Comparison of the predicted apparent rate constants based on CBS-QB3 calculations (solid lines with symbols) to those estimated using rate rules (dashed lines) for the product channels resulting from the addition of methyl to 1,3-butadiene (CH_3 + 1,3-C_4H_6) at 1 atm in N_2: (3) C=CC•CC, (I) C=CC• + C_2H_4, (II) cyclopentene + H, and (IV) C=CC=CC + H.)

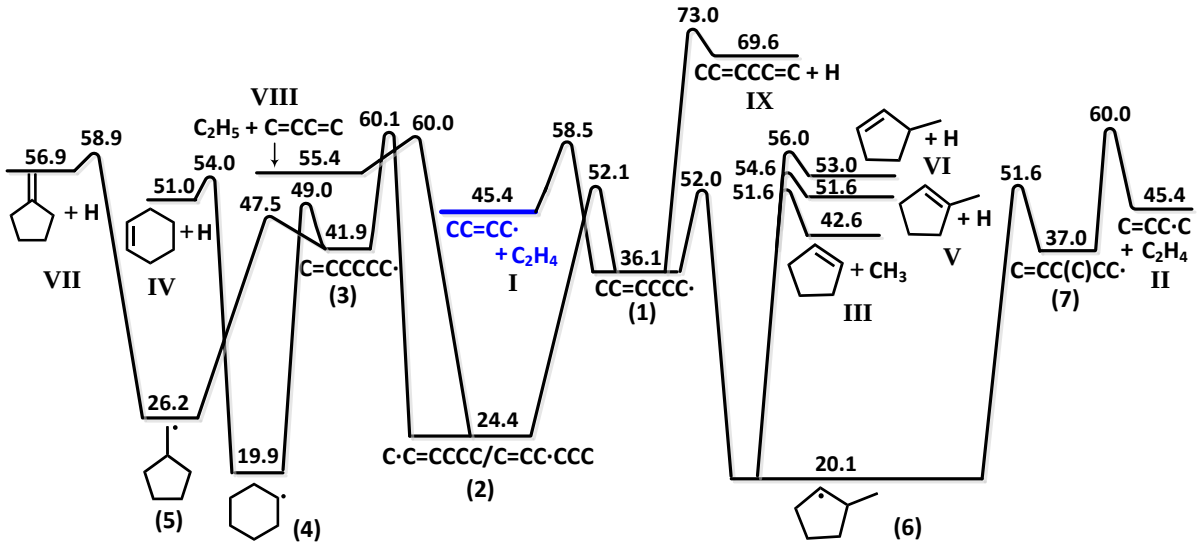

Figure 19: Simplified PES for the addition of 1-methyl-allyl to ethylene (CC=CC•/C=CC•C + C_2H_4) constructed based on rate rule estimates.

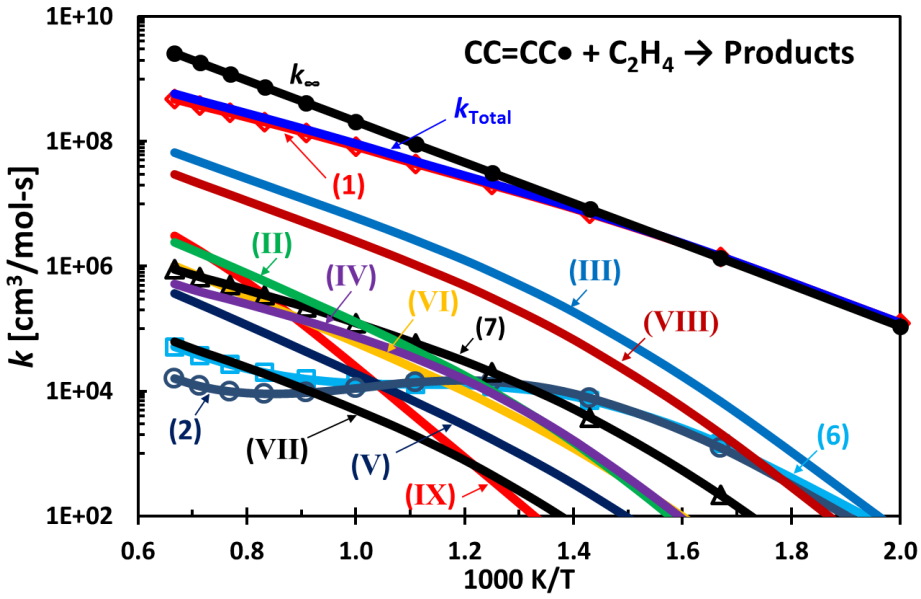

Figure 20: Predicted apparent rate constants based on rate rule estimates for the product channels resulting from the addition of 1-methyl-allyl to ethylene (CC=CC•/C=CC•C + C_2H_4) at 1 atm in N_2. (Lines with symbols are intermediate isomers and without symbols are bimolecular products. Product structures shown in Figure 19: (1) CC=CCCC•, (2) C•C=CCCC/C=CC•CCC, (6) 2-methyl-cyclopente-1-yl, (7) C=CC(C)CC•, (II) C=CC•C + C_2H_4, (III) cyclopentene + CH_3, (IV) cyclohexene + H, (V) 1-methyl-cyclopentene + H, (VI) 3-methyl-cyclopentene + H, (VII) methylene-cyclopentane + H, (VIII) C_2H_5 + C=CC=C, and (IX) CC=CCC=C + H.)

Table 1: Reaction Rate Constants for Abstraction by CH_3 from Alkenes and Comparison between Individual TST Rate Constants and the Rate Estimation Rule.

Category	Reactions	Modified Arrhenius parameters[c]				Arrhenius parameters[c]		$\Delta_R H^{(298)}$	k(TST,	k(rate rule)[c]/k(TST)		
		n_H	A_H	n	E	A'_H	Ea	(kcal/mol)	1000K)/#n_H[a]	500 K	1000 K	1500 K
Primary	trans-CC=CC + CH_3 ⇄ trans-CC=CC• + CH_4	6	26.0	3.24	7.01	3.52E+12	13.4	-18.7	4.05E+09	1.18	1.03	0.97
	cis-CC=CC + CH_3 ⇄ cis-CC=CC• + CH_4	6	11.7	3.31	6.66	2.63E+12	13.2	-19.9	3.38E+09	1.23	1.24	1.20
	CC=CCC + CH_3 ⇄ CCC=CC• + CH_4	3	26.3	3.24	7.03	3.38E+12	13.5	-18.7	3.87E+09	1.24	1.08	1.02
	C=CC + CH_3 ⇄ C=CC• + CH_4	3	18.4	3.27	7.15	3.04E+12	13.6	-18.2	3.17E+09	1.65	1.32	1.19
	C=C(C)CC + CH_3 ⇄ C=C(C•)CC + CH_4	3	64.3	3.13	7.32	3.68E+12	13.5	-17.1	4.03E+09	1.29	1.04	0.97
	C=CC_2 + CH_3 ⇄ C=CC_2• + CH_4	6	29.7	3.22	7.04	3.31E+12	13.4	-17.0	3.85E+09	1.23	1.09	1.03
	CC=CC_2 + CH_3 ⇄ trans-CC=CC_2• + CH_4	3	28.6	3.23	6.91	3.36E+12	13.3	-18.3	4.13E+09	1.08	1.01	0.97
	CC=CC_2 + CH_3 ⇄ cis-CC=CC_2• + CH_4	3	11.9	3.34	6.52	3.59E+12	13.2	-18.3	4.77E+09	0.83	0.88	0.86
	CC=CC_2 + CH_3 ⇄ C•C=CC_2 + CH_4	3	16.9	3.30	6.48	3.49E+12	13.0	-20.0	4.97E+09	0.77	0.84	0.85
	Rate rule		**20.0**	**3.26**	**6.67**	**3.33E+12**	**13.4**		**4.03E+09**			
	Standard deviation					**3.22E+11**	**0.20**		**5.76E+08**			
	K_{eq}		**1.83E-02**	**0.33**	**-19.9**							
Secondary	C=CCCC=C + CH_3 ⇄ C=CC•CC=C + CH_4	4	23.0	3.22	5.48	5.01E+12	11.9	-20.8	1.28E+10	1.05	0.94	0.87
	CC=CCC + CH_3 ⇄ CC=CC•C + CH_4	2	120.0	3.09	5.73	4.69E+12	11.9	-21.6	1.20E+10	1.16	1.01	0.94
	C=CCC + CH_3 ⇄ C=CC•C + CH_4	2	80.50	3.12	5.82	4.26E+12	12.0	-21.4	1.01E+10	1.50	1.20	1.09
	C=CCCC + CH_3 ⇄ C=CC•CC + CH_4	2	84.70	3.12	5.78	4.21E+12	12.0	-21.2	1.02E+10	1.44	1.18	1.08
	C=C(C)CC + CH_3 ⇄ C=C(C)C•C + CH_4	2	275.00	3.08	6.18	4.99E+12	12.3	-19.6	1.03E+10	1.70	1.17	1.02
	Rate rule		**90.3**	**3.10**	**5.37**	**4.63E+12**	**12.0**		**1.11E+10**			
	Standard deviation					**3.83E+11**	**0.17**		**1.25E+09**			
	K_{eq}		**9.53E-02**	**0.00**	**-23.3**							
Tertiary	C=CCC_2 + CH_3 ⇄ C=CC•C_2 + CH_4	1	333.0	2.92	4.37	3.38E+12	10.2	-23.4	2.04E+10	0.71	0.83	0.83
	C=CC(C)CC + CH_3 ⇄ C=CC•(C)CC + CH_4	1	1110.0	2.73	4.91	2.61E+12	10.3	-22.9	1.44E+10	1.15	1.17	1.17
	Rate rule		**6.30E+02**	**2.82**	**4.72**	**3.00E+12**	**10.2**		**1.74E+10**			
	Standard deviation					**5.48E+11**	**0.12**		**4.24E+09**			
	K_{eq}		**0.86**	**-0.24**	**-23.9**							
Secondary (Cyclics)	CYC_5H_8 + CH_3 ⇄ CYPE3• + CH_4	4	429.5	2.95	5.32	5.95E+12	11.2	-21.6	2.13E+10	0.99	0.95	0.92
	CYC_6H_{10} + CH_3 ⇄ CYC_6H_9A + CH_4	4	427.5	2.93	5.24	4.90E+12	11.1	-21.8	1.88E+10	1.06	1.08	1.07
	Rate rule		**4.21E+02**	**2.94**	**5.21**	**5.43E+12**	**11.1**		**2.01E+10**			
	Standard deviation					**7.37E+11**	**0.10**		**1.77E+09**			
	K_{eq}		**3.16**	**-0.24**	**-21.6**							
Tertiary (Cyclics)	$MeCYC_5H_8$ + CH_3 ⇄ MeCYPE3• + CH_4	1	945.0	2.84	4.01	5.14E+12	9.64	-23.9	4.02E+10	1.22	1.16	1.12
	$MeCYC_6H_{10}$ + CH_3 ⇄ $MeCYC_6H_9A$ + CH_4	1	890.0	2.86	3.72	5.83E+12	9.39	-24.0	5.16E+10	0.84	0.90	0.91
	Rate rule		**9.04E+02**	**2.85**	**3.83**	**5.49E+12**	**9.52**		**4.59E+10**			
	Standard deviation					**4.89E+11**	**0.17**		**8.06E+09**			
	K_{eq}		**3.91**	**-0.23**	**-24.2**							
Extended resonance	C=CCC=C + CH_3 ⇄ C=CC•C=C + CH_4	2	21.0	3.21	3.77	2.20E+12	10.1	-31.7	1.34E+10			
	C=CC=CC + CH_3 ⇄ C=CC=CC• + CH_4	3	299.7	2.84	5.77	1.65E+12	11.4	-24.4	5.30E+09	0.69	0.89	1.01
	C=CC(C)=CC + CH_3 ⇄ CH4+C=CC(C)=CC• + CH_4	3	10.5	3.31	5.63	2.37E+12	12.2	-23.8	5.12E+09	0.94	0.92	0.86
	C=CC=CC_2 + CH_3 ⇄ C=CC=CC_2• + CH_4	6	8.32	3.29	5.46	1.62E+12	12.0	-24.2	3.88E+09	1.11	1.21	1.18
	Rate rule		**29.7**	**3.15**	**5.72**	**1.88E+12**	**11.9**		**4.77E+09**			
	Standard deviation					**4.24E+11**	**0.41**		**7.70E+08**			
	K_{eq}		**3.86E-02**	**0.17**	**-24.8**							
Extended resonance (Cyclics)	CHD14 + CH_3 ⇄ CYC_6H_7 + CH_4	4	667.5	2.90	3.45	5.90E+12	9.20	-31.1	5.75E+10	0.60	0.75	0.80
	CHD13 + CH_3 ⇄ CYC_6H_7 + CH_4	4	570.0	2.91	4.67	5.64E+12	10.5	-31.0	2.93E+10	2.18	1.48	1.27
	MeCY13PD + CH_3 ⇄ MeCY13PD5• + CH_4	1	1500.0	2.80	3.38	5.94E+12	8.93	-27.2	6.62E+10	0.47	0.66	0.74
	CY13PD + CH_3 ⇄ CY13PD5• + CH_4	2	590.0	2.90	5.06	5.46E+12	10.8	-22.7	2.35E+10	3.30	1.85	1.49
	Rate rule		**7.05E+02**	**2.88**	**3.89**	**5.73E+12**	**9.85**		**4.41E+10**			
	Standard deviation					**2.25E+11**	**0.93**		**2.09E+10**			
	K_{eq}		**0.65**	**-0.05**	**-30.6**							
Aromatics	Benzene + CH_3 ⇄ Phenyl + CH_4	6	1.52E+03	2.93	15.92	1.68E+13	21.73	10.0	2.98E+08			
	K_{eq}		**29.8**	**-0.34**	**10.1**							
	Toulene + CH_3 ⇄ Benzyl + CH_4	3	6.07	3.42	8.66	3.39E+12	15.46	-14.5	1.42E+09			
	K_{eq}		**8.48E-03**	**0.33**	**-14.9**							

Note: [a] The units for A_H, A'_H, and k(TST,1000 K) are cm^3/mol-s, and are kcal/mol for $\Delta_R H^{(298)}$, E and E_a; the A terms are normalized by the number of equivalent hydrogens.

[b] The k(rate rule) term has been calculated using the bold rate rule listed at the bottom of each subset.

[c] Molecule structures are presented in abbreviated form (H atoms missing, radical site marked with "•") to improve readability. For example, C=CC_2 represents isobutene, C=CC• represents allyl. Other abbreviations:

CYC_5H_8—cyclopentene, CYC_6H_{10}—cyclohexene, $MeCYC_5H_8$—methyl-cyclopentene, $MeCYC_6H_{10}$—methyl-cyclohexene, CHD13—1,3-cyclohexadiene, CHD14—1,4-cyclohexadiene, CY13PD—1,3-cyclopentadiene, MeCY13PD—methy-1,3-cyclopentadiene.

Table 2: Comparison of Rate Constants for H-Abstraction Reactions by Methyl and Allyl.

Reaction	Modified Arrhenius parameters[a]			Arrhenius parameters[a]		k (1000K)[a]	$\Delta_R H^{298}$ (kcal/mol)	k (C=CC•)/k (CH_3) (1000 K)	A'(C=CC•)/ A'(CH_3)	Ea(C=CC•) - Ea(CH_3)
	A	n	E	A'	Ea					
C=CC + CH_3 ⇄ C=CC• + CH_4	54.4	3.27	7.15	9.12E+12	13.7	9.59E+09	-19.49			
C=CC + C=CC• ⇄ C=CC• + C=CC	12.6	3.62	16.0	3.36E+13	23.2	2.91E+08	0.00	3.0E-02	3.68	9.52
C=CCC + CH_3 ⇄ C=CC•C + CH_4	161	3.12	5.82	8.52E+12	12.0	1.97E+10	-22.68			
C=CCC + C=CC• ⇄ C=CC•C + C=CC	13.9	3.45	13.5	9.90E+12	20.3	3.49E+08	-3.19	1.8E-02	1.16	8.32
CC=CC + CH_3 ⇄ CC=CC• + CH_4	154.0	3.24	7.01	2.11E+13	13.5	2.37E+10	-19.98			
CC=CC + C=CC• ⇄ CC=CC• + C=CC	29.5	3.52	14.8	3.63E+13	21.8	6.16E+08	-0.43	2.6E-02	1.72	8.36
C=C(C)C + CH_3 ⇄ C=C(C)C• + CH_4	176.0	3.22	7.04	1.99E+13	13.4	2.33E+10	-18.27			
C=C(C)C + C=CC• ⇄ C=C(C)C• + C=CC	56.6	3.51	15.4	6.54E+13	22.4	8.31E+08	1.22	3.6E-02	3.29	8.92
CY13PD + CH_3 ⇄ CY13PD5• + CH_4 [b]	1180	2.90	5.06	1.09E+13	10.8	4.63E+10	-23.95			
CY13PD + C=CC• ⇄ CY13PD5• + C=CC [b]	191	3.14	11.5	1.20E+13	17.8	1.53E+09	-4.46	3.3E-02	1.10	6.92
C=CC(C)C + CH_3 ⇄ C=CC•(C)C + CH_4	333	2.92	4.37	3.38E+12	10.2	2.12E+10	-24.67			
C=CC(C)C + C=CC• ⇄ C=CC•(C)C + C=CC	53.7	3.22	11.2	6.16E+12	17.6	8.68E+08	-5.18	4.1E-02	1.82	7.47
CC=CCC + CH_3 ⇄ CC=CC•C + CH_4	240	3.09	5.73	9.38E+12	11.9	2.50E+10	-22.82			
CC=CCC + C=CC• ⇄ CC=CC•C + C=CC	17	3.41	13.2	8.42E+12	20.0	3.75E+08	-3.33	1.5E-02	0.90	8.10
CC=CCC + CH_3 ⇄ CCC=CC• + CH_4	77.9	3.24	7.03	1.01E+13	13.5	1.19E+10	-19.92			
CC=CCC + C=CC• ⇄ CCC=CC• + C=CC	8.7	3.57	14.7	1.60E+13	21.8	2.71E+08	-0.43	2.3E-02	1.59	8.34
C=CC=CC + CH_3 ⇄ C=CC=CC• + CH_4	899.0	2.84	5.77	4.95E+12	11.4	1.63E+10	-25.69			
C=CC=CC + C=CC• ⇄ C=CC=CC• + C=CC	3.51	3.62	12.9	9.09E+12	20.1	3.82E+08	-6.28	2.3E-02	1.84	8.68
							Average	**0.027**	**1.90**	**8.29**
							STDEV	**0.008**	**0.97**	**0.76**

Note: [a] Parameters fitted over temperature range 300-2500 K; Units for A, A' and k(1000K) are cm^3/mol-s, for E and E_a kcal/mol; [b] CY13PD and CY13PD5• are cyclopentadiene (C_5H_6) and cyclopentadienyl (C_5H_5).

Table 3: Reaction Rate Constants for Abstraction by Allyl from Alkenes and Comparison between TST Rate Constants and the Rate Estimation Rule.

Category	Reaction	Modified Arrhenius parameters[a]				Arrhenius parameters[a]		$\Delta_R H^{(298K)}$	*k* (TST,	*k* (rate rule)[b]/*k* (TST)		
		n_H	A_H	n	E	A'_H	Ea	(kcal/mol)	1000K)/n_H[a]	500 K	1000 K	1500 K
Primary	C=C(C)C + C=CC• ⇄ C=C(C)C• + C=CC	6	4.72	3.51	15.4	5.45E+12	22.4	1.22	7.05E+07	2.27	1.61	1.39
	C=CC + C=CC• ⇄ C=CC• + C=CC	3	4.20	3.62	16.0	1.12E+13	23.2	0	9.57E+07	2.47	1.19	0.89
	trans-CC=CC + trans-CC=CC• ⇄ CC=CC• + CC=CC	6	2.25	3.63	15.3	6.54E+12	22.5	0	7.97E+07	2.08	1.42	1.19
	CC=C(C)C + C=CC• ⇄ trans-CC=C(C)C• + C=CC	3	1.93	3.60	14.0	4.50E+12	21.1	-0.05	1.08E+08	0.79	1.05	1.11
	CCC=CC + C=CC• ⇄ CCC=CC• + C=CC	3	3.38	3.57	14.7	6.28E+12	21.8	-0.43	1.08E+08	0.79	1.05	1.11
	trans-CC=CC + C=CC• ⇄ trans-CC=CC• + C=CC	6	4.92	3.52	14.8	6.05E+12	21.8	-0.49	1.03E+08	1.18	1.10	1.05
	CC=C(C)C + C=CC• ⇄ C•C=C(C)C + C=CC	3	1.70	3.62	13.9	4.47E+12	21.1	-1.76	1.07E+08	0.79	1.06	1.12
	Rate Rule		**8.04**	**3.46**	**14.8**	**6.35E+12**	**22.0**		**9.58E+07**			
	Standard deviation					**2.28E+12**	**0.74**		**1.50E+07**			
	K_{eq}		**1.47**	**0.03**	**-1.05**							
Secondary	C=CCCC=C + C=CC• ⇄ C=CC•CC=C + C=CC	4	1.81	3.60	13.3	4.19E+12	20.4	-2.60	1.44E+08	1.38	1.16	1.04
	C=CCC + CC=CC• ⇄ C=CC•C + CC=CC	2	3.40	3.51	13.6	3.99E+12	20.5	-2.70	1.28E+08	1.72	1.31	1.15
	C=CCCC + C=CC• ⇄ C=CC•CC + C=CC	2	2.62	3.48	13.1	3.54E+12	20.0	-2.92	1.50E+08	1.10	1.12	1.09
	C=CCC + C=CC• ⇄ C=CC•C + C=CC	2	6.95	3.45	13.5	4.95E+12	20.3	-3.21	1.77E+08	1.13	0.95	0.87
	CC=CCC + C=CC• ⇄ CC=CC•C + C=CC	2	8.50	3.41	13.2	4.21E+12	20.0	-3.33	1.82E+08	0.91	0.92	0.90
	Rate Rule		**12.0**	**3.35**	**13.3**	**4.17E+12**	**20.3**		**1.56E+08**			
	Standard deviation					**5.13E+11**	**0.26**		**2.26E+07**			
	K_{eq}		**0.62**	**0.04**	**-3.40**							
Tertiary	C=CC(C)CC + C=CC• ⇄ C=CC•(C)CC + C=CC	1	109.6	3.08	11.5	4.17E+12	17.6	-4.64	5.82E+08	1.38	1.29	1.24
	C=CC(C)C + C=CC• ⇄ C=CC(C)C• + C=CC	1	53.7	3.22	11.2	6.16E+12	17.6	-5.18	8.69E+08	0.88	0.87	0.82
	Estimate Rate Rule		**1.31E+02**	**3.08**	**11.3**	**5.17E+12**	**17.6**		**7.26E+08**			
	K_{eq}		**21.3**	**-0.37**	**-5.43**							
Secondary (Cyclics)	CYC_5H_8 + C=CC• ⇄ CYPE3• + C=CC	4	33.3	3.26	12.8	5.11E+12	19.3	-3.39	3.10E+08	1.45	1.10	0.97
	CYC_6H_{10} + C=CC• ⇄ CYC_6H_9• + C=CC	4	32.0	3.24	12.5	4.27E+12	18.9	-3.61	3.08E+08	1.23	1.11	1.03
	Rate Rule		**80.2**	**3.12**	**12.5**	**4.69E+12**	**19.1**		**3.09E+08**			
	K_{eq}		**16.2**	**-0.17**	**-3.44**							
Tertiary (Cyclics)	$MeCYC_5H_8$ + C=CC• ⇄ MeCYPE3• + C=CC	1	96.8	3.10	10.7	4.12E+12	16.8	-5.62	8.56E+08	1.51	1.21	1.10
	$MeCYC_6H_{10}$ + C=CC• ⇄ $MeCYC_6H_9$• + C=CC	1	74.9	3.12	10.2	3.87E+12	16.4	-5.79	1.01E+09	1.01	1.03	1.00
	Rate Rule		**1.81E+02**	**3.01**	**10.4**	**4.00E+12**	**16.6**		**9.33E+08**			
	K_{eq}		**3.18E+02**	**-0.51**	**-5.4**							
Extended resonance	C=CCC=C + C=CC• ⇄ C=CC•C=C + C=CC	2	0.12	3.78	9.33	1.14E+12	16.8	-13.5	2.38E+08			
	C=CC=C(C)C + C=CC• ⇄ C=CC=C(C)C• + C=CC	6	1.54	3.56	12.9	2.53E+12	19.9	-6.03	1.11E+08	1.54	1.25	1.12
	C=CC=CC + C=CC• ⇄ C=CC=CC• + C=CC	3	1.17	3.62	12.9	3.03E+12	20.1	-6.28	1.23E+08	1.50	1.13	0.99
	C=CC(C)=CC + C=CC• ⇄ C=CC(C)=CC• + C=CC	3	0.65	3.64	11.9	2.06E+12	19.1	-7.41	1.38E+08	0.79	1.00	1.03
	Rate Rule		**2.00**	**3.52**	**12.4**	**2.54E+12**	**19.7**		**1.24E+08**			
	Standard deviation					**4.87E+11**	**0.54**		**1.37E+07**			
	K_{eq}		**2.34**	**-0.13**	**-6.50**							
Extended resonance (cyclics)	CY13PD + C=CC• ⇄ CY13PD5• + C=CC	2	95.5	3.14	11.5	5.98E+12	17.7	-4.46	7.85E+08	5.71	1.91	1.30
	MeCY13PD + C=CC• ⇄ MeCY13PD5• + C=CC	1	301.0	2.97	9.16	4.60E+12	15.1	-9.01	2.35E+09	0.51	0.64	0.70
	CHD13 + C=CC• ⇄ CYC_6H_7• + C=CC	4	47.0	3.18	9.86	3.86E+12	16.2	-12.8	1.13E+09	1.77	1.33	1.18
	CHD14 + C=CC• ⇄ CYC_6H_7• + C=CC	4	97.3	3.12	9.48	5.18E+12	15.7	-12.9	1.92E+09	0.82	0.78	0.75
	Rate Rule		**1.00E+02**	**3.08**	**9.45**	**4.90E+12**	**16.2**		**1.55E+09**			
	Standard deviation					**8.95E+11**	**1.15**		**7.18E+08**			
	K_{eq}		**1.30E+02**	**-0.44**	**-11.7**							

Note: [a] The units for A_H, A'_H, and *k*(TST,1000 K) are cm^3/mol-s, and are kcal/mol for $\Delta_R H^{(298)}$, E and E_a; the A terms are normalized by the number of equivalent hydrogens.

[b] The *k*(rate rule) term has been calculated using the bold rate rule listed at the bottom of each subset.

[c] Molecule structures are presented in abbreviated form (H atoms missing, radical site marked with "•") to improve readability. Molecule structures are presented in abbreviated form as these in Table 1

Table 4: Comparison of Predicted Rate Constants for Allyl Addition versus Abstraction from Alkenes.

Reaction types	Reactions	A (cm^3/mol/s)	*n*	E (kcal/mol)	*k* (Addition)/*k* (Addition + H-abs)		
					500 K	1000 K	1500 K
H-abs	C=CC• + C_2H_4 ⇄ C=CC + C_2H_3	2.58E+03	3.06	26.4	1.00	0.99	0.92
Addition	C=CC• + C_2H_4 ⇄ C=CCCC•	2.70E+03	2.70	11.3			
H-abs	C=CC• + C=CC ⇄ C=CC + C=CC•	1.26E+01	3.62	16.0	0.96	0.54	0.27
Addition	C=CC• + C=CC ⇄ C=CCCC•C	1.56E+03	2.53	11.0			
	C=CC• + C=CC ⇄ C=$CCCC_2$•	1.37E+02	2.84	12.2			
H-abs	C=CC• + C=CCC ⇄ C=CC + CC=CC•	1.39E+01	3.45	13.5	0.88	0.55	0.37
Addition	C=CC• + C=CCC ⇄ C=CCCC•CC	1.31E+03	2.62	10.9			
	C=CC• + C=CCC ⇄ C=CCC(C•)CC	1.22E+01	3.06	11.7			
H-abs	C=CC• + CC=CC ⇄ C=CC + CC=CC•	2.95E+01	3.52	14.8	0.88	0.40	0.21
Addition	C=CC• + CC=CC ⇄ C=CCC_2C•C	9.53E+02	2.70	11.2			

Reactions of Allylic Radicals that Impact Molecular Weight Growth Kinetics

Kun Wang, Stephanie M. Villano, and Anthony M. Dean*

Supporting Information

Table S1: Apparent temperature-and pressure-dependent rate constants for the recombination reactions of two stabilized radicals from 0.001-50 atm and 300-2500 K.

Figure S1: Pathways leading to formation of aromatic species after recombination of methyl-allyl and allyl radicals.

Figure S2: Simplified C_6H_9 PES depicting the energetics of the reaction sequence after hydrogen abstraction from the initially-formed linear adduct in the recombination of two allyl radicals. (The numbers are enthalpies (kcal/mol) at 298K based on CBS-QB3 calculations; the numbers in parenthesis are based on rate rule estimates)

Table S2: High pressure limit rate constants for reactions shown in the C_6H_9 PES in Figure S2 and Figure 5 in text (based on CBS-QB3 calculations).

Table S3: Rate constants at 1 atm for the reactions shown in the C_6H_9 PES in Figure S2 and Figure 5 in text for the temperature range 300- 2500 K.

Figure S3: A more complete C_5H_9 PES by CBS-QB3.

Figure S4: Comparison of the rate constant for formation of cyclopentene in the reaction allyl + ethylene calculated in this study with literature values at 1 atm.

Table S4: High pressure limit rate constants for reactions shown in the C_5H_9 PES in Figure 7 in text (CBS-QB3 calculations vs. rate rule estimates).

Table S5: Rate constants at 1 atm for 500- 1800 K for the C_5H_9 PES, entering the surface from the C=CC• + C_2H_4 channel.

Figure S5: Simplified C_5H_{11} potential energy surface calculated at the CBS-QB3 level of theory, showing enthalpies in kcal/mol at 298 K. Numbers in parenthesis are based on rate rule estimates.

Table S6: High pressure limit rate constants for reactions shown in the C_5H_{11} PES in Figure S5 and Figure 10 in text (CBS-QB3 calculations vs. rate rule estimates). The solid lines are obtained from the CBS-QB3 high pressure rate constants, while the dashed lines are obtained from the estimated high pressure rate constants.

Figure S6: Predicted apparent rate constants at 1 atm for the C_5H_{11} PES, entering from the CCC• + C_2H_4 channel.

Table S7: Rate constants at 1 atm and 500- 1800 K for the C_5H_{11} PES, entering from the CCC• + C_2H_4 channel.

Figure S7: Simplified C_7H_{11} potential energy surface calculated at the CBS-QB3 level of theory, showing the enthalpies in kcal/mol at 298 K.

Table S8: High pressure limit rate constants for reactions shown in the C_7H_{11} PES in Figure S7 (CBS-QB3 calculations vs. estimation).

Table S9: Rate constants at 1 atm and 500-1800 K for the C_7H_{11} PES in Figure S7, entering the surface from the allyl + C=CC=C.

Table S10: Rate constants for abstraction by resonant radicals from CH_4 and comparison between TST rate constants and the rate estimation rules.

Table S11: Reaction rate constants for abstraction by resonant radicals from propene and comparison between TST rate constants and the rate estimation rules.

Table S12: High pressure limit rate constants for the reactions shown in the C_6H_{11} PES in Figure 19 in the text.

Table S13: Rate constants at 1 atm and 500- 1800 K for the C_6H_{11} PES, entering the surface from the CC=CC• + C_2H_4 channel.

Table S1: Apparent temperature-and pressure-dependent rate constants for the recombination reactions of two stabilized radicals from 0.001-50 atm and 300-2500 K.

Reactions	Forward				Reverse				Note (Pressure in atm)
	A (cm^3/mol-s)	n	Ea (kcal/mol)	*k* (1000K) (cm^3/mol-s)	A (s^{-1})	n	Ea (kcal/mol)	*k* (1000K) (s^{-1})	
C=CC• + C=CC• ⇄ C=CCCC=C	**1.12E+13**	**0**	**-0.31**	1.31E+13	2.37E+15	0	59.54	2.27E+02	High P limit
	4.99E+52	**-12.66**	**11.48**	1.65E+12	1.35E+55	-12.69	71.38	2.83E+01	0.001
	1.64E+45	**-10.18**	**9.69**	3.70E+12	3.97E+47	-10.20	69.57	6.33E+01	0.01
	7.11E+36	**-7.47**	**7.39**	6.75E+12	1.49E+39	-7.47	67.24	1.15E+02	0.1
	2.23E+28	**-4.77**	**4.81**	1.00E+13	3.94E+30	-4.75	64.63	1.68E+02	1
	7.47E+20	**-2.42**	**2.39**	1.21E+13	1.18E+23	-2.39	62.17	2.00E+02	10
	9.99E+16	**-1.22**	**1.07**	1.27E+13	1.86E+19	-1.22	60.86	2.07E+02	50
C=CC• + CC=CC• ⇄ C=CCCC=CC	**1.12E+13**	**0**	**-0.31**	1.31E+13	5.70E+14	0.00	59.89	4.56E+01	High P limit
	1.23E+55	**-13.29**	**12.76**	2.62E+12	8.92E+56	-13.34	73.05	9.25E+00	0.001
	1.17E+46	**-10.37**	**10.31**	5.16E+12	7.07E+47	-10.39	70.56	1.80E+01	0.01
	1.79E+36	**-7.24**	**7.38**	8.25E+12	8.87E+37	-7.24	67.59	2.86E+01	0.1
	5.63E+26	**-4.25**	**4.34**	1.09E+13	2.37E+28	-4.23	64.52	3.75E+01	1
	1.32E+19	**-1.88**	**1.79**	1.24E+13	6.12E+20	-1.87	61.96	4.15E+01	10
	4.58E+15	**-0.81**	**0.60**	1.27E+13	3.55E+17	-0.87	60.83	4.22E+01	50
C=CC• + C=CC•C ⇄ C=CCC(C)C=C	**1.12E+13**	**0**	**-0.31**	1.31E+13	2.24E+15	0.00	61.44	8.21E+01	High P limit
	1.98E+59	**-14.66**	**13.90**	1.89E+12	5.83E+61	-14.71	75.74	1.21E+01	0.001
	5.37E+50	**-11.86**	**11.68**	4.02E+12	1.34E+53	-11.88	73.49	2.53E+01	0.01
	1.27E+41	**-8.77**	**8.90**	6.96E+12	2.61E+43	-8.77	70.67	4.38E+01	0.1
	1.81E+31	**-5.66**	**5.82**	9.90E+12	3.07E+33	-5.64	67.55	6.15E+01	1
	3.49E+22	**-2.94**	**2.96**	1.19E+13	5.47E+24	-2.91	64.66	7.28E+01	10
	8.84E+17	**-1.52**	**1.39**	1.25E+13	1.70E+20	-1.52	63.11	7.55E+01	50
CC=CC• + CC=CC• ⇄ CC=CCCC=CC	**1.12E+13**	**0**	**-0.31**	1.31E+13	1.15E+15	0	59.51	1.11E+02	High P limit
	1.15E+17	**-1.24**	**1.08**	1.25E+13	1.35E+19	-1.27	60.90	1.03E+02	50
	2.09E+21	**-2.56**	**2.53**	1.20E+13	1.80E+23	-2.54	62.32	9.89E+01	10
	5.68E+29	**-5.20**	**5.31**	1.02E+13	5.08E+31	-5.18	65.12	8.47E+01	1
	3.27E+39	**-8.28**	**8.37**	7.19E+12	3.52E+41	-8.28	68.22	6.07E+01	0.1
	1.37E+49	**-11.36**	**11.16**	4.13E+12	1.81E+51	-11.39	71.05	3.56E+01	0.01
	5.11E+57	**-14.16**	**13.38**	1.96E+12	7.95E+59	-14.22	73.29	1.69E+01	0.001
C=CC•C + C=CC•C ⇄ C=CC(C)C(C)C=C	**1.12E+13**	**0**	**-0.31**	1.31E+13	7.99E+15	0.00	57.09	2.62E+03	High P limit
	4.76E+23	**-3.30**	**3.31**	1.15E+13	3.00E+26	-3.29	60.69	2.25E+03	50
	7.29E+29	**-5.24**	**5.32**	9.87E+12	4.88E+32	-5.23	62.72	1.95E+03	10
	4.02E+39	**-8.32**	**8.34**	6.76E+12	3.24E+42	-8.33	65.77	1.35E+03	1
	1.16E+49	**-11.36**	**11.03**	3.78E+12	1.14E+52	-11.40	68.51	7.62E+02	0.1
	2.18E+57	**-14.08**	**13.10**	1.71E+12	2.52E+60	-14.14	70.61	3.48E+02	0.01
	8.60E+63	**-16.33**	**14.39**	6.21E+11	1.12E+67	-16.41	71.91	1.27E+02	0.001

Note: The forward rate constants are based on literature measurements as discussed in the text; the reverse rate constants are calculated using the principle of microscopic reversibility, using thermochemical parameters for each reactant.

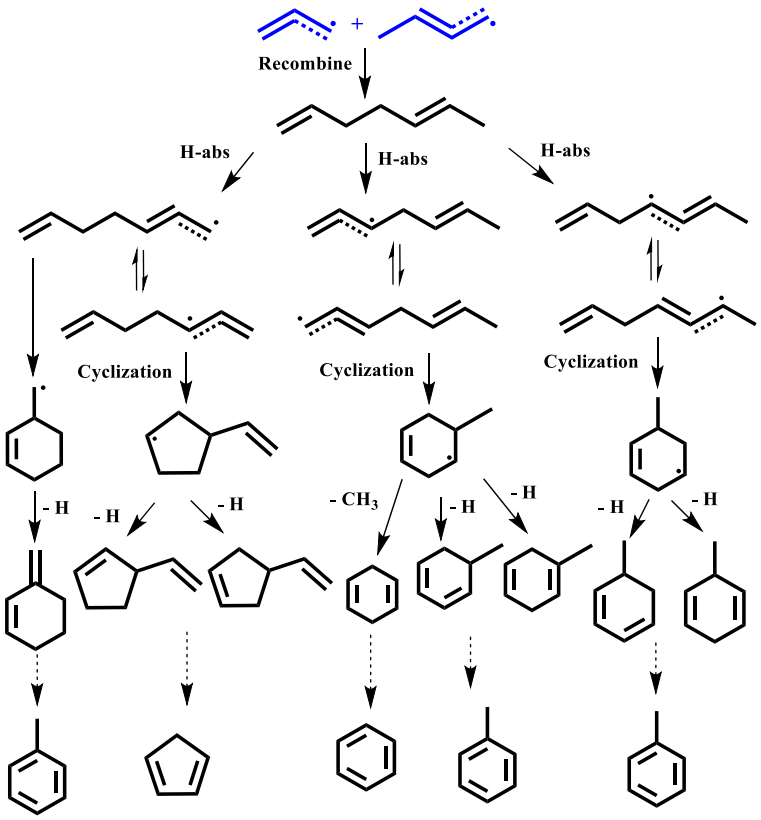

Figure S1: Pathways leading to formation of aromatic species after recombination of methyl-allyl and allyl radicals.

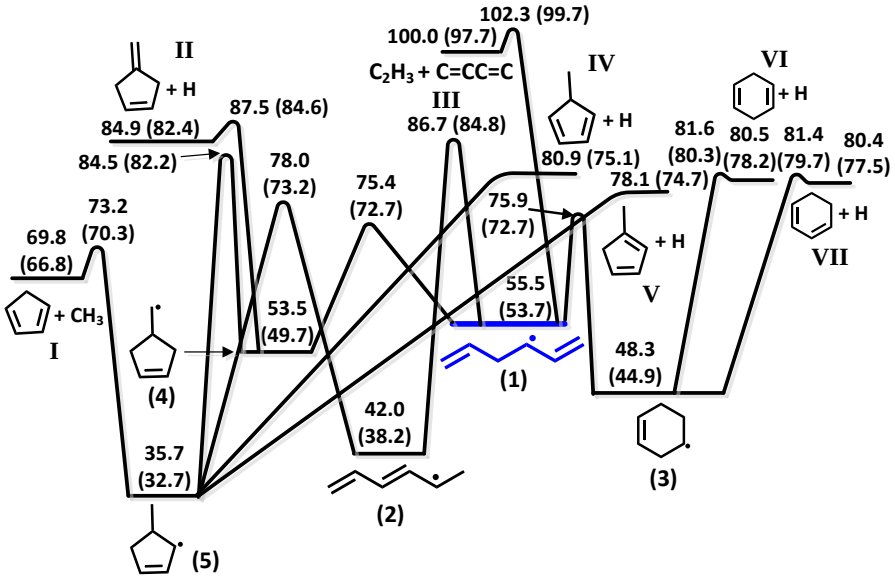

Figure S2: Simplified C_6H_9 PES depicting the energetics of the reaction sequence after hydrogen abstraction from the initially-formed linear adduct in the recombination of two allyl radicals. (The numbers are enthalpies (kcal/mol) at 298K based on CBS-QB3 calculations; the numbers in parenthesis are based on rate rule estimates).

Table S2: High pressure limit rate constants for reactions shown in the C_6H_9 PES in Figure S2 and Figure 5 in text (based on CBS-QB3 calculations).

Reactions	Forward			Reverse		
	A (s^{-1})	Ea (kcal/mol)	*k* (1000K) (s^{-1})	A (s^{-1} or cm^3/mol-s)	Ea (kcal/mol)	*k* (1000K) (s^{-1} or cm^3/mol-s)
C=CCC•C=C <=> 2	1.84E+12	31.3	2.68E+05	1.32E+13	44.8	2.12E+03
C=CCC•C=C <=> 3	1.10E+11	21.1	2.67E+06	5.03E+13	28.8	2.60E+07
C=CCC•C=C <=> 4	4.29E+11	20.9	1.14E+07	4.68E+13	23.4	3.52E+08
C=CCC•C=C <=> III	1.71E+15	45.1	2.35E+05	1.38E+13	2.31	4.30E+12
2 <=> 5	2.45E+12	36.6	2.40E+04	5.30E+13	43.2	1.88E+04
3 <=> VI	2.01E+14	35.0	4.40E+06	4.15E+14	3.71	6.41E+13
3 <=> VII	8.94E+13	34.6	2.44E+06	1.32E+14	3.33	2.47E+13
4 <=> 5	5.84E+12	30.5	1.24E+06	8.28E+12	48.1	2.47E+02
4 <=> II	2.85E+13	35.9	4.01E+05	2.47E+13	4.94	2.05E+12
5 <=> I	9.89E+14	38.9	3.11E+06	1.50E+13	6.83	4.82E+11
5 <=> IV	4.95E+12	46.4	3.57E+02	2.60E+13	2.16	8.76E+12
3 <=> V	1.54E+13	43.0	5.98E+03	2.60E+13	2.16	8.76E+12

Table S3: Rate constants at 1 atm for the reactions shown in the C_6H_9 PES in Figure S2 and Figure 5 in text for the temperature range 300- 2500 K.

Reactions			A (s^{-1})	n	E (kcal/mol)	k (1000K) (s^{-1})	Reactions			A (s^{-1})	n	E (kcal/mol)	k (1000K) (s^{-1})
C=CCC•C=C	<=>	III	2.13E+37	-7.08	51.56	6.65E+04	3	<=>	III	8.11E+48	-10.32	65.18	4.88E+03
C=CCC•C=C	<=>	3	3.90E+41	-9.86	29.57	3.46E+05	3	<=>	VI	8.03E+35	-7.18	40.16	3.86E+05
C=CCC•C=C	<=>	VI	2.90E+41	-9.04	41.53	1.82E+05	3	<=>	VII	8.58E+35	-7.28	39.95	2.24E+05
C=CCC•C=C	<=>	VII	1.70E+41	-9.06	41.32	1.00E+05	3	<=>	4	1.08E+57	-13.93	48.56	4.28E+04
C=CCC•C=C	<=>	4	5.84E+39	-9.31	27.77	6.02E+05	3	<=>	II	1.38E+52	-12.09	59.40	7.43E+02
C=CCC•C=C	<=>	II	3.99E+36	-7.78	42.68	8.25E+03	3	<=>	5	5.29E+61	-15.54	57.95	2.70E+02
C=CCC•C=C	<=>	2	2.94E+36	-7.63	38.84	1.24E+05	3	<=>	I	8.14E+55	-12.90	62.29	3.77E+03
C=CCC•C=C	<=>	5	1.57E+45	-11.02	39.86	2.66E+03	3	<=>	V	1.24E+51	-12.15	62.29	1.03E+01
C=CCC•C=C	<=>	I	2.12E+39	-8.29	45.03	4.09E+04	3	<=>	IV	1.45E+48	-11.54	62.40	7.76E-01
C=CCC•C=C	<=>	V	6.95E+34	-7.62	45.35	1.15E+02	4	<=>	III	2.41E+43	-8.75	58.26	2.45E+04
C=CCC•C=C	<=>	IV	1.97E+32	-7.11	45.80	8.84E+00	4	<=>	VI	4.92E+51	-11.86	51.23	8.04E+04
2	<=>	III	1.88E+43	-8.47	73.41	6.47E+01	4	<=>	VII	4.19E+51	-11.93	51.14	4.45E+04
2	<=>	3	1.48E+49	-11.64	60.42	1.10E+01	4	<=>	II	3.67E+25	-4.50	36.91	9.86E+03
2	<=>	VI	9.97E+49	-11.10	68.66	4.94E+01	4	<=>	5	4.29E+46	-11.49	37.64	8.60E+03
2	<=>	VII	7.28E+49	-11.15	68.59	2.65E+01	4	<=>	I	1.36E+33	-6.58	40.17	4.15E+04
2	<=>	4	2.07E+43	-9.87	57.36	1.45E+01	4	<=>	V	5.57E+27	-5.64	40.36	1.01E+02
2	<=>	II	1.24E+43	-9.27	67.63	3.21E+00	4	<=>	IV	5.17E+24	-4.98	40.89	6.97E+00
2	<=>	5	1.21E+43	-9.98	44.90	2.14E+03	5	<=>	III	3.89E+41	-8.44	77.70	1.96E-01
2	<=>	I	8.69E+32	-5.99	49.91	1.13E+04	5	<=>	VI	5.44E+54	-12.92	75.35	3.20E-01
2	<=>	V	4.88E+28	-5.38	50.83	2.81E+01	5	<=>	VII	5.22E+54	-13.00	75.32	1.74E-01
2	<=>	IV	4.98E+26	-5.01	52.02	1.99E+00	5	<=>	II	7.53E+32	-6.90	62.65	3.06E-02
							5	<=>	I	6.50E+42	-8.96	46.77	5.03E+05
							5	<=>	V	7.82E+39	-8.70	50.15	6.53E+02
							5	<=>	IV	1.24E+38	-8.37	52.70	2.79E+01

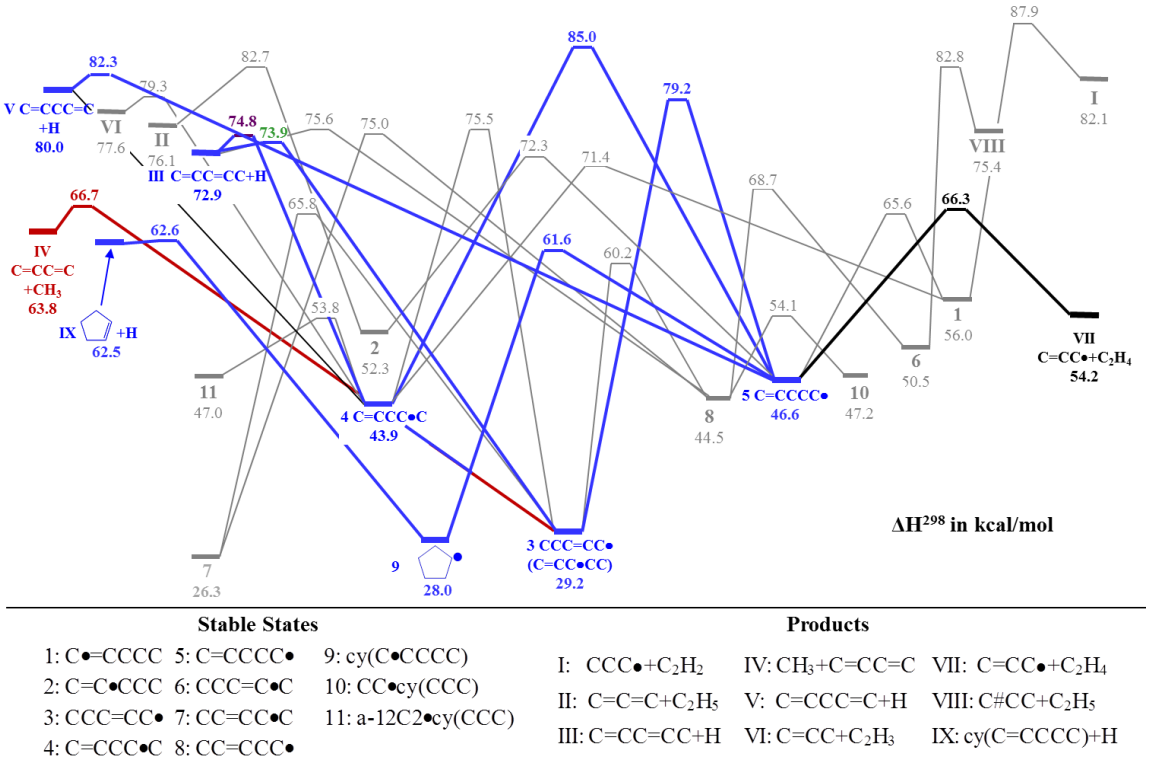

Figure S3: A more complete C_5H_9 PES by CBS-QB3.

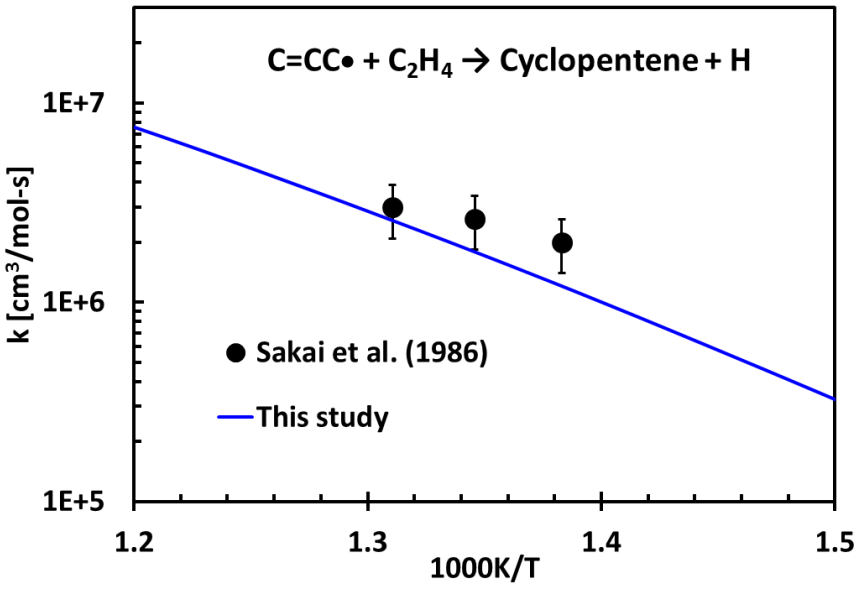

Figure S4: Comparison of the rate constant for formation of cyclopentene + H from the reaction allyl + ethylene calculated in this study with literature values at 1 atm.

Table S4: High pressure limit rate constants for reactions shown in the C_5H_9 PES in Figure 7 in text (CBS-QB3 calculations vs. rate rule estimates).

	Forward reaction			Reverse reaction				Note
	Rate constants from CBS-QB3 calculation							
Reactions	A (s^{-1} or cm^3/mol-s)	Ea (kcal/mol)	k(1000K) (s^{-1} cm^3/mol-s)	A (s^{-1} or cm^3/mol-s)	n	Ea (kcal/mol)	k(1000K) (s^{-1} cm^3/mol-s)	
I ⇄ 1	2.13E+12	14.7	1.28E+09	1.48E+13	0	20.7	4.44E+08	
1 ⇄ II	1.44E+13	36.9	1.22E+05	9.74E+13	0	3.66	1.54E+13	
1 ⇄ 4	7.67E+10	16.4	1.99E+07	3.28E+13	0	14.3	2.46E+10	
4 ⇄ VI	3.00E+14	38.7	1.03E+06	1.30E+13	0	1.6	5.93E+12	
1 ⇄ 5	7.69E+10	15.4	3.30E+07	1.70E+14	0	34.5	4.80E+06	
5 ⇄ IV	4.41E+14	36.1	5.71E+06	1.78E+14	0	2.18	5.93E+13	All rate constants are based on CBS-QB3 calculation
1 ⇄ 3	1.62E+12	32.2	1.50E+05	1.27E+13	0	49.6	1.84E+02	
3 ⇄ III	1.62E+14	46.6	1.03E+04	1.02E+14	0	3.02	2.23E+13	
3 ⇄ V	6.16E+14	38.0	2.95E+06	5.82E+12	0	5.44	3.76E+11	
1 ⇄ 2	9.01E+12	38.1	4.26E+04	1.10E+13	0	41.3	1.01E+04	
2 ⇄ II	2.38E+13	39.2	6.52E+04	2.60E+13	0	1.56	1.19E+13	
2 ⇄ III	1.45E+13	33.9	5.72E+05	5.84E+13	0	4.39	6.39E+12	
	Rate constants based on estimation techniques							
I ⇄ 1	**2.00E+12**	**13.1**	2.80E+09	1.09E+13	0	20.3	3.90E+08	Estimated A-factor, Ea from CBS-QB3 calculation of Saeys et al. (2004)
1 ⇄ II	1.95E+12	36.7	1.80E+04	**1.26E+12**	**0.29**	**2.77**	2.36E+12	Rate rules for H + larger olefin
1 ⇄ 4	**4.21E+10**	**12.9**	6.35E+07	8.52E+12	0.00	8.98	9.26E+10	4-member ring, Estrain=5, Eaddion analogy to C_2H_5+C_3H_6_CCC(C)C. at 1000 K
4 ⇄ VI	3.71E+13	35.1	7.73E+05	**1.26E+12**	**0.29**	**2.77**	2.36E+12	Rate rules for H + larger olefin
1 ⇄ 5	**4.21E+10**	**15.0**	2.21E+07	3.37E+14	0	33.4	1.65E+07	5-member ring, E_{strain}=6, E_{addion} analogy to C_2H_5+C_3H_6_2-C_5H_{11} at 1000 K
5 ⇄ IV	1.26E+14	36.5	1.31E+06	**1.26E+12**	**0.29**	**2.77**	2.36E+12	Rate rules for H + larger olefin
1 ⇄ 3	**2.99E+11**	**32.9**	1.91E+04	3.37E+14	0	48.4	8.99E+03	1,3-H transfer, E_{strain}=22.8, E_{abs} analogy to C_2H_5+C_3H_6_C_2H_6+aC_3H_5 at 1000 K
3 ⇄ III	9.70E+13	45.0	1.42E+04	**1.26E+12**	**0.29**	**2.77**	2.36E+12	Rate rules for H + larger olefin
3 ⇄ V	1.25E+15	36.8	1.14E+07	**5.71E+12**	**0**	**5.49**	3.61E+11	From CBS-QB3 calculation (Saeys at el.)
1 ⇄ 2	**1.96E+13**	**38.7**	6.74E+04	1.95E+13	0	41.8	1.41E+04	1,2-H transfer, E_{strain}=24.4, E_{abs} analogy to C_2H_5+C_3H_8_C_2H_6+iC_3H_7 at 1000 K
2 ⇄ II	4.01E+12	39.6	8.57E+03	**2.52E+12**	**0.29**	**2.77**	4.72E+12	Rate rules for H + larger olefin
2 ⇄ III	2.56E+12	32.6	1.92E+05	**1.26E+12**	**0.29**	**2.77**	2.36E+12	Rate rules for H + larger olefin

Note: The bold blue are the initially estimated numbers; the reverse rate constants are calculated from the thermodynamic data.

Table S5: Rate constants at 1 atm for 500- 1800 K for the C_5H_9 PES, entering from the C=CC• + C_2H_4.

Reactions			A (s^{-1} or cm^3/mol-s)	n	Ea (kcal/mol)	*k* (1000K) (s^{-1} or cm^3/mol-s)
I	<=>	(3)	1.41E+48	-11.83	37.87	2.37E+04
I	<=>	III	4.23E+28	-4.89	38.25	3.91E+05
I	<=>	IV	6.90E+19	-2.68	38.02	3.09E+03
I	<=>	(1)	5.30E+26	-5.02	16.49	1.13E+08
I	<=>	V	6.41E+16	-1.31	33.58	3.44E+05
I	<=>	(2)	9.45E+42	-9.61	43.74	3.89E+04
I	<=>	IV	1.89E+37	-7.09	51.61	5.30E+04
I	<=>	V	1.40E+34	-6.23	52.37	1.02E+04
I	<=>	(5)	8.31E+66	-17.33	36.70	8.19E+06
I	<=>	II	1.13E+42	-9.01	34.21	3.61E+07
I	<=>	(4)	6.65E+24	-5.29	17.97	1.03E+05
I	<=>	VI	4.14E+12	-0.55	34.50	2.71E+03
(3)	<=>	III	2.32E+56	-12.97	53.12	6.92E+05
(3)	<=>	IV	2.20E+50	-11.61	57.46	8.73E+02
(3)	<=>	(1)	8.00E+41	-10.23	52.66	4.92E-01
(3)	<=>	V	2.75E+29	-6.31	59.82	2.75E-03
(3)	<=>	(2)	5.99E+50	-13.09	68.21	3.94E-04
(3)	<=>	IV	6.44E+42	-10.06	73.56	3.53E-04
(3)	<=>	V	6.57E+37	-8.68	73.13	5.93E-05
(3)	<=>	(5)	1.01E+68	-18.50	64.12	3.04E-02
(3)	<=>	II	6.54E+58	-14.92	66.65	3.03E-01
(3)	<=>	(4)	1.46E+39	-10.31	52.79	5.04E-04
(3)	<=>	VI	3.94E+22	-4.81	58.95	1.92E-05
(1)	<=>	III	6.90E+22	-3.90	35.53	2.35E+03
(1)	<=>	IV	6.11E+11	-1.07	34.28	1.20E+01
(1)	<=>	V	6.57E+07	0.57	29.14	1.44E+03
(1)	<=>	(2)	2.61E+29	-6.22	38.40	2.29E+02
(1)	<=>	IV	4.50E+23	-3.82	45.92	1.40E+02
(1)	<=>	V	6.21E+19	-2.77	46.37	2.19E+01
(1)	<=>	(5)	3.83E+60	-15.73	31.93	2.51E+06
(1)	<=>	II	1.47E+46	-10.81	34.50	1.56E+06
(1)	<=>	(4)	6.82E+28	-7.01	15.17	3.00E+04
(1)	<=>	VI	8.41E+02	1.53	29.93	9.09E+00
(2)	<=>	III	6.09E+38	-8.66	56.63	2.64E+00
(2)	<=>	IV	2.28E+30	-6.62	55.42	2.42E-02
(2)	<=>	V	1.17E+30	-6.01	53.07	2.69E+00
(2)	<=>	IV	2.49E+40	-8.41	44.35	3.00E+05
(2)	<=>	V	3.41E+41	-8.77	49.43	2.56E+04
(2)	<=>	(5)	4.88E+50	-13.14	49.95	2.19E+00
(2)	<=>	II	1.29E+48	-11.34	55.72	8.18E+01
(2)	<=>	(4)	3.93E+26	-6.20	41.93	6.69E-02
(2)	<=>	VI	7.57E+24	-5.00	52.80	2.21E-02

(5)	<=>	III	1.08E+59	-14.24	69.72	1.21E+01
(5)	<=>	IV	8.89E+45	-10.87	67.08	4.71E-02
(5)	<=>	V	8.96E+41	-9.21	61.93	5.91E+00
(5)	<=>	IV	2.26E+52	-12.04	76.05	4.10E-01
(5)	<=>	V	6.14E+47	-10.80	76.09	5.59E-02
(5)	<=>	II	6.88E+56	-13.26	50.66	9.34E+05
(5)	<=>	(4)	2.15E+68	-17.82	56.85	2.79E+02
(5)	<=>	VI	4.92E+35	-7.89	61.87	3.19E-02
(4)	<=>	III	1.50E+26	-4.89	36.84	2.89E+03
(4)	<=>	IV	1.34E+15	-2.05	35.63	1.54E+01
(4)	<=>	V	1.75E+11	-0.43	30.53	1.84E+03
(4)	<=>	IV	4.38E+27	-4.99	47.54	1.86E+02
(4)	<=>	V	5.59E+23	-3.93	47.99	2.97E+01
(4)	<=>	II	3.05E+50	-12.10	36.39	1.74E+06
(4)	<=>	VI	1.33E+02	2.31	29.09	4.78E+02

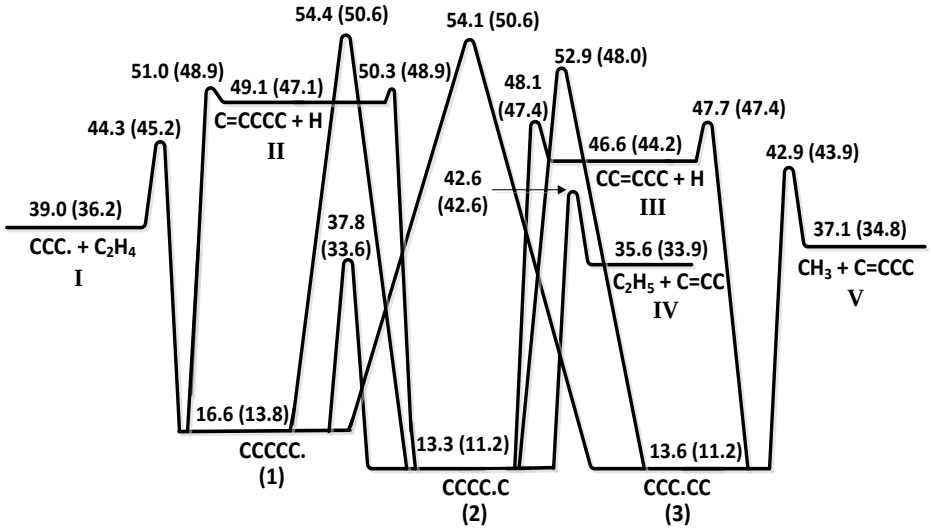

Figure S5: Simplified C_5H_{11} potential energy surface calculated at the CBS-QB3 level of theory, showing enthalpies in kcal/mol at 298 K. Numbers in parenthesis are based on rate rule estimates.

Table S6: High pressure limit rate constants for reactions shown in the C_5H_{11} PES in Figure S5 and Figure 10 in text (CBS-QB3 calculations vs. rate rule estimates). The solid lines are obtained from the CBS-QB3 high pressure rate constants, while the dashed lines are obtained from the estimated high pressure rate constants.

Reactions	Forward reaction			Reverse reaction			Note
	Rate constants by CBS-QB3 calculation						
	A (s^{-1} or cm^3/mol-s)	Ea (kcal/mol)	*k* (1000K) (s^{-1} or cm^3/mol-s)	A (s^{-1} or cm^3/mol-s)	Ea (kcal/mol)	*k* (1000K) (s^{-1} or cm^3/mol-s)	
I ⇄ 1	1.32E+12	8.52	1.81E+10	1.96E+13	28.5	1.13E+07	CBS-QB3 calculation
1 ⇄ II	2.03E+13	36.1	2.57E+05	1.20E+14	4.35	1.34E+13	
1 ⇄ 2 (Duplicate reaction)	3.27E+10	20.8	9.22E+05	1.68E+11	24.6	6.87E+05	
1 ⇄ 2 (Duplicate reaction)	1.79E+12	37.3	1.25E+04	9.21E+12	41.1	9.36E+03	
1 ⇄ 3	4.77E+11	36.7	4.40E+03	1.84E+12	40.3	2.85E+03	
2 ⇄ IV	4.82E+13	28.9	2.28E+07	4.74E+12	8.27	7.39E+10	
2 ⇄ II	1.56E+14	38.6	5.78E+05	1.80E+14	2.96	4.05E+13	
2 ⇄ III	4.29E+13	36.8	3.89E+05	8.80E+13	3.86	1.26E+13	
2 ⇄ 3	5.50E+12	39.2	1.45E+04	4.14E+12	39.0	1.26E+04	
3 ⇄ III	4.06E+13	36.2	4.93E+05	1.10E+14	3.56	1.83E+13	
3 ⇄ V	1.43E+14	30.9	2.46E+07	6.08E+12	8.99	6.57E+10	
	Rate constants from estimation						
I ⇄ 1	**2.11E+12**	**8.99**	2.29E+10	**2.12E+13**	**28.6**	1.18E+07	From CBS-QB3 calculation
1 ⇄ II	1.58E+13	36.0	2.11E+05	**1.16E+13**	**3.23**	2.28E+12	H inner addition to C=CC by Curran 2006
1 ⇄ 2 (Duplicate reaction)	**2.99E+11**	**19.1**	1.99E+07	2.86E+11	22.1	4.17E+06	1,4-H transfer, E_{strain}=5.8, E_{abs} analogy to CH_3+C_2H_6_CH_4+C_2H_5 at 1000 K
1 ⇄ 2 (Duplicate reaction)	**1.96E+13**	**37.7**	1.12E+05	1.87E+13	40.7	2.33E+04	1,2-H transfer, E_{strain}=24.4, E_{abs} analogy to CH_3+C_2H_6_CH_4+C_2H_5 at 1000 K
1 ⇄ 3	**2.42E+12**	**36.1**	3.09E+04	4.60E+12	39.1	1.28E+04	1,3-H transfer, E_{strain}=22.8, E_{abs} analogy to CH_3+C_2H_6_CH_4+C_2H_5 at 1000 K
2 ⇄ IV	5.33E+13	29.0	2.39E+07	**7.38E+12**	**8.71**	9.20E+10	From CBS-QB3 calculation
2 ⇄ II	2.55E+13	37.6	1.50E+05	**1.96E+13**	**1.84**	7.77E+12	H inner addition to C=CC by Curran 2006
2 ⇄ III	1.51E+13	39.0	4.40E+04	**1.16E+13**	**3.23**	2.28E+12	H inner addition to C=CC by Curran 2006
2 ⇄ 3	**1.96E+13**	**37.7**	1.12E+05	3.91E+13	37.7	2.23E+05	1,2-H transfer, E_{strain}=24.4, E_{abs} analogy to CH_3+C_2H_6_CH_4+C_2H_5 at 1000 K
3 ⇄ III	3.01E+13	39.0	8.78E+04	**1.16E+13**	**3.23**	2.28E+12	H inner addition to C=CC by Curran 2006
3 ⇄ V	1.79E+14	30.8	3.24E+07	**4.95E+12**	**8.56**	6.64E+10	From CBS-QB3 calculation

Note: The bold blue are the initially estimated numbers; reverse rate constants are calculated from the thermodynamic data.

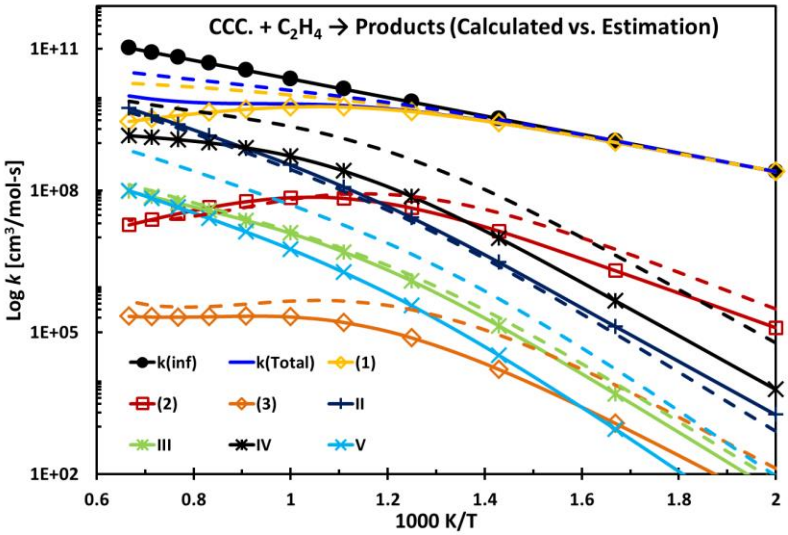

Figure S6: Predicted apparent rate constants at 1 atm for the C_5H_{11} PES, entering from the CCC• + C_2H_4 channel.

Table S7: Rate constants at 1 atm and 500- 1800 K for the C_5H_{11} PES, from the CCC• + C_2H_4 channel.

Reactions			A (s^{-1} or cm^3/mol-s)	*n*	Ea (kcal/mol)	*k* (1000K) (s^{-1} or cm^3/mol-s)	Note
I	<=>	1	2.69E+24	-4.36	9.48	1.92E+09	
I	<=>	II	4.82E+20	-2.41	25.3	8.50E+07	Duplicate reaction
I	<=>	2	7.10E+54	-13.2	27.7	1.78E+09	Duplicate reaction
I	<=>	II	8.77E+39	-7.94	34.2	4.42E+08	Duplicate reaction
I	<=>	III	4.77E+41	-8.58	34.3	2.79E+08	Duplicate reaction
I	<=>	IV	1.31E+52	-11.4	35.5	1.11E+10	Duplicate reaction
I	<=>	2	1.13E+32	-7.12	25.3	1.42E+05	Duplicate reaction
I	<=>	II	2.85E+22	-3.24	33.4	2.78E+05	Duplicate reaction
I	<=>	III	3.91E+23	-3.70	33.4	1.57E+05	Duplicate reaction
I	<=>	IV	3.14E+31	-5.83	33.9	3.83E+06	Duplicate reaction
I	<=>	3	1.79E+54	-13.6	35.6	5.50E+05	Duplicate reaction
I	<=>	III	3.80E+36	-7.55	38.2	3.78E+05	Duplicate reaction
I	<=>	V	1.69E+44	-9.51	39.5	1.20E+07	
1	<=>	II	1.10E+17	-1.95	32.4	1.28E+04	Duplicate reaction
1	<=>	2	9.63E+52	-12.8	34.1	1.11E+07	Duplicate reaction
1	<=>	II	4.23E+41	-8.92	45.2	9.87E+04	Duplicate reaction
1	<=>	III	1.43E+44	-9.77	45.5	7.70E+04	Duplicate reaction
1	<=>	IV	2.95E+56	-13.1	46.9	7.46E+06	Duplicate reaction
1	<=>	2	2.17E+34	-8.13	37.3	6.44E+01	Duplicate reaction
1	<=>	II	2.84E+17	-2.36	41.7	1.74E+01	Duplicate reaction
1	<=>	III	1.46E+19	-2.99	41.9	1.11E+01	Duplicate reaction
1	<=>	IV	3.60E+29	-5.80	43.4	4.51E+02	Duplicate reaction
1	<=>	3	1.55E+58	-14.9	49.6	4.01E+02	Duplicate reaction
1	<=>	III	2.19E+38	-8.57	50.3	4.32E+01	Duplicate reaction
1	<=>	V	6.84E+47	-11.0	52.6	2.00E+03	Duplicate reaction
2	<=>	II	6.53E+41	-9.60	50.8	8.25E+01	Duplicate reaction
2	<=>	II	8.70E+33	-6.68	42.2	4.74E+04	Duplicate reaction
2	<=>	III	2.74E+35	-7.25	41.6	3.89E+04	Duplicate reaction
2	<=>	IV	1.94E+42	-9.07	38.2	5.08E+06	Duplicate reaction
2	<=>	2	3.14E+53	-14.0	53.6	5.25E-01	Duplicate reaction
2	<=>	II	6.64E+33	-7.60	54.9	1.06E-01	Duplicate reaction
2	<=>	III	1.34E+36	-8.38	55.5	6.98E-02	Duplicate reaction
2	<=>	IV	2.20E+48	-11.7	58.4	3.13E+00	Duplicate reaction
2	<=>	3	4.09E+54	-13.8	49.2	2.18E+02	Duplicate reaction
2	<=>	III	4.74E+37	-8.35	52.2	1.69E+01	Duplicate reaction
2	<=>	V	4.73E+46	-10.6	54.0	8.31E+02	Duplicate reaction
2	<=>	II	2.07E+24	-4.47	48.7	1.77E+00	Duplicate reaction
2	<=>	II	1.56E+42	-9.57	57.0	1.05E+01	Duplicate reaction
2	<=>	III	3.85E+44	-10.4	57.7	7.05E+00	Duplicate reaction
2	<=>	IV	1.01E+57	-13.7	60.7	3.37E+02	Duplicate reaction
2	<=>	II	7.64E+36	-7.59	43.3	4.50E+04	Duplicate reaction
2	<=>	III	2.27E+38	-8.15	42.8	3.69E+04	Duplicate reaction
2	<=>	IV	1.06E+45	-9.92	39.3	4.85E+06	Duplicate reaction
2	<=>	3	1.63E+57	-14.6	50.2	2.09E+02	Duplicate reaction
2	<=>	III	4.80E+40	-9.27	53.3	1.60E+01	Duplicate reaction
2	<=>	V	4.36E+49	-11.6	55.1	7.92E+02	Duplicate reaction
3	<=>	II	3.84E+28	-5.98	50.1	5.05E-01	Duplicate reaction
3	<=>	II	3.52E+40	-9.16	53.8	2.00E+01	Duplicate reaction
3	<=>	III	8.53E+42	-9.97	54.3	1.38E+01	Duplicate reaction
3	<=>	IV	2.01E+55	-13.3	57.0	7.57E+02	Duplicate reaction
3	<=>	II	9.43E+39	-9.02	53.5	1.72E+01	Duplicate reaction
3	<=>	III	2.38E+42	-9.83	54.0	1.18E+01	Duplicate reaction
3	<=>	IV	6.99E+54	-13.2	56.7	6.57E+02	Duplicate reaction
3	<=>	III	6.32E+43	-9.79	44.6	4.84E+04	Duplicate reaction
3	<=>	V	1.18E+49	-11.1	42.5	4.32E+06	

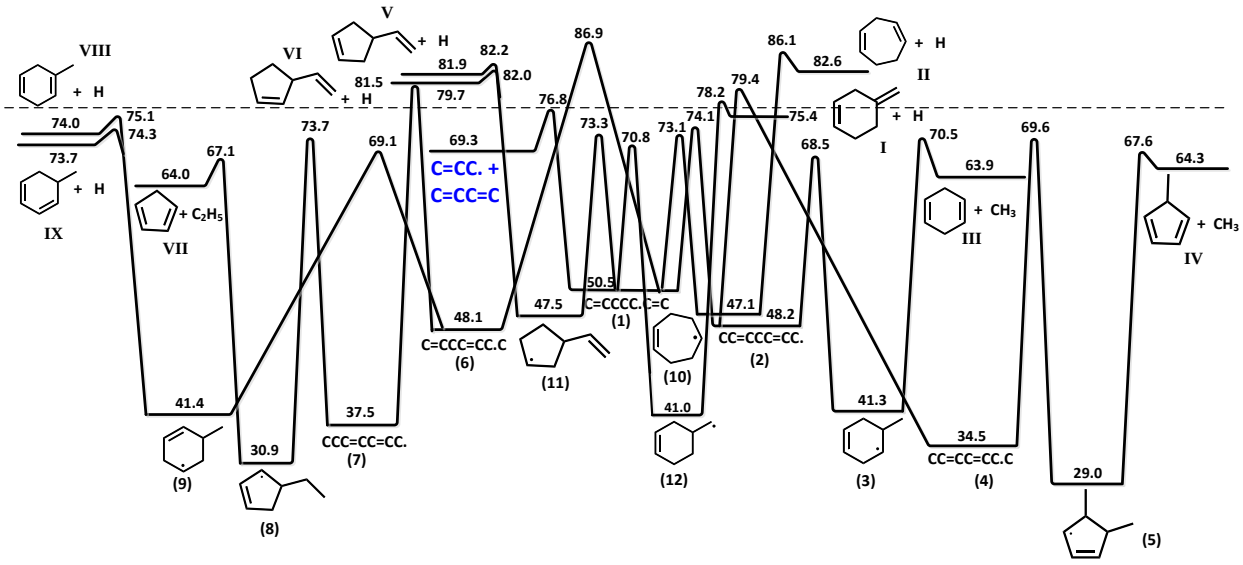

Figure S7: Simplified C_7H_{11} potential energy surface calculated at the CBS-QB3 level of theory, showing the enthalpies in kcal/mol at 298 K. (Note that this is the same as Figure 12 in the text, however the numbering of the product channels differs. This numbering corresponds to Tables S8 and S9 below.)

Table S8: High pressure limit rate constants for reactions shown in the C_7H_{11} PES in Figure S7 (CBS-QB3 calculations).

Reactions	Forward			Reverse		
	A (s^{-1} or cm^3/mol-s)	Ea (kcal/mol)	*k* (1000K) (s^{-1} or cm^3/mol-s)	A (s^{-1} or cm^3/mol-s)	Ea (kcal/mol)	*k* (1000K) (s^{-1} or cm^3/mol-s)
C=CC• + C=CC=C <=> 1	1.76E+12	11.06	6.71E+09	2.74E+13	28.11	1.95E+07
1 <=> 2	5.41E+11	24.01	3.03E+06	1.13E+12	26.40	1.91E+06
2 <=> 3	1.04E+11	21.25	2.34E+06	7.54E+13	28.46	4.51E+07
3 <=> III	5.44E+14	30.25	1.32E+08	1.32E+13	9.89	9.08E+10
2 <=> 4	1.77E+12	31.15	2.73E+05	1.41E+13	44.97	2.07E+03
4 <=> 5	1.78E+12	35.63	2.88E+04	5.08E+13	41.10	5.23E+04
5 <=> IV	1.95E+15	40.00	3.49E+06	1.52E+13	6.68	5.25E+11
1 <=> 6	3.77E+12	35.95	5.18E+04	1.34E+13	38.71	4.60E+04
6 <=> 7	5.25E+12	31.69	6.17E+05	1.38E+13	41.91	9.45E+03
7 <=> 8	2.33E+12	36.95	1.94E+04	5.64E+13	43.81	1.48E+04
8 <=> VII	3.02E+14	36.99	2.46E+06	2.15E+13	6.78	7.07E+11
6 <=> 9	1.33E+11	22.06	2.00E+06	5.49E+13	28.72	2.88E+07
9 <=> VIII	8.11E+13	34.83	1.96E+06	4.34E+13	3.12	9.04E+12
9 <=> IX	8.14E+13	34.79	2.01E+06	6.90E+13	3.28	1.32E+13
1 <=> 10	7.75E+09	23.17	6.65E+04	1.68E+13	27.12	1.98E+07
10 <=> II	2.44E+14	38.23	1.06E+06	8.00E+13	3.50	1.37E+13
1 <=> 11	4.94E+10	23.49	3.61E+05	1.92E+13	26.72	2.75E+07
11 <=> V	2.51E+14	36.80	2.25E+06	1.25E+14	3.42	2.23E+13
11 <=> VI	4.10E+14	36.60	4.07E+06	1.57E+14	2.90	3.65E+13
1 <=> 12	1.22E+11	20.32	4.39E+06	1.67E+14	32.59	1.25E+07
12 <=> I	1.72E+14	39.96	3.16E+05	2.06E+14	3.92	2.85E+13

Table S9: Rate constants from 500- 1800 K at 1 atm for the C_7H_{11} PES (Figure S7), from allyl + C=CC=C.

Reactions			A (s^{-1} or cm^3/mol-s)	n	Ea (kcal/mol)	*k* (1000K) (s^{-1} or cm^3/mol-s)
C=CC• + C=CC=C	<=>	1	1.47E+31	-6.00	17.26	2.51E+09
C=CC• + C=CC=C	<=>	2	1.80E+52	-11.94	36.63	2.70E+08
C=CC• + C=CC=C	<=>	6	2.23E+44	-9.59	39.77	7.51E+06
C=CC• + C=CC=C	<=>	10	1.51E+57	-14.34	36.56	1.51E+06
C=CC• + C=CC=C	<=>	II	3.04E+54	-12.68	48.27	7.86E+05
C=CC• + C=CC=C	<=>	11	2.64E+60	-15.13	37.48	7.03E+06
C=CC• + C=CC=C	<=>	VI	5.01E+59	-13.99	49.38	8.37E+06
C=CC• + C=CC=C	<=>	V	1.69E+59	-13.92	49.36	4.66E+06
C=CC• + C=CC=C	<=>	12	1.08E+63	-15.83	36.03	4.62E+07
C=CC• + C=CC=C	<=>	I	3.76E+57	-13.39	46.23	2.00E+07
C=CC• + C=CC=C	<=>	3	1.42E+74	-19.52	46.69	2.36E+05
C=CC• + C=CC=C	<=>	III	4.93E+69	-16.77	53.16	5.82E+07
C=CC• + C=CC=C	<=>	4	4.80E+69	-16.82	55.12	1.47E+07
C=CC• + C=CC=C	<=>	5	1.07E+82	-21.16	63.83	3.88E+04
C=CC• + C=CC=C	<=>	IV	6.25E+81	-19.81	72.57	3.12E+06
C=CC• + C=CC=C	<=>	7	9.41E+66	-15.90	58.89	2.47E+06
C=CC• + C=CC=C	<=>	9	1.39E+59	-14.58	47.74	9.26E+04
C=CC• + C=CC=C	<=>	IX	1.91E+64	-15.20	59.53	4.56E+05
C=CC• + C=CC=C	<=>	VIII	1.71E+64	-15.19	59.53	4.48E+05
C=CC• + C=CC=C	<=>	8	1.07E+73	-18.23	65.71	9.45E+03
C=CC• + C=CC=C	<=>	VII	2.23E+79	-18.95	76.82	5.12E+05
1	<=>	2	1.27E+37	-7.93	33.09	1.17E+06
1	<=>	6	1.09E+34	-6.97	41.90	9.42E+03
1	<=>	10	1.59E+44	-10.82	34.78	1.36E+04
1	<=>	II	5.42E+49	-11.69	53.68	8.32E+02
1	<=>	11	1.92E+47	-11.53	35.98	6.92E+04
1	<=>	VI	1.63E+55	-13.05	55.11	1.02E+04
1	<=>	V	5.56E+54	-12.98	55.11	5.57E+03
1	<=>	12	1.26E+52	-12.87	34.61	8.14E+05
1	<=>	I	3.38E+52	-12.31	50.57	3.42E+04
1	<=>	3	5.29E+66	-17.68	48.69	1.06E+03
1	<=>	III	1.48E+62	-15.00	55.92	8.82E+04
1	<=>	4	2.65E+56	-13.32	56.16	1.49E+04
1	<=>	5	1.15E+74	-19.13	68.97	3.80E+01
1	<=>	IV	3.41E+72	-17.52	77.27	1.20E+03
1	<=>	7	9.07E+52	-12.19	60.87	1.24E+03
1	<=>	9	4.54E+53	-13.27	53.55	1.34E+02
1	<=>	IX	7.87E+56	-13.48	64.58	2.17E+02
1	<=>	VIII	6.97E+56	-13.47	64.57	2.13E+02
1	<=>	8	1.61E+62	-15.41	70.35	3.97E+00
1	<=>	VII	2.05E+67	-15.86	80.91	1.07E+02

2	<=>	6	7.74E+51	-11.96	59.69	8.92E+02
2	<=>	10	3.80E+64	-16.54	56.66	3.67E+02
2	<=>	II	3.16E+64	-15.81	69.32	8.44E+01
2	<=>	11	3.50E+67	-17.24	57.56	1.77E+03
2	<=>	VI	6.70E+69	-17.13	70.63	9.71E+02
2	<=>	V	2.20E+69	-17.06	70.60	5.37E+02
2	<=>	12	3.54E+71	-18.34	56.68	1.35E+04
2	<=>	I	2.38E+68	-16.72	67.69	2.64E+03
2	<=>	3	1.74E+50	-12.89	31.03	5.96E+04
2	<=>	III	1.46E+37	-7.66	36.76	1.41E+06
2	<=>	4	4.12E+28	-5.11	37.07	1.54E+05
2	<=>	5	3.49E+53	-12.95	55.55	3.54E+02
2	<=>	IV	8.14E+53	-11.83	66.26	8.72E+03
2	<=>	7	6.03E+70	-17.21	77.10	1.90E+02
2	<=>	9	3.31E+67	-17.16	68.46	1.20E+01
2	<=>	IX	7.15E+71	-17.67	79.26	3.27E+01
2	<=>	VIII	6.38E+71	-17.66	79.25	3.21E+01
2	<=>	8	1.00E+77	-19.59	84.19	6.60E-01
2	<=>	VII	7.77E+81	-19.99	94.11	2.25E+01
3	<=>	1	4.81E+73	-18.54	63.88	1.22E+04
3	<=>	2	1.87E+62	-15.33	44.41	3.79E+06
3	<=>	6	2.09E+75	-18.96	80.92	5.60E+00
3	<=>	10	4.68E+92	-24.80	80.65	4.42E+00
3	<=>	II	1.29E+89	-23.16	91.20	5.01E-01
3	<=>	11	1.84E+95	-25.37	81.45	2.20E+01
3	<=>	VI	3.46E+94	-24.50	92.65	6.09E+00
3	<=>	V	1.07E+94	-24.42	92.61	3.35E+00
3	<=>	I	1.24E+94	-24.38	90.08	1.86E+01
3	<=>	III	2.61E+57	-13.67	43.27	8.86E+06
3	<=>	4	1.37E+59	-14.15	61.69	1.56E+03
3	<=>	5	2.38E+80	-20.91	78.48	3.08E+00
3	<=>	IV	7.97E+76	-18.74	86.99	4.43E+01
3	<=>	7	3.05E+91	-23.43	97.22	8.41E-01
3	<=>	9	4.20E+91	-24.33	90.31	7.87E-02
3	<=>	IX	5.52E+94	-24.54	100.38	1.44E-01
3	<=>	VIII	4.90E+94	-24.53	100.37	1.42E-01
3	<=>	8	1.57E+98	-25.94	104.85	2.75E-03

4	<=>	1	2.12E+57	-13.22	72.41	7.05E+01
4	<=>	2	2.48E+29	-5.06	50.91	1.20E+03
4	<=>	6	1.35E+69	-16.58	90.24	4.45E-01
4	<=>	10	3.04E+77	-19.94	86.58	5.29E-02
4	<=>	II	4.20E+79	-19.81	98.39	4.66E-02
4	<=>	11	5.01E+79	-20.44	86.94	2.31E-01
4	<=>	VI	2.45E+83	-20.70	98.83	4.85E-01
4	<=>	V	9.03E+82	-20.64	98.81	2.72E-01
4	<=>	12	7.21E+80	-20.71	85.19	1.30E+00
4	<=>	I	1.17E+82	-20.30	96.57	1.10E+00
4	<=>	3	1.75E+55	-13.76	63.75	1.08E+00
4	<=>	III	1.06E+54	-11.96	72.74	1.79E+02
4	<=>	5	1.96E+52	-12.52	49.87	6.52E+03
4	<=>	IV	2.99E+52	-11.44	63.78	1.65E+04
4	<=>	7	1.47E+92	-23.07	108.53	1.71E-01
4	<=>	9	2.33E+80	-20.54	96.12	5.24E-03
4	<=>	IX	1.65E+91	-22.91	109.75	2.98E-02
4	<=>	VIII	1.52E+91	-22.91	109.75	2.93E-02
4	<=>	8	8.33E+98	-25.61	115.53	6.72E-04
5	<=>	1	6.93E+77	-19.41	92.11	3.02E-01
5	<=>	2	1.88E+57	-13.31	76.31	4.69E+00
5	<=>	6	1.68E+81	-20.42	103.78	1.92E-03
5	<=>	10	1.39E+93	-24.76	102.88	2.28E-04
5	<=>	II	2.05E+90	-23.25	110.96	1.99E-04
5	<=>	11	1.54E+95	-25.21	103.18	9.92E-04
5	<=>	VI	1.15E+94	-24.13	111.43	2.05E-03
5	<=>	V	3.79E+93	-24.05	111.37	1.15E-03
5	<=>	12	1.29E+97	-25.69	102.06	5.46E-03
5	<=>	I	1.26E+94	-24.12	110.10	4.67E-03
5	<=>	3	1.34E+79	-20.87	86.43	4.17E-03
5	<=>	III	2.11E+75	-18.38	92.83	7.66E-01
5	<=>	4	5.00E+54	-12.79	55.91	1.27E+04
5	<=>	IV	2.86E+54	-12.21	54.20	9.29E+05
5	<=>	7	7.25E+99	-25.66	119.05	7.21E-04
5	<=>	9	1.08E+91	-23.97	108.77	2.24E-05
5	<=>	IX	3.12E+98	-25.39	119.97	1.24E-04
5	<=>	VIII	2.83E+98	-25.38	119.96	1.22E-04

6	<=>	10	1.56E+54	-13.51	58.84	6.48E+00
6	<=>	II	3.98E+53	-12.57	69.61	4.53E+00
6	<=>	11	3.28E+56	-14.03	59.28	2.88E+01
6	<=>	VI	9.15E+57	-13.63	70.34	4.77E+01
6	<=>	V	3.16E+57	-13.57	70.30	2.68E+01
6	<=>	12	1.77E+58	-14.46	57.76	1.68E+02
6	<=>	I	6.16E+56	-13.29	68.05	1.12E+02
6	<=>	3	2.70E+72	-19.08	69.11	1.17E+00
6	<=>	III	6.02E+69	-16.92	75.53	3.30E+02
6	<=>	4	1.77E+68	-16.53	76.41	8.91E+01
6	<=>	5	5.05E+78	-20.33	83.83	2.36E-01
6	<=>	IV	2.33E+81	-19.88	93.56	1.86E+01
6	<=>	7	1.52E+30	-5.38	38.52	4.22E+05
6	<=>	9	1.88E+40	-9.23	31.65	4.55E+05
6	<=>	IX	3.82E+46	-10.26	49.77	8.17E+04
6	<=>	VIII	3.49E+46	-10.25	49.78	7.97E+04
6	<=>	8	2.40E+51	-11.91	58.06	9.05E+02
6	<=>	VII	7.80E+58	-13.06	71.46	1.22E+04
7	<=>	1	1.18E+56	-12.78	75.37	1.73E+01
7	<=>	2	4.08E+74	-18.12	89.72	4.39E+00
7	<=>	6	4.65E+30	-5.40	48.72	6.35E+03
7	<=>	10	1.66E+72	-18.41	86.10	1.41E-02
7	<=>	II	5.94E+76	-18.96	98.11	2.82E-02
7	<=>	11	2.46E+73	-18.62	85.89	5.64E-02
7	<=>	VI	5.03E+79	-19.60	98.13	2.71E-01
7	<=>	V	1.89E+79	-19.55	98.11	1.52E-01
7	<=>	12	8.23E+73	-18.68	84.18	2.85E-01
7	<=>	I	3.95E+78	-19.26	96.31	5.63E-01
7	<=>	3	7.97E+92	-24.67	97.49	3.66E-03
7	<=>	III	2.35E+93	-23.40	104.79	1.78E+00
7	<=>	4	7.48E+92	-23.36	105.51	5.46E-01
7	<=>	9	3.53E+57	-13.75	65.60	8.78E+01
7	<=>	IX	5.72E+68	-16.21	82.18	1.41E+02
7	<=>	VIII	5.32E+68	-16.20	82.19	1.38E+02
7	<=>	8	6.03E+44	-10.23	47.85	4.35E+03
7	<=>	VII	1.03E+50	-10.73	62.95	1.11E+04

8	<=>	1	1.38E+66	-15.82	91.90	3.83E-02
8	<=>	2	3.70E+81	-20.28	103.85	1.03E-02
8	<=>	6	1.07E+54	-12.13	76.08	9.79E+00
8	<=>	10	1.03E+79	-20.53	100.30	3.09E-05
8	<=>	II	3.77E+80	-20.23	109.87	7.32E-05
8	<=>	11	9.62E+79	-20.68	100.02	1.20E-04
8	<=>	VI	3.84E+83	-20.90	109.99	6.89E-04
8	<=>	V	1.36E+83	-20.84	109.94	3.86E-04
8	<=>	12	1.79E+81	-20.95	98.91	6.01E-04
8	<=>	I	1.85E+83	-20.78	108.75	1.41E-03
8	<=>	3	3.39E+99	-26.75	111.41	8.55E-06
8	<=>	III	2.63E+98	-25.03	117.42	4.49E-03
8	<=>	4	9.06E+96	-24.72	117.34	1.40E-03
8	<=>	7	1.61E+47	-10.51	55.35	3.64E+03
8	<=>	9	6.24E+72	-18.21	87.07	1.35E-01
8	<=>	IX	2.96E+80	-19.71	99.96	3.14E-01
8	<=>	VIII	2.68E+80	-19.69	99.96	3.07E-01
8	<=>	VII	8.63E+45	-9.78	48.60	9.38E+05
9	<=>	1	9.15E+59	-14.12	65.58	1.79E+03
9	<=>	2	2.78E+74	-18.29	78.58	2.52E+02
9	<=>	6	1.06E+44	-9.56	38.89	6.93E+06
9	<=>	10	6.46E+75	-19.61	77.13	1.26E+00
9	<=>	II	1.25E+71	-17.57	84.72	7.27E-01
9	<=>	11	9.44E+77	-20.09	77.53	5.71E+00
9	<=>	VI	3.24E+75	-18.64	85.51	7.83E+00
9	<=>	V	9.95E+74	-18.56	85.45	4.35E+00
9	<=>	12	3.62E+80	-20.76	76.60	3.37E+01
9	<=>	I	5.20E+75	-18.68	84.12	1.89E+01
9	<=>	3	3.13E+93	-25.06	86.84	2.19E-01
9	<=>	III	9.91E+88	-22.39	91.78	5.57E+01
9	<=>	4	1.88E+85	-21.38	91.39	1.45E+01
9	<=>	5	8.57E+93	-24.66	97.70	3.78E-02
9	<=>	IV	9.51E+92	-23.21	104.92	2.56E+00
9	<=>	7	4.03E+61	-14.26	63.59	8.20E+04
9	<=>	IX	7.32E+35	-7.17	40.51	3.19E+05
9	<=>	VIII	6.64E+35	-7.16	40.53	3.10E+05
9	<=>	8	2.49E+75	-18.71	77.81	1.73E+02
9	<=>	VII	6.07E+78	-18.73	88.19	2.01E+03

10	<=>	1	4.48E+49	-11.38	40.17	5.19E+06
10	<=>	2	2.09E+69	-16.98	60.11	1.73E+05
10	<=>	6	5.81E+58	-13.98	62.17	1.71E+03
10	<=>	II	1.15E+33	-6.17	42.59	1.69E+05
10	<=>	11	6.06E+76	-19.77	61.83	8.72E+03
10	<=>	VI	1.98E+78	-19.61	74.09	1.88E+03
10	<=>	V	5.92E+77	-19.52	74.04	1.03E+03
10	<=>	12	1.11E+83	-21.51	62.13	8.38E+04
10	<=>	I	1.49E+78	-19.57	71.69	6.03E+03
10	<=>	3	1.14E+93	-25.07	71.61	1.55E+02
10	<=>	III	2.48E+88	-22.43	77.38	1.55E+04
10	<=>	4	1.68E+81	-20.37	76.27	2.81E+03
10	<=>	5	5.08E+94	-25.00	86.20	7.11E+00
10	<=>	IV	3.28E+91	-22.97	92.74	2.13E+02
10	<=>	7	3.17E+73	-18.05	77.65	2.28E+02
10	<=>	9	1.62E+75	-19.38	71.72	2.46E+01
10	<=>	IX	1.55E+77	-19.30	81.00	3.91E+01
10	<=>	VIII	1.37E+77	-19.28	80.99	3.86E+01
10	<=>	8	4.14E+79	-20.39	84.96	7.19E-01
10	<=>	VII	1.82E+83	-20.47	94.19	1.77E+01
11	<=>	1	8.28E+50	-11.79	40.00	6.19E+06
11	<=>	2	1.76E+72	-17.90	60.43	2.22E+05
11	<=>	6	4.62E+60	-14.62	61.58	2.15E+03
11	<=>	10	3.36E+76	-19.94	61.08	2.24E+03
11	<=>	II	5.37E+74	-18.91	71.92	1.88E+02
11	<=>	VI	7.80E+35	-7.01	41.76	5.44E+05
11	<=>	V	3.21E+35	-6.96	41.86	2.95E+05
11	<=>	12	5.83E+84	-22.06	62.01	1.06E+05
11	<=>	I	2.42E+80	-20.30	71.30	7.68E+03
11	<=>	3	2.70E+95	-25.83	71.56	2.02E+02
11	<=>	III	6.33E+90	-23.22	77.08	1.96E+04
11	<=>	4	9.71E+82	-20.97	75.58	3.45E+03
11	<=>	5	8.43E+95	-25.45	85.19	8.74E+00
11	<=>	IV	3.07E+92	-23.37	91.48	2.45E+02
11	<=>	7	2.55E+74	-18.43	76.41	2.65E+02
11	<=>	9	3.85E+76	-19.87	70.84	3.10E+01
11	<=>	IX	2.81E+78	-19.77	79.89	4.57E+01
11	<=>	VIII	2.46E+78	-19.76	79.88	4.46E+01
11	<=>	8	1.74E+80	-20.68	83.56	8.24E-01
11	<=>	VII	3.10E+83	-20.66	92.53	1.88E+01

12	<=>	1	1.98E+54	-12.54	46.85	2.80E+06
12	<=>	2	7.23E+76	-18.98	69.26	6.15E+04
12	<=>	6	2.18E+65	-15.71	71.02	4.64E+02
12	<=>	10	6.30E+81	-21.19	70.39	7.11E+02
12	<=>	II	8.54E+79	-20.15	81.74	4.01E+01
12	<=>	11	9.68E+83	-21.63	71.10	3.65E+03
12	<=>	VI	1.80E+85	-21.45	83.22	5.06E+02
12	<=>	V	4.99E+84	-21.36	83.15	2.76E+02
12	<=>	I	7.04E+39	-8.30	47.03	4.64E+04
12	<=>	III	1.22E+96	-24.49	86.73	4.41E+03
12	<=>	4	1.59E+87	-21.93	84.82	7.09E+02
12	<=>	IV	2.26E+96	-24.22	100.91	4.32E+01
12	<=>	7	5.93E+77	-19.13	85.46	4.82E+01
12	<=>	9	9.94E+81	-21.17	80.83	6.73E+00
12	<=>	IX	3.23E+82	-20.68	89.32	8.42E+00
12	<=>	VIII	2.81E+82	-20.67	89.30	8.19E+00
12	<=>	8	1.06E+84	-21.51	93.04	1.44E-01
12	<=>	VII	3.36E+87	-21.55	102.32	3.13E+00

Table S10: Rate constants for abstraction by resonant radicals from CH_4 and comparison between TST rate constants and the rate estimation rules.

Category	Reactions	Modified Arrhenius parameters[a]				Arrhenius parameters[a]		$\Delta_R H^{298K}$	k (TST,	k (rate rule)[b] / k (TST)		
		n_H	A_H	n	E	A'_H	Ea	(kcal/mol)	1000K)/#n_H[a]	500 K	1000 K	1500 K
Primary	trans-CC=CC• + CH_4 ⇄ trans-CC=CC + CH_3	6	82.5	3.19	26.1	1.27E+12	32.4	18.2	6.32E+05	1.57	1.67	1.61
	cis-CC=CC• + CH_4 ⇄ cis-CC=CC + CH_3	6	181.7	3.04	26.9	8.14E+11	32.9	19.9	3.18E+05	4.08	3.31	2.99
	CCC=CC• + CH_4 ⇄ CC=CCC + CH_3	3	188.0	3.18	26.0	5.18E+12	32.3	18.7	1.34E+06	0.71	0.79	0.77
	C=CC• + CH_4 ⇄ C=CC + CH_3	3	626.7	3.10	25.7	9.03E+12	31.9	18.2	2.96E+06	0.26	0.36	0.38
	C=C(C•)CC + CH_4 ⇄ C=C(C)CC + CH_3	3	436.7	3.13	24.7	8.17E+12	30.9	17.1	4.30E+06	0.11	0.25	0.30
	C=CC_2• + CH_4 ⇄ C=CC_2 + CH_3	6	106.7	3.24	24.4	2.27E+12	30.8	17.0	2.53E+06	0.17	0.42	0.52
	trans-CC=CC_2• + CH_4 ⇄ CC=CC_2 + CH_3	3	185.7	3.16	25.5	4.37E+12	31.8	18.3	1.47E+06	0.50	0.72	0.76
	cis-CC=CC_2• + CH_4 ⇄ CC=CC_2 + CH_3	3	50.5	3.32	25.2	4.28E+12	31.8	18.3	7.37E+05	0.93	1.43	1.53
	C•C=CC_2 + CH_4 ⇄ CC=CC_2 + CH_3	3	119.7	3.22	26.8	4.35E+12	33.2	20.0	7.30E+05	2.00	1.44	1.21
	Average					**4.42E+12**	**32.0**		**1.67E+06**			
	Standard deviation					**2.82E+12**	**0.80**		**1.33E+06**			
Secondary	C=CC•CC=C + CH_4 ⇄ C=CCCC=C + CH_3	4	75.3	3.30	26.5	2.19E+17	33.1	20.8	1.28E+10	0.46	1.12	1.43
	CC=CC•C + CH_4 ⇄ CC=CCC + CH_3	2	202.5	3.31	27.6	3.45E+17	34.1	21.6	1.20E+10	0.45	0.64	0.69
	C=CC•C + CH_4 ⇄ C=CCC + CH_3	2	402.5	3.20	27.5	2.49E+17	33.8	21.4	1.01E+10	0.42	0.67	0.76
	C=CC•CC + CH_4 ⇄ C=CCCC + CH_3	2	133.5	3.24	27.2	2.25E+17	33.6	21.1	1.02E+10	0.70	1.28	1.51
	C=C(C)C•C + CH_4 ⇄ C=C(C)CC + CH_3	2	77.5	3.42	26.0	1.50E+17	32.8	19.6	1.03E+10	0.86	1.32	1.45
	Average					**2.38E+17**	**33.5**		**1.11E+10**			
	Standard deviation					**7.03E+16**	**0.55**		**1.25E+09**			
Tertiary	C=CC•C_2 + CH_4 ⇄ C=CCC_2 + CH_3	1	58.4	3.40	28.0	7.90E+17	34.7	23.4	2.04E+10	0.83	0.88	0.84
	C=CC•(C)CC + CH_4 ⇄ C=CC(C)CC + CH_3	1	92.7	3.30	28.2	5.82E+17	34.8	22.9	1.44E+10	1.27	1.21	1.13
	Average					**6.86E+17**	**34.8**		**1.74E+10**			
	Standard deviation					**1.47E+17**	**0.06**					
Secondary (Cyclics)	CYPE3• + CH_4 ⇄ CYC_5H_8 + CH_3	4	232.3	3.11	26.9	3.69E+17	33.1	21.6	2.13E+10	1.00	1.00	1.00
	CYC_6H_9A + CH_4 ⇄ CYC_6H_{10} + CH_3	4	225.5	3.12	27.1	3.51E+17	33.3	21.8	1.88E+10	1.10	1.02	0.99
	Average					**3.60E+17**	**33.2**		**2.01E+10**			
	Standard deviation					**1.26E+16**	**0.11**					
Tertiary (Cyclics)	MeCYPE3• + CH_4 ⇄ $MeCYC_5H_8$ + CH_3	1	37.9	3.29	27.8	1.25E+18	34.3	23.8	4.02E+10	1.30	1.26	1.19
	$MeCYC_6H_9A$ + CH_4 ⇄ $MeCYC_6H_{10}$ + CH_3	1	43.4	3.31	27.6	1.54E+18	34.2	24.0	5.16E+10	0.85	0.87	0.84
	Average					**1.40E+18**	**34.2**		**4.59E+10**			
	Standard deviation					**2.08E+17**	**0.05**					
Extended resonance	C=CC•C=C + CH_4 ⇄ C=CCC=C + CH_3	2	2.51E+04	2.84	36.1	1.77E+19	41.7	31.7	1.34E+10			
	C=CC=CC• + CH_4 ⇄ C=CC=CC + CH_3	3	513.3	3.14	30.5	5.57E+17	36.7	24.5	5.30E+09	0.57	0.51	0.47
	C=CC(C)=CC• + CH_4 ⇄ C=CC(C)=CC + CH_3	3	136.3	3.30	29.8	4.48E+17	36.3	23.8	5.12E+09	0.39	0.43	0.41
	C=CC=CC_2• + CH_4 ⇄ C=CC=CC_2 + CH_3	6	59.0	3.22	30.0	3.49E+17	36.4	24.3	3.88E+09	1.72	1.87	1.79
	Average					**4.76E+18**	**37.8**		**6.91E+09**			
	Standard deviation					**8.61E+18**	**2.63**		**4.34E+09**			
Extended resonance (Cyclics)	CYC_6H_7 + CH_4 ⇄ CHD14 + CH_3	4	272.5	3.11	34.6	4.66E+19	40.8	31.1	5.75E+10	1.40	1.18	1.07
	CYC_6H_7 + CH_4 ⇄ CHD13 + CH_3	4	277.5	3.15	35.7	4.36E+19	42.0	31.0	2.93E+10	3.48	1.61	1.18
	MeCY13PD5• + CH_4 ⇄ MeCY13PD + CH_3	1	26.8	3.36	30.5	8.65E+18	37.1	27.2	6.62E+10	0.05	0.26	0.42
	CY13PD5• + CH_4 ⇄ CY13PD + CH_3	2	32.5	3.05	27.7	5.50E+17	33.7	22.7	2.35E+10	0.02	0.48	1.41
	Average					**2.49E+19**	**38.4**		**4.41E+10**			
	Standard deviation					**2.37E+19**	**3.73**		**2.09E+10**			
Aromatics	Phenyl + CH_3 ⇄ Benzene + CH_4	6	63.7	3.24	5.97	1.54E+11	12.4	-10.1	2.98E+08			
	Benzyl + CH_3 ⇄ Toulene + CH_4	3	723.3	3.09	23.5	4.28E+15	29.6	14.5	1.42E+09			

Note: [a] The units for A_H, A'_H, and k(TST,1000 K) are cm^3/mol-s, and are kcal/mol for $\Delta_R H^{(298)}$, E and E_a; [b] The rate constant k(rate rule) has been calculated using the bold estimate rate rule listed at the bottom of the each subset. The rows of estimate rate rule list refitted parameters with the averaged values of rate constants of each group in the temperature range of 300 - 2500 K. Molecule structures are presented in abbreviated form as these in Table 1 in the text, with CYC5H8—cyclopentene, CYC6H10—cyclohexene, MeCYC5H8—methyl-cyclopentene, MeCYC6H10—methyl-cyclohexene, CHD13—1,3-cyclohexadiene, CHD14—1,4-cyclohexadiene, CY13PD—1,3-cyclopentadiene, MeCY13PD—methy-1,3-cyclopentadiene.

Table S11: Reaction rate constants for abstraction by resonant radicals from propene and comparison between TST rate constants and the rate estimation rules.

Category	Reactions	Modified Arrhenius parameters[a]				Arrhenius parameters[a]		$\Delta_R H^{(298K)}$	k (TST,	k (rate rule)[b]/k (TST)		
		n_H	A_H	n	E	A'_H	Ea	(kcal/mol)	1000K)/n_H[a]	500 K	1000 K	1500 K
Primary	C=C(C)C• + C=CC ⇄ C=C(C)C + C=CC•	6	0.99	3.70	14.2	5.05E+12	21.5	-1.21	9.93E+07	0.21	0.39	0.45
	C=CC• + C=CC ⇄ C=CC + C=CC•	3	4.20	3.62	16.0	1.12E+13	23.2	0	9.57E+07	0.50	0.40	0.35
	CC=CC• + CC=CC ⇄ CC=CC + CC=CC•	6	2.25	3.63	15.3	6.54E+12	22.5	0	7.97E+07	0.42	0.48	0.48
	trans-CC=C(C)C• + C=CC ⇄ CC=C(C)C + C=CC•	3	0.73	3.71	14.0	3.94E+12	21.4	0.05	8.20E+07	0.24	0.47	0.55
	CCC=CC• + C=CC ⇄ CCC=CC + C=CC•	3	0.20	3.69	15.1	9.29E+11	22.5	0.43	1.14E+07	2.88	3.37	3.38
	trans-CC=CC• + C=CC ⇄ trans-CC=CC + C=CC•	6	0.46	3.64	15.3	1.47E+12	22.6	0.49	1.72E+07	2.03	2.24	2.18
	C•C=C(C)C + C=CC ⇄ CC=C(C)C + C=CC•	3	0.71	3.71	15.7	3.79E+12	23.1	1.76	3.40E+07	1.33	1.13	1.01
	Average (restricted fits)					**4.70E+12**	**22.4**		**5.99E+07**			
	Standard deviation					**3.45E+12**	**0.69**		**3.78E+07**			
Secondary	C=CC•CC=C + C=CC ⇄ C=CCCC=C + C=CC•	4	0.17	3.85	15.8	2.93E+12	23.4	2.60	2.21E+07	0.83	0.88	0.81
	C=CC•C + CC=CC ⇄ C=CCC + CC=CC	2	2.59	3.64	16.2	1.62E+13	23.4	2.70	1.23E+08	0.31	0.32	0.30
	C=CC•CC + C=CC ⇄ C=CCCC + C=CC•	2	0.12	3.77	15.9	3.29E+12	23.4	2.92	2.51E+07	1.46	1.56	1.45
	C=CC•C + C=CC ⇄ C=CCC + C=CC•	2	0.98	3.70	16.6	4.91E+12	24.0	3.21	2.84E+07	1.76	1.38	1.16
	CC=CC•C + C=CC ⇄ CC=CCC + C=CC•	2	0.84	3.80	16.5	9.24E+12	24.0	3.33	5.20E+07	0.97	0.75	0.63
	Average (restricted fits)					**7.32E+12**	**23.6**		**5.01E+07**			
	Standard deviation					**5.58E+12**	**0.31**		**4.24E+07**			
Tertiary	C=CC•(C)CC + C=CC ⇄ C=CC(C)CC + C=CC•	1	0.27	3.83	16.3	3.72E+12	23.9	4.64	2.24E+07	1.49	1.36	1.23
	C=CC(C)C• + C=CC ⇄ C=CC(C)C + C=CC•	1	0.27	3.87	16.3	5.55E+12	24.0	5.18	3.21E+07	1.01	0.95	0.85
	Average (restricted fits)					**4.64E+12**	**23.9**		**2.73E+07**			
Secondary (Cyclics)	CYPE3• + C=CC ⇄ CYC_5H_8 + C=CC•	4	0.52	3.59	15.9	1.07E+12	23.0	3.39	1.00E+07	1.46	1.24	1.10
	CYC_6H_9A + C=CC ⇄ CYC_6H_{10} + C=CC•	4	0.49	3.60	15.8	1.15E+12	22.9	3.61	1.11E+07	1.29	1.12	1.00
	Average (restricted fits)					**1.11E+12**	**23.0**		**1.06E+07**			
Tertiary (Cyclics)	MeCYPE3• + C=CC ⇄ $MeCYC_5H_8$ + C=CC•	1	0.11	3.72	15.9	6.65E+11	23.3	5.62	5.44E+06	1.52	1.28	1.15
	$MeCYC_6H_9A$ + C=CC ⇄ $MeCYC_6H_{10}$ + C=CC•	1	74.9	3.12	10.2	2.77E+10	16.4	5.79	7.23E+06	0.98	0.96	0.91
	Average (restricted fits)					**3.46E+11**	**19.8**		**6.34E+06**			
Extended resonance	C=CC•C=C + C=CC ⇄ C=CCC=C + C=CC•	2	3.63	3.60	23.1	8.46E+12	30.3	13.5	2.03E+06			
	C=CC=C(C)C• + C=CC ⇄ C=CC=C(C)C + C=CC•	6	0.32	3.66	18.8	1.21E+12	26.1	6.03	2.37E+06	2.16	2.30	2.26
	C=CC=CC• + C=CC ⇄ C=CC=CC + C=CC•	3	0.06	4.08	19.1	6.12E+12	27.2	6.28	7.05E+06	1.13	0.77	0.61
	C=CC(C)=CC• + C=CC ⇄ C=CC(C)=CC + C=CC•	3	0.11	4.10	19.2	1.32E+13	27.4	7.41	1.38E+07	0.64	0.39	0.30
	Average (restricted fits)					**6.86E+12**	**26.9**		**7.74E+06**			
	Standard deviation					**6.05E+12**	**0.67**		**5.75E+06**			
Extended resonance (cyclics)	CY13PD5• + C=CC ⇄ CY13PD + C=CC	2	0.2	3.46	15.6	1.15E+11	22.4	4.46	1.44E+06	0.03	0.47	1.22
	MeCY13PD5• + C=CC ⇄ MeCY13PD + C=CC•	1	0.2	3.71	17.7	8.34E+11	25.0	9.01	2.80E+06	0.05	0.24	0.40
	CYC_6H_7• + C=CC ⇄ CHD13 + C=CC•	4	0.3	3.58	22.3	6.78E+11	29.5	12.8	2.45E+05	5.33	2.78	2.18
	CYC_6H_7• + C=CC ⇄ CHD14 + C=CC•	4	1.2	3.51	22.1	1.29E+12	29.0	12.9	5.80E+05	1.84	1.18	1.00
	Average (restricted fits)					**7.28E+11**	**26.5**		**1.27E+06**			
	Standard deviation					**4.84E+11**	**3.36**		**1.14E+06**			

Note: [a] The units for A_H, A'_H, and k(TST,1000 K) are cm^3/mol-s, and $\Delta_R H^{(298)}$, E and Ea are kcal/mol; [b] The rate constant k(rate rule) has been calculated using the values of estimate rate rule listed at the bottom of the table. The rows of estimate rate rule list refitted parameters with the averaged values of rate constants of each group in the temperature range of 300 - 2500 K. The ratio uses the original k(TST) value. Molecule structures are presented in abbreviated form as these in Table 1 in the text, with CYC5H8—cyclopentene, CYC6H10—cyclohexene, MeCYC5H8—methyl-cyclopentene, MeCYC6H10—methyl-cyclohexene, CHD13—1,3-cyclohexadiene, CHD14—1,4-cyclohexadiene, CY13PD—1,3-cyclopentadiene, MeCY13PD—methy-1,3- cyclopentadiene.

Table S12: High pressure limit rate constants for the reactions shown in the C_6H_{11} PES in Figure 19 in the text.

Reactions	Forward			Reverse			Note
	A (s^{-1} or cm^3/mol-s)	Ea (kcal/mol)	*k* (1000K) (s^{-1} or cm^3/mol-s)	A (s^{-1} or cm^3/mol-s)	Ea (kcal/mol)	*k* (1000K) (s^{-1} or cm^3/mol-s)	
I <=> 1	**4.55E+11**	**15.0**	2.37E+08	4.15E+12	19.0	2.89E+08	From CBS-QB3 calculation
II <=> 7	**5.35E+11**	**15.0**	2.79E+08	4.39E+12	21.2	1.01E+08	From CBS-QB3 calculation
1 <=> IX	3.78E+12	36.7	3.57E+04	**1.16E+13**	**3.2**	2.28E+12	Rate rules for H + larger olefin*
1 <=> 6	**4.21E+10**	**15.9**	1.40E+07	2.41E+14	33.7	1.02E+07	5-member ring, E_{strain}=6, E_{addion} analogy to CH_3+C_3H_6_2-C_4H_9*
1 <=> 2	**5.55E+10**	**15.8**	1.90E+07	5.13E+11	31.5	6.48E+04	1,6-H thift, Estrain=2.3, Ebi analogy to CCC.+2-C_4H_8_CCC+CC=CC.*
6 <=> IV	1.94E+14	36.0	2.64E+06	**1.16E+13**	**3.2**	2.28E+12	Rate rules for H + larger olefin*
6 <=> V	3.32E+14	34.5	9.36E+06	**1.16E+13**	**3.2**	2.28E+12	Rate rules for H + larger olefin*
6 <=> VI	5.28E+15	30.2	1.28E+09	**4.44E+12**	**9.1**	4.59E+10	Rate rules for CH_3 + larger olefin*
6 <=> 7	4.79E+14	31.9	5.16E+07	**4.21E+10**	**15.2**	2.05E+07	5-member ring, Estrain=6, Eaddion analogy to C_2H_5+C_3H_6_CCCC.C*
2 <=> VIII	4.12E+15	34.8	9.94E+07	**7.43E+13**	**5.8**	3.93E+12	From CBS-QB3 calculation
2 <=> 3	2.12E+14	29.7	6.69E+07	**3.70E+10**	**18.2**	3.88E+06	1,4-H thift, Estrain=5.8, Ebi analogy to CCC.+1-C4H8_CCC+C=CC.C*
3 <=> 4	**5.10E+09**	**8.3**	7.81E+07	1.04E+14	27.9	8.36E+07	6-member ring, E_{strain}=8, E_{addion} analogy to CH_3+C_3H_6_2-C_4H_9*
4 <=> IV	7.96E+13	33.9	3.09E+06	**2.32E+13**	**3.2**	4.57E+12	Rate rules for H + larger olefin*
3 <=> 5	**4.21E+10**	**8.8**	5.01E+08	5.54E+14	25.7	1.32E+09	5-member ring, E_{strain}=6, E_{addion} analogy to CH_3+C_3H_6_2-C_4H_9*
5 <=> VII	3.53E+13	35.1	7.48E+05	**2.32E+13**	**3.2**	4.57E+12	Rate rules for H + larger olefin*

Table S13: Rate constants at 1 atm for 500- 1800 K for the C_6H_{11} PES, from *CC=CC• + C_2H_4.*

Reactions			A (cm^3/mol-s or s^{-1})	n	Ea (kcal/mol)	*k* (1000K) (cm^3/mol-s or s^{-1})
I	<=>	(1)	3.33E+20	-2.96	17.0	8.65E+07
I	<=>	IX	9.84E+34	-6.88	45.4	2.53E+04
I	<=>	(6)	1.90E+36	-8.96	23.2	2.16E+04
I	<=>	III	1.63E+48	-11.01	38.1	7.26E+06
I	<=>	V	2.83E+41	-9.57	38.4	2.23E+04
I	<=>	VI	9.44E+42	-9.92	38.3	7.20E+04
I	<=>	(2)	1.71E+59	-15.91	33.3	1.74E+04
I	<=>	VIII	9.80E+50	-11.88	40.5	3.06E+06
I	<=>	(3)	8.05E+54	-13.46	40.7	4.29E+05
I	<=>	(4)	3.66E+84	-23.36	49.8	4.10E+03
I	<=>	IV	5.26E+72	-18.71	53.2	9.28E+04
I	<=>	(5)	7.98E+66	-18.20	41.8	1.43E+03
I	<=>	VII	1.14E+60	-15.20	48.8	5.98E+03
I	<=>	(7)	7.56E+51	-12.69	39.5	1.50E+05
I	<=>	II	1.17E+63	-15.54	51.4	1.65E+05
(1)	<=>	IX	1.10E+13	-0.67	33.8	4.33E+03
(1)	<=>	(6)	3.41E+34	-8.60	17.2	9.36E+04
(1)	<=>	III	5.82E+38	-8.50	29.6	6.20E+06
(1)	<=>	V	5.51E+29	-6.40	29.4	1.33E+04
(1)	<=>	VI	7.09E+31	-6.92	29.3	4.71E+04
(1)	<=>	(2)	2.41E+56	-15.18	27.3	7.30E+04
(1)	<=>	VIII	3.93E+42	-9.66	33.1	2.41E+06
(1)	<=>	(3)	3.45E+48	-11.80	34.1	4.96E+05
(1)	<=>	(4)	5.06E+83	-23.19	46.6	8.67E+03
(1)	<=>	IV	1.18E+67	-17.26	47.8	7.13E+04
(1)	<=>	(5)	8.04E+62	-17.18	36.4	2.64E+03
(1)	<=>	VII	5.92E+49	-12.44	40.8	3.46E+03
(1)	<=>	(7)	2.30E+43	-10.36	32.2	1.72E+05
(1)	<=>	II	3.40E+49	-11.78	42.9	6.63E+04
(6)	<=>	IX	6.21E+22	-3.83	53.9	3.38E-01
(6)	<=>	III	1.82E+48	-10.81	37.7	3.96E+07
(6)	<=>	V	1.15E+34	-7.19	36.6	3.20E+04
(6)	<=>	VI	5.39E+37	-8.17	36.9	1.45E+05
(6)	<=>	(2)	4.48E+83	-23.10	58.4	3.81E+01
(6)	<=>	VIII	1.07E+63	-15.83	58.5	5.48E+02
(6)	<=>	(3)	4.14E+70	-18.40	60.7	1.40E+02
(6)	<=>	(4)	1.91+103	-28.96	72.7	
(6)	<=>	IV	1.34E+86	-23.03	72.5	1.57E+01
(6)	<=>	(5)	9.37E+84	-23.70	63.6	9.38E-01
(6)	<=>	VII	4.01E+68	-18.18	65.2	6.48E-01
(6)	<=>	(7)	3.70E+48	-11.30	39.4	1.12E+06
(6)	<=>	II	1.16E+43	-9.32	47.6	4.75E+04

(2)	<=>	IX	2.69E+33	-7.89	60.1	4.23E-04
(2)	<=>	III	1.18E+86	-23.27	70.1	8.13E+00
(2)	<=>	V	7.24E+72	-20.04	67.3	1.03E-02
(2)	<=>	VI	1.53E+76	-20.90	68.0	4.22E-02
(2)	<=>	VIII	4.41E+60	-14.38	48.9	6.50E+06
(2)	<=>	(3)	6.15E+60	-14.73	45.9	3.79E+06
(2)	<=>	(4)	6.87E+94	-25.38	61.4	1.96E+05
(2)	<=>	IV	8.09E+89	-23.31	67.7	1.54E+05
(2)	<=>	(5)	2.92E+75	-19.96	49.4	6.38E+04
(2)	<=>	VII	4.75E+68	-17.49	57.6	3.92E+03
(2)	<=>	(7)	6.83E+84	-23.34	70.5	2.54E-01
(2)	<=>	II	2.72E+81	-22.21	75.2	2.26E-02
(3)	<=>	IX	1.46E+35	-8.43	58.7	1.10E-03
(3)	<=>	III	9.49E+70	-18.98	61.9	3.33E+00
(3)	<=>	V	2.29E+60	-16.47	60.2	6.37E-03
(3)	<=>	VI	8.58E+62	-17.11	60.6	2.34E-02
(3)	<=>	VIII	2.10E+46	-10.28	43.2	1.09E+06
(3)	<=>	(4)	3.68E+47	-11.87	21.7	1.58E+07
(3)	<=>	IV	3.97E+40	-8.82	32.7	9.63E+06
(3)	<=>	(5)	6.23E+44	-11.39	16.6	1.04E+07
(3)	<=>	VII	1.88E+18	-2.62	22.7	2.82E+05
(3)	<=>	(7)	9.94E+71	-19.75	62.9	9.89E-02
(3)	<=>	II	3.52E+74	-20.26	70.2	2.64E-02
(4)	<=>	IX	1.48E+61	-15.92	88.7	1.03E-06
(4)	<=>	III	6.44+107	-29.52	97.5	
(4)	<=>	V	3.71E+95	-26.57	94.8	1.31E-05
(4)	<=>	VI	4.17E+98	-27.35	95.5	5.02E-05
(4)	<=>	VIII	7.01E+88	-22.45	81.9	3.83E+03
(4)	<=>	IV	2.42E+53	-12.34	48.1	7.26E+05
(4)	<=>	(5)	4.03E+86	-22.83	59.9	1.02E+05
(4)	<=>	VII	2.19E+70	-17.55	66.7	1.33E+03
(4)	<=>	(7)	1.39+107	-29.77	97.9	
(4)	<=>	II	5.58+105	-29.22	102.8	
(5)	<=>	IX	3.47E+47	-11.97	77.1	5.97E-06
(5)	<=>	III	5.07E+89	-24.33	83.0	3.87E-02
(5)	<=>	V	1.04E+78	-21.52	80.7	6.30E-05
(5)	<=>	VI	7.90E+80	-22.25	81.3	2.40E-04
(5)	<=>	VIII	4.55E+66	-16.11	64.5	1.70E+04
(5)	<=>	IV	9.91E+68	-16.99	57.5	2.88E+05
(5)	<=>	IV	1.19E+30	-6.09	35.5	1.10E+04
(5)	<=>	(7)	4.84E+89	-24.77	83.7	1.19E-03
(5)	<=>	II	9.55E+89	-24.67	89.9	2.03E-04

(7)	<=>	IX	2.33E+31	-6.85	47.0	3.44E+00
(7)	<=>	III	6.93E+40	-8.98	31.0	1.30E+07
(7)	<=>	V	6.90E+32	-7.17	31.4	2.82E+04
(7)	<=>	VI	4.50E+34	-7.61	31.2	9.99E+04
(7)	<=>	VIII	3.16E+62	-16.18	49.9	1.11E+03
(7)	<=>	IV	2.84E+83	-22.78	62.2	3.30E+01
(7)	<=>	IV	5.22E+69	-18.99	57.1	1.84E+00
(7)	<=>	II	1.15E+22	-3.04	24.0	5.10E+07